Equations of State for Technical Applications. II. Results for Nonpolar Fluids

R. Span[1] and W. Wagner[2]

New functional forms have been developed for multiparameter equations of state for non- and weakly polar fluids and for polar fluids. The resulting functional forms, which were established with an optimization algorithm which considers data sets for different fluids simultaneously, are suitable as a basis for equations of state for a broad variety of fluids. The functional forms were designed to fulfill typical demands of advanced technical applications with regard to the achieved accuracy. They are numerically very stable and their substance-specific coefficients can easily be fitted to restricted data sets. In this way, a fast extension of the group of fluids for which accurate empirical equations of state are available becomes possible. This article deals with the results found for the non- and weakly polar fluids methane, ethane, propane, iso-butane, *n*-butane, *n*-pentane, *n*-hexane, *n*-heptane, *n*-octane, argon, oxygen, nitrogen, ethylene, cyclohexane, and sulfur hexafluoride. The substance-specific parameters of the new equations of state are given as well as statistical and graphical comparisons with experimental data. General features of the new class of equations of state such as their extrapolation behavior and their numerical stability have been discussed in a preceding article. Results for typical polar fluids will be discussed in a subsequent article.

KEY WORDS: argon; cyclohexane; equation of state; ethane; ethylene; fundamental equation; Helmholtz energy; isobutane; methane; *n*-butane; *n*-heptane; *n*-hexane; *n*-octane; *n*-pentane; nitrogen; nonpolar fluids; oxygen; propane; sulfur hexafluoride

---

[1] To whom correspondence should be addressed. Lehrstuhl für Thermodynamik und Energie-technik, Universität Paderborn, D-33095 Paderborn, Germany. E-mail: Roland.Span@thet.uni-paderborn.de

[2] Lehrstuhl für Thermodynamik, Ruhr-Universität Bochum, D-44780 Bochum, Germany. E-mail: Wagner@thermo.ruhr-uni-bochum.de

1. INTRODUCTION

Optimized functional forms are a common feature of modern highly accurate equations of state for well measured reference fluids. To make use of the advantages of optimized functional forms for the description of less well measured fluids, Span et al. [1] presented a new kind of optimization algorithm which considers data sets for different substances simultaneously. The chosen functional form is not the one which yields the best results for a certain fluid, but the one which yields on average the best results for all fluids. If the considered fluids are typical representatives of a certain group of fluids, such as the group of non- or weakly polar fluids, equations of state using the simultaneously optimized functional form can be fitted to data sets for different fluids out of the same group without significant disadvantages.

As a first application, we used the simultaneous optimization algorithm to establish functional forms for equations of state which are able to satisfy advanced technical demands on accuracy for typical nonpolar and polar fluids but which are *not* intended as reference equations for well measured substances. The necessary background information on the development of the new class of equations of state, on the general aspects such as their extrapolation behavior and their numerical stability, and on the selected functional forms are given in a preceding article [2]. The present article summarizes the necessary substance-specific information for the considered non- and weakly polar fluids methane, ethane, propane, isobutane, *n*-butane, *n*-pentane, *n*-hexane, *n*-heptane, *n*-octane, argon, oxygen, nitrogen, ethylene, cyclohexane, and sulfur hexafluoride. In Section 2, the functional form of the equations is given together with the required substance-specific parameters and coefficients. In Section 3, the performance of the new class of equations of state is discussed based on graphical and statistical comparisons with the selected experimental data for all substances. For the considered polar fluids, the corresponding information is given in a subsequent article [3].

2. THE NEW EQUATIONS OF STATE FOR NON- AND WEAKLY POLAR FLUIDS

The new class of equations of state for technical applications of non- and weakly polar fluids is formulated in the reduced Helmholtz energy. As usual, the reduced Helmholtz energy is split into one part which describes the behavior of the hypothetical ideal gas (superscript o) at given values of temperature and density and a second part which describes the residual

behavior (superscript r) of the real fluid. Thus, the general form of the new equation of state reads

$$\frac{a(T, \rho)}{RT} = \frac{a^{\circ}(T, \rho) + a^{\mathrm{r}}(T, \rho)}{RT} = \alpha^{\circ}(\tau, \delta) + \alpha^{\mathrm{r}}(\tau, \delta), \qquad (1)$$

where a is the specific or molar Helmholtz energy, R the corresponding gas constant, T the temperature, ρ the density, $\tau = T_{\mathrm{c}}/T$ the inverse reduced temperature, and $\delta = \rho/\rho_{\mathrm{c}}$ the reduced density. Since the Helmholtz energy as a function of temperature and density is one of the variable sets which are suitable for the formulation of so called fundamental equations, all thermodynamic properties can be calculated by combinations of α° and α^{r} and their derivatives with respect to τ and δ. For some relevant properties, the corresponding relations were given in Ref. 2; for more details see Ref. 4.

The required relation for the ideal gas part, $\alpha^{\circ}(\tau, \delta)$, can easily be obtained from an integrable equation for the heat capacity of the ideal gas, $c_p^{\circ}(T)$, which is known rather accurately for many technically important fluids. The development of equations for $c_p^{\circ}(T)$ and the required integration is described in detail in Ref. 4. This article focuses on the description of the residual part of the reduced Helmholtz energy, $\alpha^{\mathrm{r}}(\tau, \delta)$. For the considered substances, references for the correlations used to describe $\alpha^{\circ}(\tau, \delta)$ are given in Table I together with the values used for the molar mass and for the critical parameters. Where necessary, critical temperatures were converted to the ITS-90 temperature scale according to the procedures given by Preston-Thomas [20] and Rusby [21]. Critical pressures were rounded to 0.001 MPa. The molar masses of the molecules were calculated based on the IUPAC recommended atomic masses published by Coplen [22] and rounded to 0.001 g·mol^{-1}.

As discussed in Ref. 2, the simultaneous optimization algorithm resulted in the following functional form for the residual part of the reduced Helmholtz energy of non- or weakly polar fluids:

$$\alpha(\tau, \delta) = \alpha^{\circ}(\tau, \delta) + \alpha^{\mathrm{r}}(\tau, \delta)$$

$$= \alpha^{\circ}(\tau, \delta) + n_1 \delta \tau^{0.250} \quad + n_2 \delta \tau^{1.125} \quad + n_3 \delta \tau^{1.500}$$

$$+ n_4 \delta^2 \tau^{1.375} \quad + n_5 \delta^3 \tau^{0.250} \quad + n_6 \delta^7 \tau^{0.875}$$

$$+ n_7 \delta^2 \tau^{0.625} e^{-\delta} \quad + n_8 \delta^5 \tau^{1.750} e^{-\delta} \quad + n_9 \delta \tau^{3.625} e^{-\delta^2}$$

$$+ n_{10} \delta^4 \tau^{3.625} e^{-\delta^2} + n_{11} \delta^3 \tau^{14.5} e^{-\delta^3} + n_{12} \delta^4 \tau^{12.0} e^{-\delta^3}. \qquad (2)$$

Table I. References for the Correlations Used for the Caloric Properties of the Ideal Gases, Molar Masses, Critical Parameters and Acentric Factors of the Considered Substances

Substance	Correlation used for α°	M (g·mol^{-1})	T_c (K)	p_c (Mpa)	ρ_c (kg·m^{-3})	Reference T_c, p_c, ρ_c	ω
		Normal alkanes					
Methane	Setzmann and Wagner [5]	16.043	190.564	4.599	162.66	[5]	0.011
Ethane	Jaeschke and Schley [6]	30.070	305.322	4.872	206.60	[7]	0.099
Propane	Jaeschke and Schley [6]	44.097	369.825	4.248	220.48	[8]	0.153
n-Butane	Jaeschke and Schley [6]	58.123	425.125	3.796	227.84	[8]	0.200
n-Pentane	Jaeschke and Schley [6]	72.150	469.70	3.370	232.00	[9, 10]	0.251
n-Hexane	Jaeschke and Schley [6]	86.177	507.82	3.034	233.18	[10, 11]	0.299
n-Heptane	Jaeschke and Schley [6]	100.204	540.13	2.736	232.00	[11, 12]	0.349
n-Octane	Jaeschke and Schley [6]	114.231	569.32	2.497	234.90	[11, 12]	0.395
		Other non- or weakly polar substances					
Argon	Tegeler et al. [13]	39.948	150.687	4.863	535.60	[13]	−0.002
Oxygen	Schmidt and Wagner [14]	31.999	154.595	5.043	436.14	[14]	0.022
Nitrogen	Span et al. [15]	28.013	126.192	3.396	313.30	[15]	0.038
Ethylene	Smukala et al. [16]	28.054	282.35	5.042	214.24	[16]	0.087
Isobutane	Jaeschke and Schley [6]	58.123	407.817	3.640	224.36	[8]	0.185
Cyclohexane	Penoncello et al. [17]	84.161	553.60	4.078	273.02	[17]	0.209
SF$_6$	Cole and de Reuck [18]	146.054	318.7232	3.755	742.15	[19]	0.218

According to Ref. 23, the value used for the universal gas constant is

$$R_m = 8.314510 \, \text{J} \cdot \text{mol}^{-1} \cdot \text{K}^{-1}. \tag{3}$$

The more recent, internationally agreed on value published by Mohr and Taylor [24] became available after the work on the equations presented in this article was finished. It was not taken into account since a shift of −0.0005% in the gas constant is negligible on the level of accuracy aspired here. Where applicable, specific gas constants were calculated as

$$R = R_m / M \tag{4}$$

with the molar masses given in Table I. Values for the substance-specific coefficients n_1 to n_{12} are given in Table II.

Table III gives values for the isobaric heat capacity of the ideal gas, for the pressure, for the isobaric heat capacity and for enthalpy and entropy differences calculated from Eq. (2) in order to enable verification of computer programs. To reproduce the caloric values exactly, the reduced ideal gas contribution, α°, has to be evaluated considering the gas constant

Table II. Coefficients n_i of the Simultaneously Optimized Equations for the Helmholtz Energy of Non- and Weakly Polar Fluids, Eq. (2)

i	Methane n_i	Ethane n_i	Propane n_i	n-Butane n_i	n-Pentane n_i
1	$0.892\,696\,76 \times 10^{+0}$	$0.976\,280\,68 \times 10^{+0}$	$0.104\,039\,73 \times 10^{+1}$	$0.106\,262\,77 \times 10^{+1}$	$0.109\,686\,43 \times 10^{+1}$
2	$-0.254\,382\,82 \times 10^{+1}$	$-0.269\,052\,51 \times 10^{+1}$	$-0.283\,184\,04 \times 10^{+1}$	$-0.286\,209\,52 \times 10^{+1}$	$-0.299\,888\,88 \times 10^{+1}$
3	$0.649\,809\,78 \times 10^{+0}$	$0.734\,982\,22 \times 10^{+0}$	$0.843\,938\,10 \times 10^{+0}$	$0.887\,382\,33 \times 10^{+0}$	$0.995\,168\,87 \times 10^{+0}$
4	$0.207\,934\,71 \times 10^{-1}$	$-0.353\,662\,06 \times 10^{-1}$	$-0.765\,595\,92 \times 10^{-1}$	$-0.125\,705\,81 \times 10^{+0}$	$-0.161\,707\,09 \times 10^{+0}$
5	$0.701\,891\,04 \times 10^{-1}$	$0.846\,920\,31 \times 10^{-1}$	$0.946\,973\,73 \times 10^{-1}$	$0.102\,863\,09 \times 10^{+0}$	$0.113\,344\,60 \times 10^{+0}$
6	$0.237\,003\,78 \times 10^{-3}$	$0.241\,545\,94 \times 10^{-3}$	$0.247\,964\,75 \times 10^{-3}$	$0.253\,580\,41 \times 10^{-3}$	$0.267\,605\,95 \times 10^{-3}$
7	$0.166\,533\,34 \times 10^{+0}$	$0.239\,649\,54 \times 10^{+0}$	$0.277\,437\,60 \times 10^{+0}$	$0.323\,252\,00 \times 10^{+0}$	$0.409\,798\,82 \times 10^{+0}$
8	$-0.438\,556\,69 \times 10^{-1}$	$-0.427\,800\,93 \times 10^{-1}$	$-0.438\,460\,01 \times 10^{-1}$	$-0.379\,507\,61 \times 10^{-1}$	$-0.408\,764\,23 \times 10^{-1}$
9	$-0.157\,267\,80 \times 10^{+0}$	$-0.223\,088\,32 \times 10^{+0}$	$-0.269\,910\,65 \times 10^{+0}$	$-0.325\,348\,02 \times 10^{+0}$	$-0.381\,694\,82 \times 10^{+0}$
10	$-0.353\,116\,75 \times 10^{-1}$	$-0.517\,999\,54 \times 10^{-1}$	$-0.693\,134\,13 \times 10^{-1}$	$-0.790\,509\,69 \times 10^{-1}$	$-0.109\,319\,57 \times 10^{+0}$
11	$-0.295\,700\,24 \times 10^{-1}$	$-0.271\,784\,26 \times 10^{-1}$	$-0.296\,321\,46 \times 10^{-1}$	$-0.206\,367\,21 \times 10^{-1}$	$-0.320\,732\,23 \times 10^{-1}$
12	$0.140\,198\,42 \times 10^{-1}$	$0.112\,463\,05 \times 10^{-1}$	$0.140\,401\,27 \times 10^{-1}$	$0.570\,538\,09 \times 10^{-2}$	$0.168\,770\,16 \times 10^{-1}$

i	n-Hexane n_i	n-Heptane n_i	n-Octane n_i	Argon n_i	Oxygen n_i
1	$0.105\,532\,38 \times 10^{+1}$	$0.105\,437\,48 \times 10^{+1}$	$0.107\,225\,45 \times 10^{+1}$	$0.850\,957\,15 \times 10^{+0}$	$0.888\,782\,86 \times 10^{+0}$
2	$-0.261\,206\,16 \times 10^{+1}$	$-0.265\,006\,82 \times 10^{+1}$	$-0.246\,329\,51 \times 10^{+1}$	$-0.240\,032\,23 \times 10^{+1}$	$-0.248\,794\,33 \times 10^{+1}$
3	$0.766\,138\,83 \times 10^{+0}$	$0.817\,300\,48 \times 10^{+0}$	$0.653\,866\,74 \times 10^{+0}$	$0.541\,278\,41 \times 10^{+0}$	$0.597\,501\,91 \times 10^{+0}$
4	$-0.297\,703\,21 \times 10^{+0}$	$-0.304\,513\,91 \times 10^{+0}$	$-0.363\,249\,74 \times 10^{+0}$	$0.169\,197\,71 \times 10^{-1}$	$0.965\,018\,17 \times 10^{-2}$
5	$0.118\,799\,08 \times 10^{+0}$	$0.122\,538\,69 \times 10^{+0}$	$0.127\,132\,70 \times 10^{+0}$	$0.688\,259\,65 \times 10^{-1}$	$0.719\,704\,29 \times 10^{-1}$
6	$0.279\,228\,61 \times 10^{-3}$	$0.272\,664\,73 \times 10^{-3}$	$0.307\,135\,73 \times 10^{-3}$	$0.214\,280\,33 \times 10^{-3}$	$0.223\,374\,43 \times 10^{-3}$
7	$0.463\,475\,90 \times 10^{+0}$	$0.498\,658\,26 \times 10^{+0}$	$0.526\,568\,57 \times 10^{+0}$	$0.174\,298\,95 \times 10^{+0}$	$0.185\,586\,86 \times 10^{+0}$
8	$0.114\,331\,97 \times 10^{-1}$	$-0.714\,328\,15 \times 10^{-3}$	$0.193\,628\,63 \times 10^{-1}$	$-0.336\,544\,96 \times 10^{-1}$	$-0.381\,293\,68 \times 10^{-1}$
9	$-0.482\,569\,69 \times 10^{+0}$	$-0.542\,368\,96 \times 10^{+0}$	$-0.589\,394\,27 \times 10^{+0}$	$-0.135\,268\,00 \times 10^{+0}$	$-0.153\,522\,45 \times 10^{+0}$
10	$-0.937\,505\,59 \times 10^{-1}$	$-0.138\,018\,22 \times 10^{+0}$	$-0.140\,699\,64 \times 10^{+0}$	$-0.163\,873\,51 \times 10^{-1}$	$-0.267\,268\,15 \times 10^{-1}$
11	$-0.672\,732\,47 \times 10^{-2}$	$-0.615\,952\,87 \times 10^{-2}$	$-0.789\,663\,31 \times 10^{-2}$	$-0.249\,876\,67 \times 10^{-1}$	$-0.256\,752\,99 \times 10^{-1}$
12	$-0.511\,415\,84 \times 10^{-2}$	$0.486\,025\,10 \times 10^{-3}$	$0.330\,365\,98 \times 10^{-2}$	$0.887\,692\,05 \times 10^{-2}$	$0.957\,143\,02 \times 10^{-2}$

i	Nitrogen n_i	Ethylene n_i	Isobutane n_i	Cyclohexane n_i	SF$_6$ n_i
1	$0.922\,965\,67 \times 10^{+0}$	$0.909\,622\,30 \times 10^{+0}$	$0.104\,293\,32 \times 10^{+1}$	$0.102\,323\,54 \times 10^{+1}$	$0.122\,794\,03 \times 10^{+1}$
2	$-0.255\,750\,12 \times 10^{+1}$	$-0.246\,410\,15 \times 10^{+1}$	$-0.281\,842\,73 \times 10^{+1}$	$-0.292\,049\,64 \times 10^{+1}$	$-0.330\,356\,23 \times 10^{+1}$
3	$0.644\,824\,63 \times 10^{+0}$	$0.561\,753\,11 \times 10^{+0}$	$0.861\,762\,32 \times 10^{+0}$	$0.107\,366\,30 \times 10^{+1}$	$0.120\,940\,19 \times 10^{+1}$
4	$0.108\,310\,20 \times 10^{-1}$	$-0.196\,880\,13 \times 10^{-1}$	$-0.106\,136\,19 \times 10^{+0}$	$-0.195\,739\,85 \times 10^{+0}$	$-0.123\,160\,00 \times 10^{+0}$
5	$0.739\,241\,67 \times 10^{-1}$	$0.788\,311\,45 \times 10^{-1}$	$0.986\,157\,49 \times 10^{-1}$	$0.122\,281\,11 \times 10^{+0}$	$0.110\,446\,57 \times 10^{+0}$
6	$0.235\,329\,62 \times 10^{-3}$	$0.214\,787\,76 \times 10^{-3}$	$0.239\,482\,09 \times 10^{-3}$	$0.289\,433\,21 \times 10^{-3}$	$0.329\,521\,53 \times 10^{-3}$
7	$0.180\,248\,54 \times 10^{+0}$	$0.231\,513\,37 \times 10^{+0}$	$0.303\,300\,05 \times 10^{+0}$	$0.272\,317\,67 \times 10^{+0}$	$0.270\,176\,29 \times 10^{+0}$
8	$-0.456\,602\,99 \times 10^{-1}$	$-0.378\,044\,54 \times 10^{-1}$	$-0.415\,981\,56 \times 10^{-1}$	$-0.448\,333\,20 \times 10^{-1}$	$-0.629\,103\,51 \times 10^{-1}$
9	$-0.155\,210\,60 \times 10^{+0}$	$-0.201\,227\,39 \times 10^{+0}$	$-0.299\,919\,37 \times 10^{+0}$	$-0.382\,533\,34 \times 10^{+0}$	$-0.318\,288\,90 \times 10^{+0}$
10	$-0.381\,114\,90 \times 10^{-1}$	$-0.449\,601\,57 \times 10^{-1}$	$-0.803\,693\,43 \times 10^{-1}$	$-0.898\,353\,33 \times 10^{-1}$	$-0.995\,574\,19 \times 10^{-1}$
11	$-0.319\,624\,22 \times 10^{-1}$	$-0.283\,429\,60 \times 10^{-1}$	$-0.297\,613\,73 \times 10^{-1}$	$-0.248\,749\,65 \times 10^{-1}$	$-0.369\,096\,94 \times 10^{-1}$
12	$0.155\,135\,32 \times 10^{-1}$	$0.126\,528\,24 \times 10^{-1}$	$0.130\,596\,30 \times 10^{-1}$	$0.108\,361\,32 \times 10^{-1}$	$0.191\,364\,27 \times 10^{-1}$

Table III. Values for Computer Program Verification

Substance	$c_p^\circ(T_1)^a$ $(kJ \cdot kg^{-1} \cdot K^{-1})$	$p(T_1, \rho_1)^b$ (MPa)	$c_p(T_1, \rho_1)^b$ $(kJ \cdot kg^{-1} \cdot K^{-1})$	$h_2 - h_1{}^c$ $(kJ \cdot kg^{-1})$	$s_2 - s_1{}^c$ $(kJ \cdot kg^{-1} \cdot K^{-1})$
Normal alkanes					
Methane	3.6278	108.108	3.9282	142.73	0.78167
Ethane	3.2991	44.781	3.6276	209.07	0.50715
Propane	3.2350	27.175	3.5658	212.66	0.41879
n-Butane	3.2176	18.416	3.5758	213.77	0.37465
n-Pentane	3.2053	13.454	3.6052	213.42	0.34915
n-Hexane	3.1802	10.221	3.6535	213.09	0.33219
n-Heptane	3.1651	7.957	3.7079	211.90	0.31964
n-Octane	3.1537	6.363	3.8007	211.79	0.31183
Other non- or weakly polar substances					
Argon	0.5203	31.922	0.5630	25.97	0.18479
Oxygen	1.0308	41.051	1.0969	50.89	0.26457
Nitrogen	1.0979	51.268	1.1719	41.82	0.31052
Ethylene	2.7683	48.416	3.0651	174.10	0.47682
Isobutane	3.2392	19.108	3.5575	210.32	0.37469
Cyclohexane	3.0278	9.007	3.5927	206.82	0.31448
SF_6	0.9671	8.094	0.9958	52.80	0.10913

[a] Calculated for $T_1 = 700$ K.
[b] Calculated for $T_1 = 700$ K and $\rho_1 = 200$ kg·m^{-3}.
[c] Calculated between $T_2 = 750$ K and $\rho_2 = 100$ kg·m^{-3} and T_1 and ρ_1.

R_{Lit} used in the reference given for α°. To do so, the reduced ideal gas contribution can be written as

$$\alpha^\circ(\tau, \delta) = \alpha^\circ_{\text{Lit}}(\tau, \delta) \frac{R_{\text{Lit}}}{R_{\text{Eq. (4)}}}. \tag{5}$$

Enthalpy and entropy differences are given instead of absolute values in order to avoid confusion caused by possibly different reference states. In general, we assumed that the enthalpy and entropy were zero for the ideal gas at $T_0 = 298.15$ K and $p_0 = 0.101325$ MPa; for the algorithms needed to calculate the resulting integration constants see, e.g., Ref. 4.

3. DISCUSSION

The goal of this project was to develop numerically stable formulations which yield reliable results when being fitted to small data sets and which satisfy the demands on the accuracy of thermodynamic property

Table IV. Demands on the Accuracy of Thermodynamic Property Data Resulting from Typical Technical Applications; See also Ref. 2

Pressure range	$\rho(p, T)$	$w(p, T)$	Uncertainty in $c_p(p, T)$	$p_s(T)$	$\rho'(T)$	$\rho''(T)$
$p \leqslant 30$ MPa[a]	$\pm 0.2\%$[b]	$\pm 1\%$–$\pm 2\%$[c]	$\pm 1\%$–$\pm 2\%$[c]	$\pm 0.2\%$[d]	$\pm 0.2\%$	$\pm 0.4\%$[d,e]
$p > 30$ MPa[f]	$\pm 0.5\%$	$\pm 2\%$	$\pm 2\%$	–	–	–

[a] Larger uncertainties are to be expected in the extended critical region.

[b] In the extended critical region, $\Delta p/p$ is used instead of $\Delta \rho/\rho$.

[c] $\pm 1\%$ at gaseous and gas-like supercritical states, $\pm 2\%$ at liquid and liquid-like states.

[d] Larger relative uncertainties have to be tolerated for small vapor pressures and saturated vapor densities.

[e] Combination of the uncertainties of gas densities and vapor pressures; experimental data of this accuracy are available for only a few substances.

[f] States at pressures $p > 100$ MPa are not considered due to their limited technical relevance.

data summarized in Table IV, which is repeated from Ref. 2 for the sake of completeness. In a rather general way, it has been shown in Ref. 2 that the new equations of state satisfy the formulated requirements both with regard to their numerical stability, with regard to their reliability, and with regard to the achieved accuracy. In this section, the accuracy of the new equations of state will be discussed in more detail by substance-specific comparisons with selected data sets and with values calculated from other equations of state.

In general, the selected data sets contain all reliable experimental thermodynamic property data available for the corresponding fluid. Data at pressures above 100 MPa were not used due to their limited technical relevance. Data at pressures below 100 MPa were not used if their critically evaluated experimental uncertainty comes close to or exceeds the aimed at uncertainty of the equation of state as it is summarized in Table IV and if more accurate data are available in the same range of states. Data sets were used in part if they partly overlap with more accurate data sets or if outliers in the data set could be identified. Thus, the number of selected data may be substantially smaller than the total number of data in certain data sets. In some cases inconsistencies between data describing different properties led to the exclusion of the less accurate data. Such inconsistencies can only be detected during the development of a fundamental equation of state, which by definition yields a consistent description of different properties since all properties are calculated from derivatives of the same thermodynamic potential. In this way, sets of selected data were generated, which allow for expressive statistical comparisons between experimental

data and values calculated from the new equations of state. The substance-specific discussion in the following sections focuses on these sets of selected data, which were also used to optimize the functional form of Eq. (2), see Ref. 2, and to fit the coefficients of the new equations of state.

3.1. The Representation of the Critical Parameters

For reasons which were explained in Ref. 2, the new equations of state were not constrained to the selected critical parameters given in Table I. Only for n-hexane, n-heptane, n-octane, and cyclohexane, where no reliable data are available in the extended critical region, were reasonable values for the critical temperature enforced by adding one artificial data point for the density of the saturated liquid and one for the density of the saturated vapor close to the critical temperature; see Ref. 2. Table V summarizes the

Table V. Critical Parameters Resulting from an Evaluation of the New Equations of State and Deviations from the Selected Critical Parameters Given in Table I

Substance	$T_{c,\,Eq.\,(2)}$ [a] (K)	$p_{c,\,Eq.\,(2)}$ (MPa)	$\rho_{c,\,Eq.\,(2)}$ [a] (kg·m^{-3})	ΔT_c (K)	Δp_c (%)	$\Delta \rho_c$ (%)	Δp_c^* [b] (%)
			Normal alkanes				
Methane	190.612	4.606	159.97	0.048	0.141	−1.65	−0.011
Ethane	305.509	4.887	196.80	0.187	0.316	−4.74	−0.070
Propane	369.939	4.255	213.33	0.114	0.183	−3.24	−0.020
n-Butane	425.759	3.830	215.47	0.634	0.896	−5.43	−0.095
n-Pentane	469.660	3.369	235.20	−0.040	−0.036	1.38	0.028
n-Hexane	507.794[c]	3.042	222.83	−0.026	0.260	−4.44	0.297
n-Heptane	541.226[c]	2.774	224.90	1.096	1.382	−3.06	−0.133
n-Octane	569.570[c]	2.507	227.63	0.25	0.403	−3.09	0.057
			Other non- or weakly polar substances				
Argon	150.791	4.880	520.50	0.104	0.345	−2.82	−0.058
Oxygen	154.709	5.062	419.83	0.114	0.377	−3.74	−0.065
Nitrogen	126.253	3.404	307.34	0.061	0.253	−1.90	−0.041
Ethylene	282.454	5.050	206.28	0.104	0.171	−3.72	−0.060
Isobutane	407.750	3.633	217.28	−0.067	−0.192	−3.16	−0.080
Cyclohexane	553.651[c]	3.984	262.89	0.051	−2.260	−3.71	−2.321
SF$_6$	318.724	3.754	718.89	0.001	−0.017	−3.13	−0.018

[a] $T_{c,\,Eq.\,(2)}$ and $\rho_{c,\,Eq.\,(2)}$ result from an iteration of the critical point of Eq. (2). To calculate the reduced density δ and the inversely reduced temperature τ, the values given in Table I have to be used.
[b] $\Delta p_c^* / \% = 100[\,p_{c,\,Eq.\,(2)} - p_c - (T_{c,\,Eq.\,(2)} - T_c)(\partial p / \partial T)_\rho|_{T_c,\,\rho_c}\,]/p_c$.
[c] Reasonable values enforced by adding one data point for ρ' and for ρ'' close to T_c; see Ref. 2.

critical parameters resulting from an evaluation of the new equations of state, Eq. (2), in combination with the parameters given in Tables I and II, and the difference between these values and the values selected from the literature.

For substances for which the data situation in the extended critical region is reasonably good, critical temperatures resulting from Eq. (2) agree with the values selected from literature within ± 0.2 K. For an equation of state which is designed mainly for technical applications, this agreement is considered as excellent.

In most cases, the critical pressures resulting from Eq. (2) deviate from the true critical pressures by more than the 0.2% claimed for the uncertainty of pressures calculated in the critical region. However, the deviations observed for the critical pressures mainly result from shifted critical temperatures in combination with the steep plot of the vapor pressure curve close to the critical point. Pseudo-critical pressures p_c^*, which are corrected for this effect, agree with the selected values mostly within $\pm 0.1\%$ indicating that pressures in the immediate vicinity of the critical point can be calculated far within the claimed uncertainty.

In most cases, critical densities calculated from Eq. (2) are smaller than the corresponding, experimentally determined critical densities by 2 to 4%. Considering the large density gradients in the immediate vicinity of the critical point, the simplicity of the new equations of state, and their main focus, this result is also regarded as quite reasonable.

A large value of $|\Delta p_c^*|$ was found for cyclohexane. Most likely, this problem is caused not by the limitations of the new class of equations of state but by severe inconsistencies in the data available for cyclohexane in the extended critical region and at high temperatures in general. However, since cyclohexane is the only cyclic hydrocarbon considered in this study, principal limitations cannot be ruled out completely. A more detailed discussion of this topic is given in Section 3.15. Large values for $|\Delta T_c|$ observed for normal butane and normal heptane most likely result from questionable data for the saturated liquid density close to the critical temperature. In this case, principal limitations can be ruled out since no shortcomings were found for the other normal alkanes.

3.2. Results for Methane

The data set which is available for methane was described in detail by Setzmann and Wagner [5] and by Wagner and de Reuck [25]. The data set used covers fluid states from the triple-point temperature at $T_t \approx 90.7$ K ($T_t/T_c \approx 0.476$) to a temperature of $T_{max} \approx 623$ K ($T_{max}/T_c \approx 3.27$) at pressures up to $p_{max} = 100$ MPa. Data which describe thermal properties,

Table VI. Summary of the Data Sets Selected for Methane and Average Absolute Deviations between Values Calculated from the New Equation of State and the Selected Data

| Authors | No. of data | Temperature and pressure range | | Average absolute deviations (AAD), % | | | | | |
		T (K)	p (MPa)	Gas	Liq.	Crit. reg.	LD[a]	MD[a]	HD[a]
$p\rho T$ data[b]									
Schamp et al. [26]	118	273–423	1.8–26.1	–	–	–	0.023	0.055	–
Douslin et al. [27]	220	398–623	2.5–40.0	–	–	–	0.057	0.101	–
Pope [28]	134	126–191	0.1–4.4	0.028	–	–	0.045	–	–
Roe [29]	70	156–291	0.3–7.9	0.040	–	–	0.028	0.006	–
Goodwin [30][c]	229	94–300	0.4–35.2	0.076	0.036	0.091	0.070	0.079	0.118
Trappeniers et al. [31]	438	273–423	1.8–99.5	–	–	–	0.027	0.052	0.244
Mollerup [32]	51	310–310	0.2–71.7	–	–	–	0.018	0.032	0.169
Achtermann et al. [33]	35	323–323	1.1–28.7	–	–	–	0.012	0.042	–
Kleinrahm et al. [34]	206	180–193	3.3–6.7	0.080	0.067	0.019	0.024	0.150	0.091
Kleinrahm et al. [35]	169	273–323	0.1–8.1	–	–	–	0.026	–	–
Jaeschke and Hinze [36]	86	273–353	0.3–30.3	–	–	–	0.014	0.033	–
Pieperbeck et al. [37]	175	263–323	0.1–12.1	–	–	–	0.021	0.012	–
Achtermann et al. [38]	217	273–373	1.0–34.0	–	–	–	0.022	0.050	0.156
Händel et al. [39]	270	100–260	0.2–8.1	0.047	0.029	0.066	0.033	0.095	0.042
Isochoric heat capacities									
Younglove [40]	282	93–297	3.3–33.5	–	0.720	0.792	–	1.703	0.982
Roder [41]	28	147–218	5.0–23.6	–	0.224	1.439	–	0.675	–
Speeds of sound									
van Dael et al. [42]	24	94–179	0.0–3.2	–	0.937	–	–	–	–
van Itterbeek et al. [43]	91	111–190	0.1–20.0	–	0.329	–	–	–	–
Straty [44]	26	91–178	0.0–3.1	–	0.985	–	–	–	–
Straty [45]	22	150–240	1.0–14.5	0.309	–	–	0.185	0.214	–
Gammon and Douslin [46]	97	113–323	0.1–24.6	0.434	1.108	0.632	0.174	0.098	–
Baidakov et al. [47]	119	150–183	1.1–4.0	–	1.219	–	–	–	–
Sivaraman and Gammon [48]	91	193–423	1.5–26.6	–	–	1.067	0.100	0.218	–
Goodwin [49]	108	255–350	0.2–7.2	–	–	–	0.053	–	–
Lemming [50]	62	232–350	0.1–0.5	–	–	–	0.006	–	–
Trusler and Zarari [51]	80	275–375	0.4–10.1	–	–	–	0.062	–	–
Fawcett [52]	55	293–303	0.3–10.6	–	–	–	0.047	–	–
Trusler and Costa Gomes [53]	64	250–350	0.5–29.8	–	–	–	0.050	0.131	–
Saturated liquid heat capacities									
Younglove [40]	56	96–179	Sat. liq.	–	0.675	–	–	–	–
Roder [41]	3	116–122	Sat. liq.	–	0.150	–	–	–	–
Enthalpy differences									
Dawe and Snowdon [54]	37	273–367	0.1–10.0	–	–	–	0.749	–	–
Grini [55]	134	135–341	0.2–14.2	0.409	0.894	–	0.305	0.524	0.170
Owren et al. [56]	84	242–349	1.0–16.5	–	–	–	0.182	0.328	–
Day et al. [57]	212	287–590	0.2–7.0	–	–	–	0.376	–	–
Second virial coefficients									
Douslin et al. [27]	16	273–623	–	1.973	–	–	–	–	–
Roe [29]	10	156–291	–	0.475	–	–	–	–	–
Kleinrahm et al. [35]	6	273–323	–	0.781	–	–	–	–	–

Table VI. *(Continued)*

Authors	No of data	Temp. range T (K)	Average absolute deviations (AAD), %		
			$T/T_c < 0.6$	$0.6 \leqslant T/T_c \leqslant 0.98$	$T/T_c > 0.98$
Vapor pressures[d]					
Kleinrahm and Wagner [58]	119	91–191	0.380	0.062	0.014
Saturated liquid densities					
Kleinrahm and Wagner [58]	54	91–191	0.047	0.038	0.326
Saturated vapor densities					
Kleinrahm and Wagner [58]	65	91–191	0.156	0.114	0.690
Setzmann and Wagner [5]	31	91–121	0.115	0.186	–

[a] LD: $\rho/\rho_c \leqslant 0.6$; MD: $0.6 < \rho/\rho_c < 1.5$; HD: $\rho/\rho_c \geqslant 1.5$.
[b] In the extended critical region, pressure deviations are given instead of density deviations.
[c] The data of Goodwin [30] were adjusted according to Setzmann and Wagner [5].
[d] At temperatures $T/T_c < 0.6$, average absolute deviations in hPa are given.

including the saturated vapor density and caloric properties on the vapor-liquid phase boundary are available from the triple-point temperature to the critical temperature.

Table VI summarizes the data sets selected for the development of the new equation of state. The number of data tabulated corresponds to the number of selected data points; the total number of points in the corresponding data set can be substantially larger. Statistical information on the accuracy of the equation is given as percentage average absolute deviations,

$$\%\text{AAD} = \frac{100}{N} \sum_{i=1}^{N} \left| \frac{y_{\text{calc}} - y_{\text{exp}}}{y_{\text{exp}}} \right|, \tag{6}$$

for six regions, namely for the gas phase and the liquid phase at subcritical temperatures, for the extended critical region defined as $0.98 \leqslant T/T_c \leqslant 1.1$ and $0.7 \leqslant \rho/\rho_c \leqslant 1.4$, and for the supercritical fluid subdivided into a low-density range (LD, $\rho/\rho_c \leqslant 0.6$), a medium-density range (MD, $0.6 < \rho/\rho_c < 1.5$), and a high-density range (HD, $\rho/\rho_c \geqslant 1.5$). Data in the liquid and supercritical high-density range often correspond to states at $p \geqslant 30$ MPa. Thus, larger density deviations in these ranges may still be acceptable; see Table IV. For $p\rho T$ data in the extended critical region, deviations in pressure are given instead of deviations in density; see also Table IV. Results for vapor pressures and saturated liquid and vapor densities are reported separately for three temperature ranges. At very low reduced temperatures ($T/T_c < 0.6$) relative deviations between measured and calculated vapor pressures increase due to the very small absolute

values of the vapor pressure. Thus, average absolute deviations in hecto-pascal[3] are reported for vapor pressures in this temperature range. For the saturated vapor density, larger relative deviations are expected if data are available at low reduced temperatures. At temperatures close to the critical temperature $(T/T_c > 0.98)$, relative deviations of the saturation densities increase due to the strong temperature dependence of these properties. In this range, the representation of vapor pressures is a more reasonable measure of the quality of technical equations of state.

From Table VI it becomes obvious that Eq. (2) describes the selected data sets well within the uncertainties claimed in Table IV. On average, the formulated demands are by far over fulfilled. Larger deviations between values calculated from Eq. (2) and from the highly accurate reference equation published by Setzmann and Wagner [5] were observed only for speeds of sound at low temperature liquid states where the limit of $|\Delta w|/w = 2\%$ is exceeded at $p \gtrsim 30$ MPa with maximum deviations of $\Delta w/w \approx -4\%$ at $p = 100$ MPa.

As an example of the representation of thermal properties on the phase boundary, Fig. 1 shows deviations between accurate experimental data for the vapor pressure (p_s) and the saturated vapor (ρ'') and liquid (ρ') density of methane and values calculated from Eq. (2). For comparison, values calculated from the reference equation by Setzmann and Wagner [5] are plotted as dashed lines. For $T_t \leqslant T \lessgtr 0.995 T_c$, the data are represented within the uncertainties claimed for the new class of equations of state. Vapor pressures are represented accurately up to the critical temperature; for saturated vapor and liquid densities, the expected increased uncertainties are observed in the critical region.

Figure 2 shows deviations between densities calculated from Eq. (2) and selected experimental results for the density of methane at homogeneous states. The dashed line corresponds to values calculated from the reference equation by Setzmann and Wagner [5]. At pressures above 30 MPa, the observed deviations exceed $\pm 0.2\%$ but they remain well within the limit of $\pm 0.5\%$. Slightly larger deviations on the 204 to 207 K isotherms correspond to states in the extended critical region; the corresponding pressure deviations remain within $\pm 0.2\%$.
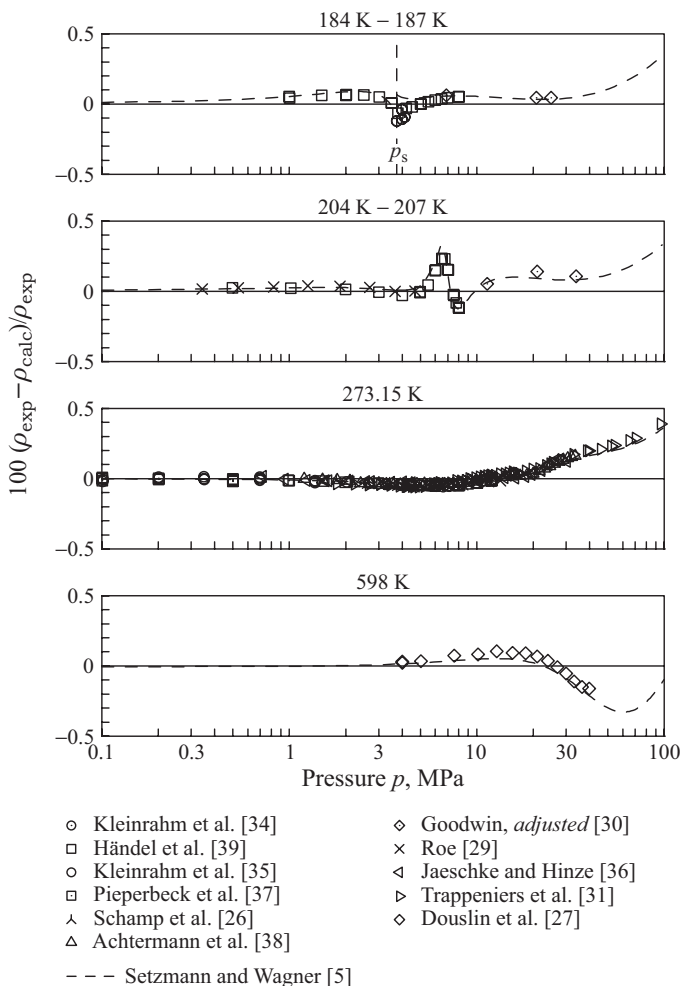
3.3. Results for Ethane

For ethane, experimental results are available for thermodynamic properties from the triple-point temperature at $T_t \approx 90.4$ K $(T_t/T_c \approx 0.296)$ to $T_{max} \approx 623$ K $(T_{max}/T_c \approx 2.04)$ at pressures up to $p_{max} \approx 52$ MPa. Detailed

---

[3] 10^2 Pa; 1 hPa corresponds to 1 mbar.
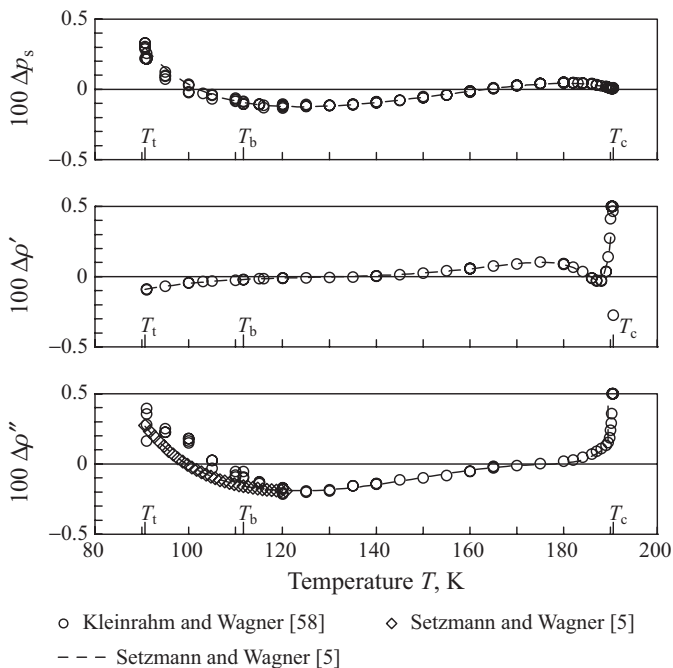
Fig. 1. Percentage deviations $\Delta y, \% = 100(y_{exp} - y_{calc})/y_{exp}$ with $y = p_s, \rho', \rho''$ between selected experimental results for thermal properties on the phase boundary of methane and values calculated from the new equation of state, Eq. (2). Values calculated from the reference equation by Setzmann and Wagner [5] are plotted for comparison.

information on the available data was published by Friend et al. [59]. When the new equation for ethane was finalized, the available data were considered sufficient for the development of technical equations of state both for thermal and caloric properties. On the phase boundary, sufficiently accurate data were available for the vapor pressure and the saturated liquid density from the triple-point temperature to the critical temperature. For the saturated vapor density, data could have been selected only for temperatures above 248 K ($T/T_c \approx 0.81$) and even these data sets showed significant inconsistencies. Thus, the new equation for ethane was not fitted to saturated vapor densities at all. The most reliable data, the data by Sliwinski [60] and Douslin and Harrison [61], were used to check whether the results predicted for the saturated vapor density are reasonable. After the new equation for ethane had been finalized, a comprehensive set of highly accurate data for the $p\rho T$ relation and for thermal properties on the phase boundary of ethane measured by Funke et al. [62, 63]

Fig. 2. Percentage deviations between selected experimental results for the density of methane and values calculated from the new equation of state, Eq. (2). Values calculated from the reference equation by Setzmann and Wagner [5] are plotted for comparison. The data by Goodwin [30] were adjusted according to Setzmann and Wagner [5].

became available. These data are included in the comparisons given in this section.

Table VII summarizes the data sets selected for ethane and gives percentage average absolute deviations between the selected experimental data and values calculated from Eq. (2). The simultaneously optimized equation

Table VII. Summary of the Data Sets Selected for Ethane and Average Absolute Deviations Between Values Calculated from the New Equation of State and the Selected Data

Authors	No. of data	Temperature and pressure range T (K)	p (MPa)	Average absolute deviations (AAD), % Gas	Liq.	Crit. reg.	Supercritical fluid LD^a	MD^a	HD^a
$p\rho T$ data[b]									
Michels and Nederbragt [64]	12	273–323	1.0–6.1	0.083	–	0.064	0.077	–	–
Michels et al. [65]	101	273–423	1.6–21.8	0.048	–	0.041	0.061	0.067	–
Pope [28]	83	210–239	0.1–0.9	0.067	–	–	–	–	–
Douslin and Harrison [61]	298	248–623	1.2–41.0	0.124	0.138	0.081	0.060	0.090	0.169
Straty and Tsumura [66]	456	92–320	0.5–38.4	0.193	0.048	0.088	0.261	0.266	0.065
Young [67]	52	250–300	0.5–1.6	0.056	–	–	–	–	–
Mansoorian et al. [68]	90	323–473	0.1–5.6	–	–	–	0.036	–	–
Lau [69]	37	240–320	1.1–34.3	–	0.038	–	–	–	0.064
Jaeschke and Humphreys [70]	326	260–360	0.1–26.8	0.060	–	0.052	0.030	0.082	0.091
Guo et al. [71]	18	273–293	1.3–3.7	0.043	–	–	–	–	–
Weber [72]	11	320–320	0.3–4.3	–	–	–	0.052	–	–
Hou et al. [73]	42	300–320	0.11–5.0	0.062	–	–	0.063	–	–
Estrada-Alexanders and Trusler [74]	389[c]	220–450	0.0–10.2	0.057	–	–	0.036	–	–
Funke et al. [62]	368[d]	95–340	0.2–12.1	0.068	0.049	0.081	0.095	0.115	0.024
Funke et al. [63]	200[d]	303–305	4.7–4.9	0.449	–	0.033	–	–	–
Isochoric heat capacities									
Roder [41]	106	131–329	2.7–32.2	1.425	0.597	1.963	0.727	0.916	0.571
Speeds of sound									
Tsumura and Straty [75]	209	91–323	0.0–36.9	–	0.455	1.104	–	0.148	0.153
Lemming [50]	186	223–351	0.0–0.6	0.018	–	–	0.027	–	–
Boyes [76]	71	210–360	0.0–1.0	0.021	–	–	0.020	–	–
Trusler and Costa Gomes [53]	52	250–350	0.0–19.6	0.056	–	–	0.052	0.209	0.182
Estrada-Alexanders and Trusler [74]	186	220–450	0.0–10.5	0.091	–	–	0.071	–	–
Isobaric heat capacities									
Bier et al. [77]	117	283–473	0.1–10.0	0.843	–	1.630	0.776	1.408	0.765
Bender [78]	30	233–298	0.1–1.5	0.288	–	–	–	–	–
Ernst and Hochberg [79]	48	303–393	0.3–52.4	0.333	0.632	1.081	0.279	0.368	0.513
Estrada-Alexanders and Trusler [74]	389[c]	220–450	0.0–10.2	0.368	–	–	0.145	–	–
Enthalpy differences									
Grini [55]	82	146–267	0.8–5.1	–	0.547	–	–	–	–

Authors	No of data	Temp. range T (K)	Average absolute deviations (AAD), % $T/T_c < 0.6$	$0.6 \leqslant T/T_c \leqslant 0.98$	$T/T_c > 0.98$
Vapor pressures[e]					
Tickner and Lossing [80]	10	91–131	0.224	–	–
Miniovich and Sorina [81]	14	303–305	–	–	0.123
Pope [28]	8	198–304	–	0.112	0.063
Regnier [82]	10	90–135	0.329	–	–

Table VII.   *(Continued)*

Authors	No of data	Temp. range T (K)	Average absolute deviations (AAD), %		
			$T/T_c < 0.6$	$0.6 \leqslant T/T_c \leqslant 0.98$	$T/T_c > 0.98$
Vapor pressures[e]					
Carruth and Kobayashi [83]	11	91–144	0.077	–	–
Douslin and Harrison [61]	18	238–305	–	0.053	0.046
Fredenslund and Mollerup [84]	4	223–293	–	0.062	–
Pal et al. [85]	41	235–305	–	0.061	0.042
Straty and Tsumura [66]	43	160–300	1.075	0.075	0.028
Barclay et al. [86]	7	198–278	–	0.150	–
Funke et al. [63]	52[d]	95–305	0.338	0.083	0.058
Saturated liquid densities					
Klosek and McKinley [87]	8	94–133	0.149	–	–
Sliwinski [60]	11	283–305	–	0.105	0.651
Tomlinson [88]	7	283–302	–	0.094	0.515
Douslin and Harrison [61]	10	248–304	–	0.172	0.563
Kahre [89]	10	267–300	–	0.131	0.574
McClune [90]	17	93–173	0.072	–	–
Haynes and Hiza [91]	22	100–270	0.057	0.092	–
Orrit and Laupretre [92]	43	102–232	0.032	0.095	–
Luo and Miller [93]	5	220–250	–	0.116	–
Pestak et al. [94]	39	299–305	–	0.055	0.441
Funke et al. [63]	43[d]	91–305	0.084	0.061	0.808
Saturated vapor densities					
Sliwinski [60]	11[f]	283–305	–	0.306	1.705
Douslin and Harrison [61]	13[f]	248–305	–	0.218	4.700
Funke et al. [63]	43[d]	91–305	0.455	0.158	3.102

[a] LD: $\rho/\rho_c \leqslant 0.6$; MD: $0.6 < \rho/\rho_c < 1.5$; HD: $\rho/\rho_c \geqslant 1.5$.

[b] In the extended critical region, pressure deviations are given instead of density deviations.

[c] Data calculated from speed of sound measurements.

[d] The data of Funke et al. [62, 63] became available after the work on the new equation was completed.

[e] At temperatures $T/T_c < 0.6$, average absolute deviations in hPa are given.

[f] Data used only for comparisons.

of state represents the available data within the demanded uncertainties without restrictions. This becomes obvious especially when looking at the very comprehensive set of $p\rho T$ data measured by Funke et al. [62, 63]. The enlarged average absolute deviation reported for the gas phase data by Funke et al. [63] results from the fact that the six data points considered in this category are located close to the border of the extended critical region. The corresponding pressure deviations remain within $\pm 0.1\%$ for all six points.

Figure 3 shows the representation of selected experimental results for the saturated vapor density of ethane. The dashed line corresponds to data
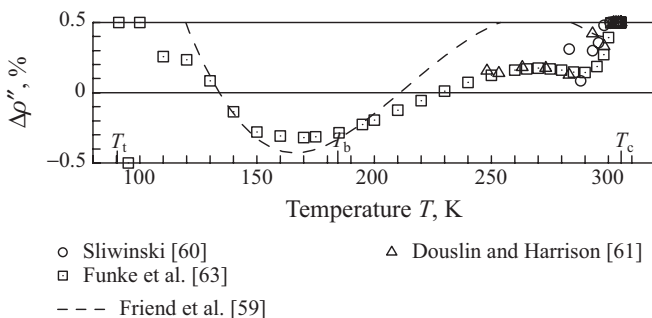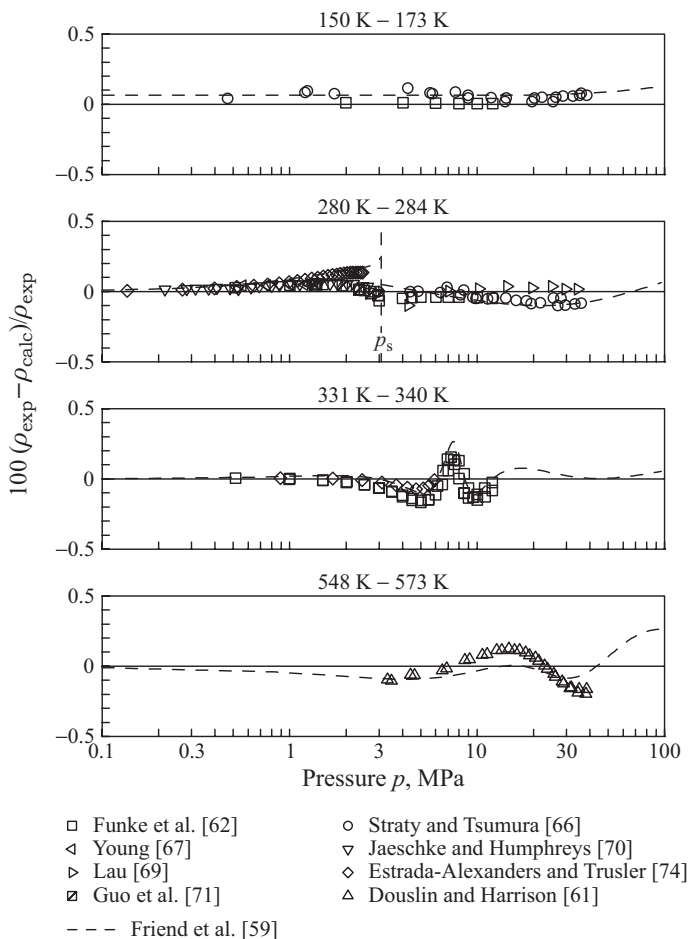
Fig. 3. Percentage deviations $\Delta\rho''$, % $= 100(\rho''_{exp} - \rho''_{calc})/\rho''_{exp}$ between selected experimental results for the saturated vapor density of ethane and values calculated from the new equation of state, Eq. (2). Values calculated from the reference equation by Friend et al. [59] are plotted for comparison.

calculated from the reference equation of state by Friend et al. [59]. From almost the triple-point temperature to $T \approx 0.98 \cdot T_c$, Eq. (2) represents the highly accurate data by Funke et al. [43] which were not used to fit the equation within the demanded accuracy of $|\Delta\rho''|/\rho'' \leqslant 0.4\%$. The increased deviations at very low temperatures remain within the experimental uncertainty of the data. Obviously, it is possible to predict saturated vapor densities with sufficient accuracy based only on experimental data for the vapor pressure and for properties in the homogeneous gas region.

As an example of the representation of $p\rho T$ data, Fig. 4 shows percentage deviations between selected experimental data and densities calculated from Eq. (2) and from the reference equation by Friend et al. [59]. Figure 5 illustrates the very good representation of accurate speed of sound data at gaseous, liquid and supercritical conditions. In the subcritical gas and liquid phase, the new 12-term equation is slightly superior to the 32-term equation by Friend et al., while the reference equation is slightly superior at supercritical conditions. However, the new class of equations of state presented in this article was not designed for use as a reference equation but as a technical equation of state. The fact that the accuracy of the new equation of state for ethane compares well with the one of a typical reference equation implies that the new class of equations of state is far superior to older technical equations of state; see also Refs. 2 and 4.

3.4. Results for Propane

For propane, reliable experimental data are available from the triple-point temperature at $T_t \approx 85.5\,\mathrm{K}$ $(T_t/T_c \approx 0.231)$ to $T_{max} \approx 623\,\mathrm{K}$

Fig. 4. Percentage deviations between selected experimental results for the density of ethane and values calculated from the new equation of state, Eq. (2). Values calculated from the reference equation by Friend et al. [59] are plotted for comparison.

$(T_{max}/T_c \approx 1.68)$; the considered data set was restricted to pressures up to $p_{max} \approx 100$ MPa. The recent work by Miyamoto and Watanabe [95] contains a review of the available data set. At liquid and liquid-like supercritical states, reliable data are available for thermal and caloric data from different authors. However, compared to methane and ethane, the data situation is quite unsatisfactory for gaseous and gas-like supercritical states. An accurate description of caloric properties at gaseous states recently became
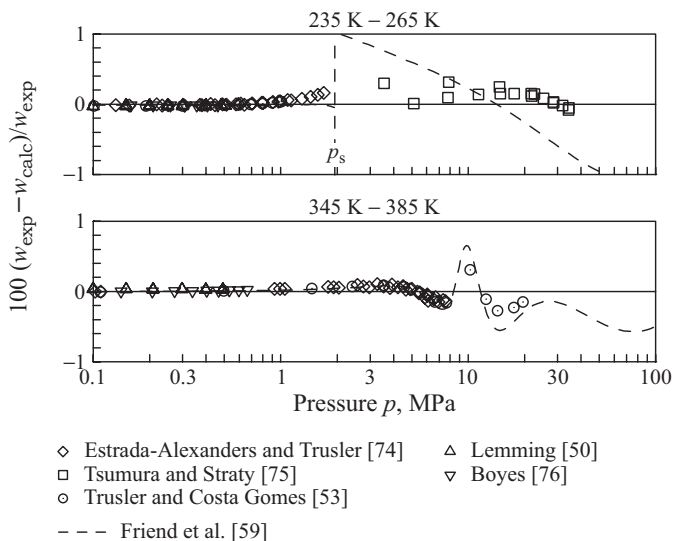
Fig. 5. Percentage deviations between selected experimental results for the speed of sound in ethane and values calculated from the new equation of state, Eq. (2). Values calculated from the reference equation by Friend et al. [59] are plotted for comparison.

possible when Trusler and Zarari [96] published their speed of sound data. Accurate experimental results for the saturated vapor density are missing. The most reasonable data sets were again used for comparison. Table VIII summarizes the selected data sets for propane and gives percentage average absolute deviations between the selected experimental data and values calculated from Eq. (2). The recent data by Abdulagatov et al. [114, 115] did not meet the selection criteria.

The new equation of state represents the available data within the demanded uncertainties without significant restrictions. This becomes obvious especially when looking at the representation of the comprehensive data set by Thomas and Harrison [101]. Large deviations up to $\Delta\rho'/\rho' \approx -0.4\%$ are observed only for saturated liquid densities at temperatures $T \lesssim 100K$ ($T/T_c \lesssim 0.271$), at reduced temperatures which are relevant only for propane. Figure 6 shows deviations between experimental results for the speed of sound in propane and values calculated from Eq. (2), from the 32-term MBWR-type equation of state by Younglove and Ely [8] which is internationally used as a reference for the properties of propane, and from the recent reference equation by Miyamato and Watanabe [95]. Even

Table VIII. Summary of the Data Sets Selected for Propane and Average Absolute Deviations Between Values Calculated from the New Equation of State and the Selected Data

Authors	No. of data	Temperature and pressure range T (K)	p (MPa)	Average absolute deviations (AAD), % Gas	Liq.	Crit. reg.	Supercritical fluid LD[a]	MD[a]	HD[a]
$p\rho T$ data[b]									
Dittmar et al. [97]	274	273–413	1.0–103.5	–	0.077	–	–	–	0.122
Babb and Robertson [98]	4	308–308	63.8–98.3	–	0.112	–	–	–	0.112
Ely and Kobayashi [99]	221	166–324	0.1–42.8	–	0.042	–	–	–	–
Warowny et al. [100]	48	373–423	0.3–6.3	–	–	–	0.177	–	–
Thomas and Harisson [101]	785	273–623	0.6–40.0	0.111	0.060	0.019	0.079	0.127	0.107
Haynes [102]	196	90–300	0.6–37.5	–	0.087	–	–	–	–
Kratzke and Müller [103]	54	247–491	2.2–61.0	–	0.068	–	–	–	0.151
Starling [104]	26	273–323	0.1–1.8	0.094	–	–	–	–	–
Straty and Palavra [105]	143	363–598	0.2–34.6	–	–	0.247	0.141	0.138	0.078
Speeds of sound									
Lacam [106]	109	298–498	10.1–91.2	–	0.248	–	–	1.030	0.564
Younglove [107]	162	90–300	1.9–35.0	–	0.539	–	–	–	–
Niepmann [108]	240	200–340	0.0–60.6	–	0.308	–	–	–	–
Trusler and Zarari [96]	68	225–375	0.0–0.9	0.012	–	–	0.017	–	–
Isobaric heat capacities									
Yesavage et al. [109]	70	117–297	1.7–13.8	–	1.171	–	–	–	–
Ernst and Büsser [110]	36	293–353	0.1–1.4	0.448	–	–	–	–	–

Authors	No of data	Temp. range T (K)	Average absolute deviations (AAD), % $T/T_c < 0.6$	$0.6 \leqslant T/T_c \leqslant 0.98$	$T/T_c > 0.98$
Vapor pressures[c]					
Kemp and Egan [111]	11	166–231	0.148	0.020	–
Kratzke [112]	14	312–368	–	0.036	0.108
Thomas and Harisson [101]	25	258–370	–	0.098	0.005
Saturated liquid densities					
Ely and Kobayashi [99]	18	166–288	0.057	0.050	–
Orrit and Laupretre [92]	20	96–205	0.066	–	–
Thomas and Harisson [101]	16	283–369	–	0.038	0.156
Saturated vapor densities					
Helgeson and Sage [113]	12[d]	278–339	–	0.410	–
Thomas and Harisson [101]	11[d]	323–369	–	0.108	0.551

[a] LD: $\rho/\rho_c \leqslant 0.6$; MD: $0.6 < \rho/\rho_c < 1.5$; HD: $\rho/\rho_c \geqslant 1.5$.
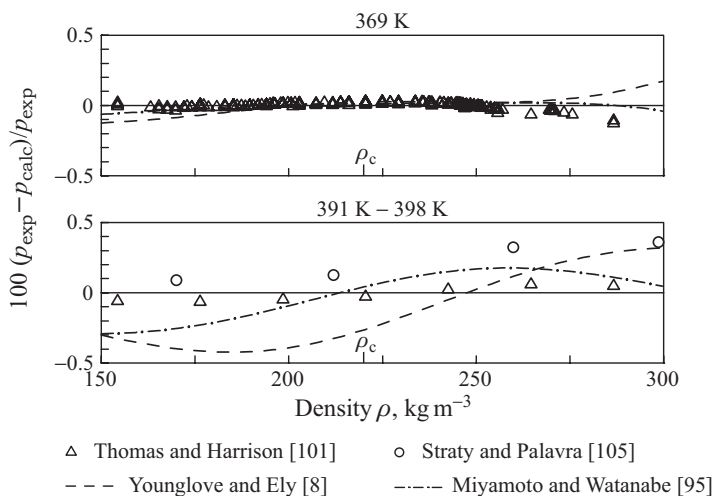[b] In the extended critical region, pressure deviations are given instead of density deviations.
[c] At temperatures $T/T_c < 0.6$, average absolute deviations in hPa are given.
[d] Data used only for comparison.
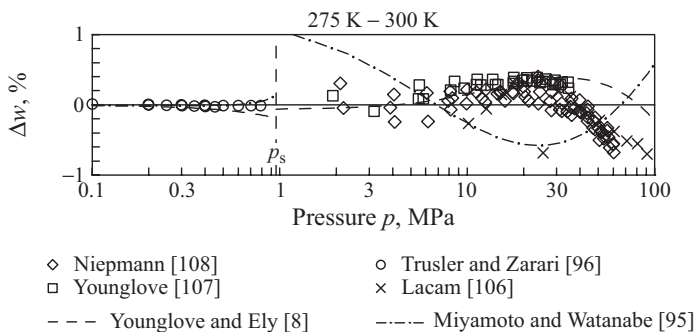
Fig. 6. Percentage deviations $\Delta w, \% = 100(w_{exp} - w_{calc})/w_{exp}$ between selected experimental results for the speed of sound in propane and values calculated from the new equation of state, Eq. (2). Values calculated from the equations by Miyamoto and Watanabe [95] and by Younglove and Ely [8] are plotted for comparison.

though Eq. (2) was not designed as a reference equation, its performance comes close to that of the reference equations. For thermal properties on the phase boundary, these equations are superior, while Eq. (2) yields comparable results for homogeneous states and is slightly superior in the extended critical region; see Fig. 7.

Fig. 7. Percentage pressure deviations between selected $p\rho T$ data in the extended critical region of propane and values calculated from the new equation of state, Eq. (2). Values calculated from the equations by Miyamoto and Watanabe [95] and by Younglove and Ely [8] are plotted for comparison.

3.5. Results for Normal Butane

For normal butane, reliable experimental data are available from the triple-point temperature at $T_t \approx 134.9 K$ ($T_t/T_c \approx 0.317$) to $T_{max} \approx 693$ K ($T_{max}/T_c \approx 1.63$) and up to pressures of $p_{max} \approx 69$ MPa. For liquid and liquid-like supercritical states, the data situation is satisfactory, while accurate data for gaseous states are rare. Some data for the second virial coefficient had to be used as substitutes for direct measurements of properties in the gas phase. For the development of technical equations of state, the vapor pressure and saturated liquid density are described by experimental data with sufficient accuracy; reliable data for the saturated vapor density are not available. An extensive review of the data set which was available in 1982 was published by Goodwin and Haynes [116]. Important new data sets for properties of gaseous n-butane include those of Gupta and Eubank [117] and Ewing et al. [118]. In the liquid region, measurements of the speed of sound published by Niepmann [108] and measurements of the isochoric heat capacity published recently by Magee and Lüddecke [119] have improved the situation with regard to caloric properties. Table IX summarizes the selected data sets for normal butane and gives percentage average absolute deviations between the selected experimental data and values calculated from Eq. (2).

From Table IX it becomes obvious that the new equation of state describes the available data within the demanded uncertainties in general. Comparisons between the recent $p\rho T$ data by Gupta and Eubank [117] and the data by Olds et al. [121] show that larger deviations found for the data by Olds et al. are caused by the uncertainty of these data. The performance of Eq. (2) is comparable to the 32-term MBWR-type equation published by Younglove and Ely [8] which is the common standard for properties of normal butane. However, at low temperature liquid states, Eq. (2) is clearly superior with regard to the representation of caloric properties. Using the isochoric heat capacity data by Magee and Lüddecke [119] as an example, this fact is illustrated in Fig. 8.

3.6. Results for Normal Pentane

For normal pentane, experimental data are available from the triple-point temperature at $T_t \approx 143.4$ K ($T_t/T_c \approx 0.305$) to $T_{max} \approx 573$ K ($T_{max}/T_c \approx 1.22$) and up to pressures of $p_{max} \approx 69$ MPa. At liquid and liquid-like states, only the $p\rho T$ data published by Kratzke et al. [130] are sufficiently accurate to develop an equation of state that satisfies the demands formulated above; basically, the same is true for vapor pressures and saturated liquid densities. Sufficiently accurate data for the saturated vapor

Table IX. Summary of the Data Sets Selected for Normal Butane and Average Absolute Deviations Between Values Calculated from the New Equation of State and the Selected Data

Authors	No. of data	Temperature and pressure range T (K)	Temperature and pressure range p (MPa)	Average absolute deviations (AAD), % Gas	Liq.	Crit. reg.	Supercritical fluid LD[a]	MD[a]	HD[a]
$p\rho T$ data[b]									
Beattie et al. [120]	35	473–573	1.7–11.9	–	–	–	0.065	0.120	–
Olds et al. [121]	216	311–511	0.1–69.0	0.272	0.096	–	0.072	0.271	0.162
Haynes [122]	104	140–300	1.7–36.1	–	0.064	–	–	–	–
Gupta and Eubank [117]	49	265–450	0.0–1.1	0.074	–	–	0.083	–	–
Isochoric heat capacities									
Magee and Lüddecke [119]	148	153–342	2.0–33.2	–	0.844	–	–	–	–
Speeds of sound									
Niepmann [108]	248	200–375	0.0–60.4	–	0.286	–	–	–	–
Isobaric/saturated liquid heat capacities									
Aston and Messerly [123]	20	140–268	Sat. liq.	–	0.980	–	–	–	–
Dailey and Felsing [124]	8	345–693	0.1–0.1	0.205	–	–	0.365	–	–
Magee and Lüddecke [119]	100	139–317	Sat. liq.	–	0.878	–	–	–	–
Second virial coefficients									
Brostow et al. [125]	3	348–400	–	1.059	–	–	–	–	–
Ewing et al. [118]	8	250–320	–	0.274	–	–	–	–	–

Authors	No of data	Temp. range T (K)	Average absolute deviations (AAD), % $T/T_c < 0.6$	$0.6 \leqslant T/T_c \leqslant 0.98$	$T/T_c > 0.98$
Vapor pressures[c]					
Kay [126]	11	368–422	–	0.151	0.121
Holldorf and Knapp [127]	20	259–357	–	0.096	–
Machin and Golding [128]	142	173–250	0.033	–	–
Sako et al. [129]	22	301–316	–	0.023	–
Saturated liquid densities					
Kay [126]	15	325–413	–	0.121	–
Kahre [89]	4	289–328	–	0.069	–
Haynes and Hiza [91]	11	135–300	0.049	0.106	–
Orrit and Laupretre [92]	50	135–275	0.049	0.090	–

[a] LD: $\rho/\rho_c \leqslant 0.6$; MD: $0.6 < \rho/\rho_c < 1.5$; HD: $\rho/\rho_c \geqslant 1.5$.
[b] In the extended critical region, pressure deviations are given instead of density deviations.
[c] At temperatures $T/T_c < 0.6$, average absolute deviations in hPa are given.

density are not available. The only reliable data for caloric properties are those published by Ewing et al. [131] for the speed of sound in the gas phase at very low pressures. In the low temperature gas region, the new equation mainly depends on the second virial coefficients derived from these data. The speed of sound measurements themselves cover a pressure range up to only 0.09 MPa and were not used to fit Eq. (2) since the residual contribution to the speed of sound is smaller than the target

$100\,(c_{v,\mathrm{exp}} - c_{v,\mathrm{calc}})/c_{v,\mathrm{exp}}$
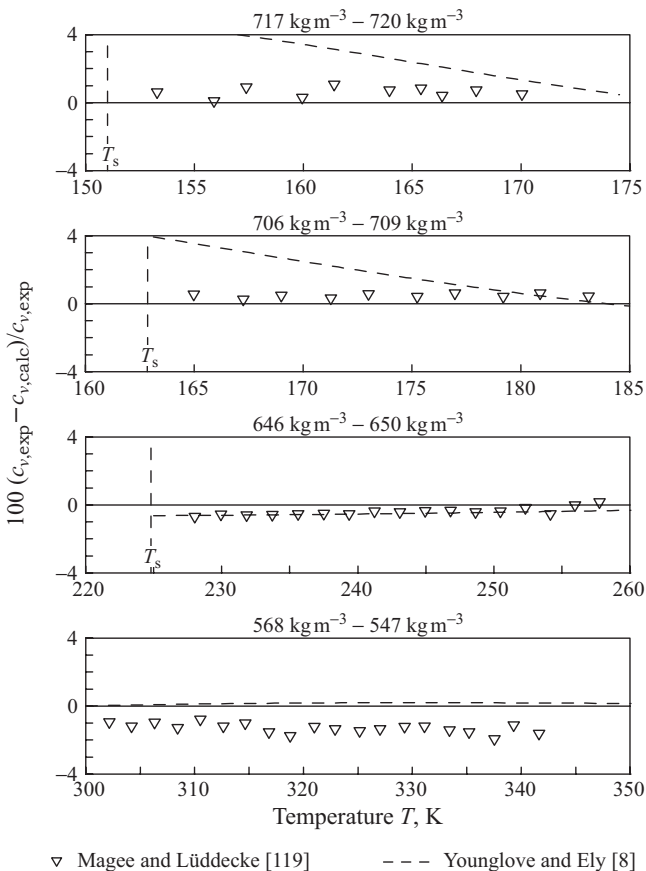
Fig. 8. Percentage deviations between experimental results for the isochoric heat capacity in the liquid region of normal butane and values calculated from the new equation of state, Eq. (2). Values calculated from the MBWR-type equation by Younglove and Ely [8] are plotted for comparison.

uncertainty of the new equation of state at most states. At higher temperatures, less accurate data for the second virial coefficient had to be considered as well in order to achieve a reasonable description of the gas phase. No complete reviews have been published for the data sets available for *n*-pentane and for the higher *n*-alkanes. Cibulka and Hnedkovsky [132] have published an extensive compilation which summarizes the available data on liquid densities considering normal alkanes from pentane to hexadecane. Very recently, vapor pressures and critical constants of normal

Table X. Summary of the Data Sets Selected for Normal Pentane and Average Absolute Deviations Between Values Calculated from the New Equation of State and the Selected Data

| Authors | No. of data | Temperature and pressure range | | Average absolute deviations (AAD), % | | | | | |
| | | T (K) | p (MPa) | Gas | Liq. | Crit. reg. | LD[a] | MD[a] | HD[a] |
							Supercritical fluid		
$p\rho T$ data[b]									
Sage and Lacey [134]	229	311–511	0.1–69.0	0.200	0.266	–	0.421	–	0.336
Beattie et al. [135]	100	469–470	3.4–3.4	–	–	0.018	–	–	–
Kratzke et al. [130]	118	238–573	0.8–60.6	–	0.096	–	–	–	0.184[c]
Second virial coefficients									
Huff and Reed [136]	8	308–511	–	1.487	–	–	–	–	–
Hajjar et al. [153]	11	313–473	–	1.239	–	–	–	–	–
Brostow et al. [125]	3	348–400	–	1.089	–	–	–	–	–
Ewing et al. [131]	7	270–330	–	0.237	–	–	–	–	–

| Authors | No of data | Temp. range T (K) | Average absolute deviations (AAD), % | | |
			$T/T_c < 0.6$	$0.6 \leqslant T/T_c \leqslant 0.98$	$T/T_c > 0.98$
Vapor pressures[d]					
Mair [137]	1	309	–	0.081	–
Willingham et al. [138]	8	286–310	–	0.069	–
Beattie et al. [135]	5	373–448	–	0.190	–
Tickner and Lossing [80]	7	177–223	0.314	–	–
Li and Canjar [139]	2	423–448	–	0.152	–
Osborn and Douslin [140]	15	269–341	0.009	0.018	–
Kratzke et al. [130]	14	350–460	–	0.035	–
Saturated liquid densities					
Carney [141]	6	243–293	0.086	0.050	–
Orrit and Laupretre [92]	14	179–249	0.030	–	–
Kratzke et al. [130]	12	237–440	0.108	0.048	–

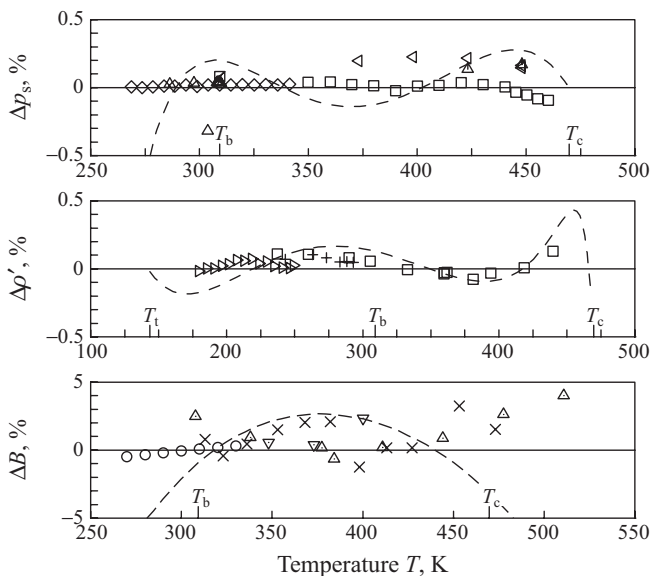[a] LD: $\rho/\rho_c \leqslant 0.6$; MD: $0.6 < \rho/\rho_c < 1.5$; HD: $\rho/\rho_c \geqslant 1.5$.
[b] In the extended critical region, pressure deviations are given instead of density deviations.
[c] Maximum deviation $\Delta\rho/\rho = 0.234\%$ at $p \approx 60$ MPa.
[d] At temperatures $T/T_c < 0.6$, average absolute deviations in hPa are given.

alkanes up to hexatriacontane have been discussed by Lemmon and Goodwin [133]. Table X summarizes the selected data sets for normal pentane and gives percentage average absolute deviations between the selected experimental data and values calculated from Eq. (2).

Based on the percentage average absolute deviations given in Table X, it becomes difficult to prove that the new equation satisfies the demands summarized in Table IV. However, more detailed comparisons between the $p\rho T$ data by Kratzke et al. [130] and the data by Sage and Lacey [134] show that the large deviations found for the most comprehensive data set, the one by Sage and Lacey, obviously result from the uncertainty of these

Fig. 9. Percentage deviations $\Delta y, \% = 100(y_{exp} - y_{calc})/y_{exp}$ with $y = p_s, \rho', B$ between selected experimental results for normal pentane and values calculated from the new equation of state, Eq. (2). Values calculated from a Bender equation of state which was fitted to the same data set are plotted for comparison.

data. The accurate representation of the saturated and compressed liquid densities by Kratzke et al. [130], of the second virial coefficients by Ewing et al. [131], and of the vapor pressures by Osborn and Douslin [140] and Kratzke et al. [130] proves that the most reliable data are represented well within the demanded uncertainty. Figure 9 shows the representation of data selected for the vapor pressure, for the saturated liquid density, and for the second virial coefficient. Since no widely accepted reference equation of state is available for normal pentane, a 19-term Bender equation of state [142] was fitted to the same data set as Eq. (2) for comparison. Equations of this type can be regarded as the most accurate technical equations of state which were available until now. For details on their advantages and disadvantages, see Refs. 2 and 4.

3.7. Results for Normal Hexane

When the functional form of the equation for non- and weakly polar fluids was finalized, reliable experimental data for normal hexane were available from $T_{min} = 263$ K ($T_{min}/T_c \approx 0.518$, $T_t/T_c \approx 0.350$) to $T_{max} \approx 548$ K ($T_{max}/T_c \approx 1.08$) and up to pressures of $p_{max} \approx 92$ MPa. Data at pressures above 100 MPa were not used due to their small technical relevance. For data compilations, see Refs. 132 and 133. The description of the gaseous phase had to rely mainly on questionable data published for the second virial coefficients. At liquid states, the $p\rho T$ data set published by Sauermann et al. [143] was the most reliable foundation for an equation of state; this reference contains vapor pressures and saturated liquid densities as well. Reliable data for the saturated vapor density were not available. Abdulagatov et al. [144] published a set of $p\rho T$ data which covers the temperature range 523 K $\leqslant T \leqslant 663$ K. Fitting Eq. (2) to a data set which contains these data results in significant inconsistencies at lower temperatures where reliable $p\rho T$ data are available and in a critical temperature which is almost 4 K higher than the literature value; see Table V for comparison. Similar problems were found when the corresponding data for *n*-octane [144] were considered, see Section 3.9, and for normal pentane reliable data in the same range of reduced temperatures could be represented without inconsistencies; see Section 3.6. Abdulagatov et al. do not compare their $p\rho T$ data with any other experimental results, and they do not discuss effects such as thermal decomposition which may limit the accuracy of their data. Thus, the data by Abdulagatov et al. [144] were not considered in the final data set, but they point out a severe shortcoming of the data sets available for higher alkanes—the complete absence of reliable data at supercritical conditions makes predictions for such states very uncertain. It may become necessary to refit the corresponding equations of state if a reliable experimental basis becomes available.

Table XI summarizes the selected data sets for normal hexane and gives percentage average absolute deviations between the selected experimental data and values calculated from Eq. (2). The new equation of state describes the selected data sets within the demanded uncertainties or within their experimental uncertainties. As an example for the performance of the new equation of state, Fig. 10 shows deviations between selected experimental data for the vapor pressure and the saturated liquid density of normal hexane and values calculated from Eq. (2). Since no widely accepted reference equation of state is available for normal hexane, a Bender equation of state [142] was again fitted to the same data set as Eq. (2) for comparison. The dash-dotted line corresponds to values calculated from an equation of state which uses the functional form of Eq. (2),

Table XI. Summary of the Data Sets Selected for Normal Hexane and Average Absolute Deviations Between Values Calculated from the New Equation of State and the Selected Data

Authors	No. of data	Temperature and pressure range T (K)	p (MPa)	Average absolute deviations (AAD), % Gas	Liq.	Crit. reg.	Supercritical fluid LD[a]	MD[a]	HD[a]
$p\rho T$ data[b]									
Kelso and Felsing [145]	27	373–548	15.6–31.6	–	0.058	–	–	–	0.129
Stewart et al. [146]	78	311–511	0.7–67.3	–	0.256	–	–	–	0.566
Kuss and Taslimi [147]	11	298–353	0.1–78.5	–	0.373	–	–	–	–
Dymond and Young [148]	9	298–373	0.1–92.1	–	0.274	–	–	–	–
Kiran and Sen [149]	40	313–448	34.2–65.9	–	0.366	–	–	–	–
Susnar et al. [150]	51	294	0.1–34.6	–	0.112	–	–	–	–
Sauermann et al. [143]	76	263–473	0.1–49.8	–	0.055	–	–	–	–
Isobaric heat capacities									
Waddington and Douslin [151]	11	334–469	0.0–0.1	0.151	–	–	–	–	–
Second virial coefficients									
McGlashan and Potter [152]	11	318–398	–	1.547	–	–	–	–	–
Hajjar et al. [153]	3	403–453	–	0.912	–	–	–	–	–
Brostow et al. [125]	2	348–400	–	0.948	–	–	–	–	–
Rodriguez et al. [154]	1	298	–	0.324	–	–	–	–	–

Authors	No of data	Temp. range T (K)	Average absolute deviations (AAD), % $T/T_c < 0.6$	$0.6 \leqslant T/T_c \leqslant 0.98$	$T/T_c > 0.98$
Vapor pressures[c]					
Willingham et al. [138]	16	286–343	0.120	0.012	–
Mousa [155]	10	485–508	–	0.159	0.085
Wieczorek and Stecki [156]	10	298–343	0.194	0.028	–
Wolff et al. [157]	8	223–293	0.295	–	–
Wolff and Shadiakhy [158]	9	293–373	0.241	0.143	–
Weiguo et al. [159]	3	298–308	0.303	0.183	–
Sauermann et al. [143]	26	308–443	–	0.047	–
Saturated liquid densities					
Maciel and Francesconi [160]	1	293	0.026	–	–
Weiguo et al. [159]	1	298	0.008	–	–
Fenclova and Dohnal [161]	1	298	0.032	–	–
Sauermann et al. [143]	11	278–428	0.012	0.050	–
Enthalpies of vaporization					
Vesely et al. [162]	6	342–434	–	0.106	–

[a] LD: $\rho/\rho_c \leqslant 0.6$; MD: $0.6 < \rho/\rho_c < 1.5$; HD: $\rho/\rho_c \geqslant 1.5$.

[b] In the extended critical region, pressure deviations are given instead of density deviations.

[c] At temperatures $T/T_c < 0.6$, average absolute deviations in hPa are given.
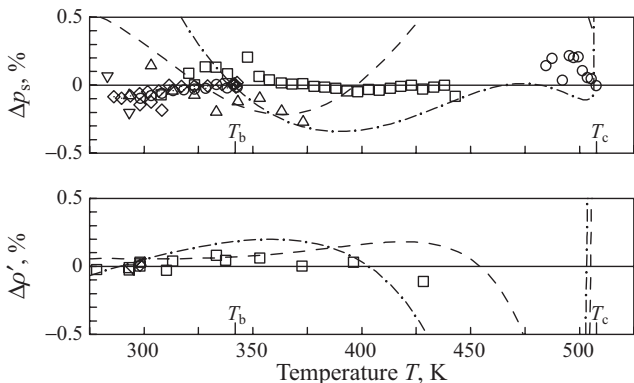
○ Mousa [155]   □ Sauermann et al. [143]
◇ Weiguo et al. [159]   ⊙ Wieczorek and Stecki [156]
◇ Willingham et al. [138]   ▽ Wolff et al. [157]
△ Wolff and Shadiakhy [158]   ⊠ Fenclova and Dohnal [161]
⬚ Maciel and Francesconi [160]

– – – Bender [142] equation, refitted
–··–··– Eq. (2), fitted to a data set including the data from Ref. [144]

Fig. 10. Percentage deviations $\Delta y, \% = 100(y_{exp} - y_{calc})/y_{exp}$ with $y = p_s$, ρ' between selected experimental results for normal hexane and values calculated from the new equation of state, Eq. (2). Values calculated from a Bender equation of state which was fitted to the same data set as Eq. (2) and from an equation which uses the functional form of Eq. (2) but which was fitted to a data set including the data by Abdulagatov et al. [144] are plotted for comparison.

but which was fitted to a data set including the data by Abdulagatov et al. [144]. The inconsistencies discussed above become obvious even when looking at the representation of thermal properties on the phase boundary.

3.8. Results for Normal Heptane

For normal heptane, accurate data on thermal and caloric properties are available from different authors in the liquid region from the triple-point temperature at $T_t \approx 182.6$ K $(T_t/T_c \approx 0.338)$ to 310 K. The most important data in this range are the $p\rho T$ and speed of sound data measured by Muringer et al. [163] and the isobaric heat capacity data derived by Sun et al. [164]. The data set used was restricted to pressures up to $p_{max} = 100$ MPa. At higher temperatures, no data were available for caloric properties while the $p\rho T$ data by Nichols et al. [165] still enabled a satisfactory description of liquid states. Again, the description of the gaseous phase had to rely on questionable data published for the second virial

coefficients. Vapor pressure data were available up to the critical temperature, but reliable data for the saturated liquid density were available only at ambient temperatures. Reliable data for the saturated vapor density were not available and no reliable data were available above $T_{\max} \approx 523$ K ($T_{\max}/T_c \approx 0.97$) when Eq. (2) was finalized. However, more recently a comprehensive set of isochoric heat capacities was made available by Abdulagatov [166]. The data set covers gaseous, liquid, and supercritical states at temperatures up to 693 K ($T/T_c \approx 1.28$). In Ref. 2, comparisons with these data were used as an argument for the good extrapolation behavior of Eq. (2). For data compilations see Refs. 132 and 133.

Table XII summarizes the selected data sets for normal heptane and gives percentage average absolute deviations between the selected experimental data and values calculated from Eq. (2). The new equation of state describes the reliable data sets well within the demanded uncertainties. This fact becomes obvious especially when looking at the representation of the $p\rho T$ and speed of sound data by Muringer et al. [163], of the isobaric heat capacities by Sun et al. [164], of the vapor pressures by Willingham et al. [138] and Weber [177], and of the saturated liquid densities by Romani et al. [181]. At supercritical states, the isochoric heat capacities by Abdulagatov et al. [166] are represented well within the demanded uncertainty, even though the corresponding data lie outside of the range where Eq. (2) was fitted to experimental data. Larger deviations in the extended critical region and at gaseous and liquid states close to the limits of the extended critical region had to be expected for simple technical equations of state. The saturated liquid heat capacities published by Zábranský and Růzicka [170] result from a reevaluation of older experimental data and were thus not considered as primary data. However, when comparing the new equation with these data, it became obvious that the saturated liquid heat capacities are very accurately predicted; see also Fig. 11. The limit of $|\Delta c_\sigma|/c_\sigma \leqslant 2\%$ is exceeded only slightly for three data points at $T \leqslant 190$ K, close to the triple-point temperature. At temperatures $T \geqslant 210$ K, saturated liquid heat capacities are predicted well within $|\Delta c_\sigma|/c_\sigma \leqslant 1\%$.

In calibration applications, normal heptane is used as a reference fluid for saturated liquid heat capacities and liquid densities around 700 kg·m^{-3}. With regard to densities, this reference status is justified at least for temperatures up to 311 K, where the $p\rho T$ surface is described by the data of Muringer et al. [163]. If an uncertainty of $|\Delta\rho|/\rho \leqslant 0.1\%$ is sufficient, Eq. (2) can be used as a reference for calibrations in this region. At higher temperatures, the scatter of the available data increases; see Fig. 12. Since no widely accepted reference equation of state is available for normal heptane, a Bender equation of state [142] was again fitted to the same data set as Eq. (2) for comparison.

Table XII. Summary of the Data Sets Selected for Normal Heptane and Average Absolute Deviations Between Values Calculated from the New Equation of State and the Selected Data

Authors	No. of data	Temperature and pressure range T (K)	p (MPa)	Gas	Liq.	Crit. reg.	Supercritical fluid LD[a]	MD[a]	HD[a]
$p\rho T$ data[b]									
Smith et al. [167]	45	303–523	0.7–35.6	–	0.184	–	–	–	–
Nichols et al. [165]	273	278–511	0.1–69.1	–	0.116	–	–	–	–
Kuss and Taslimi [147]	12	298–353	0.1–78.5	–	0.112	–	–	–	–
Muringer et al. [163]	89	198–311	0.1–91.2	–	0.037	–	–	–	–
Toscani et al. [168]	96	298–373	0.1–100	–	0.254	–	–	–	–
Susnar et al. [150]	51	294	0.1–34.6	–	0.081	–	–	–	–
Isochoric heat capacities									
Abdulagatov [166]	395[c]	375–693	0.1–19.1	2.156	1.852	3.353	0.774	0.702	0.752
Speeds of sound									
Muringer et al. [163]	46	186–311	0.1–81.0	–	0.442	–	–	–	–
Isobaric/saturated liquid heat capacities									
Sun et al. [164]	48	205–310	0.0–100	–	0.400	–	–	–	–
Osborne and Ginnings [169]	9	278–318	Sat. liq.	–	0.130	–	–	–	–
Zábranský and Růžicka [170]	53[c]	183–480	Sat. liq.	–	0.416	–	–	–	–
Enthalpy differences									
Castro-Gomez et al. [171]	11	235–367	0.9–1.2	–	0.547	–	–	–	–
Second virial coefficients									
Hirschfelder et al. [172]	4	548–623	–	2.983	–	–	–	–	–
McGlashan and Potter [152]	10	349–414	–	1.550	–	–	–	–	–
Hajjar et al. [153]	7	353–473	–	1.710	–	–	–	–	–

Authors	No of data	Temp. range T (K)	$T/T_c < 0.6$	$0.6 \leqslant T/T_c \leqslant 0.98$	$T/T_c > 0.98$
Vapor pressures[d]					
Mair [137]	1	372	–	0.089	–
Beattie and Kay [173]	8	540	–	–	0.019
Willingham et al. [138]	40	299–372	0.138	0.037	–
Forziati et al. [174]	20	299–372	0.148	0.048	–
Cook [175]	3	273–308	0.210	–	–
McMicking [176]	7	523–540	–	0.122	0.159
McMicking and Kay [12]	19	372–540	–	0.116	0.192
Carruth and Kobayashi [83]	9	185–285	0.174	–	–
Weber [177]	27	335–503	–	0.089	–
Saturated liquid densities					
Bravo et al. [178]	1	298	0.001	–	–
de la Fuente et al. [179]	1	298	0.001	–	–
Pittau et al. [180]	1	298	0.006	–	–
Romani et al. [181]	4	278–308	0.005	–	–

[a] LD: $\rho/\rho_c \leqslant 0.6$; MD: $0.6 < \rho/\rho_c < 1.5$; HD: $\rho/\rho_c \geqslant 1.5$.
[b] In the extended critical region, pressure deviations are given instead of density deviations.
[c] Data used only for comparison.
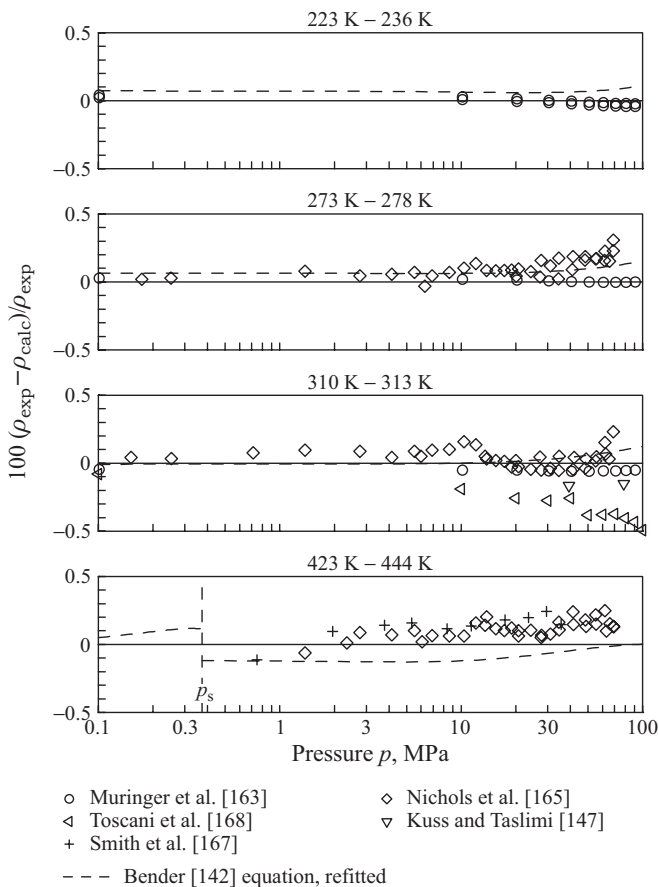[d] At temperatures $T/T_c < 0.6$, average absolute deviations in hPa are given.
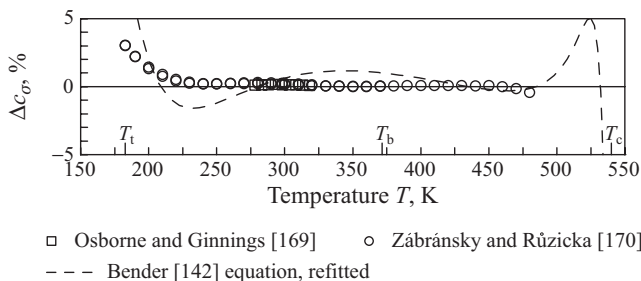
Fig. 11. Percentage deviations $\Delta c_\sigma, \% = 100(c_{\sigma,\,exp} - c_{\sigma,\,calc})/c_{\sigma,\,exp}$ between selected experimental results for the saturated liquid heat capacity of normal heptane and values calculated from the new equation of state, Eq. (2). Values calculated from a Bender equation of state which was fitted to the same data set as Eq. (2) are plotted for comparison.

3.9. Results for Normal Octane

When Eq. (2) was finalized, the data situation was satisfactory for normal octane in the liquid region at temperatures from 258 to 373 K. At higher temperatures, no data for caloric properties were available, and the only set of reasonable $p\rho T$ data scatters by more than $|\Delta\rho|/\rho = 0.2\%$. The $p\rho T$ data which were measured recently by Abdulagatov et al. [144] at $T \approx 623$ K ($T/T_c \approx 1.09$) were not selected. Equations which were fitted to data sets containing these data could not satisfactorily represent data at lower temperatures—the results published by Abdulagatov et al. [144] seem to be inconsistent with other data sets; see also Section 3.7. Accurate data for the vapor pressure were available at temperatures above 350 K, and the saturated liquid density was described with sufficient accuracy between 245 and 475 K. Sufficiently accurate data for the saturated vapor density were not available. The highest temperature for which data could be used was $T_{max} \approx 548$K ($T_{max}/T_c \approx 0.96$) and the highest pressure was $p_{max} \approx 96$MPa. Recently, a comprehensive set of data for the isochoric heat capacity of normal octane which covers the temperature range $0.78 \leqslant T/T_c \leqslant 1.22$ has been made available by Abdulagatov [166]. These data have only been used for comparisons again and were used in Ref. 2 as an argument for the good extrapolation behavior of Eq. (2).

Table XIII summarizes the selected data sets for normal octane and gives percentage average absolute deviations between the selected experimental data and values calculated from Eq. (2). The selected data are described either within the demanded accuracy or within their experimental uncertainties. At supercritical states, predicted isochoric heat capacities

Legend:
- ○ Muringer et al. [163]
- ◁ Toscani et al. [168]
- + Smith et al. [167]
- ◇ Nichols et al. [165]
- ▽ Kuss and Taslimi [147]
- – – – Bender [142] equation, refitted

Fig. 12. Percentage deviations between selected experimental results for the density of normal heptane and values calculated from the new equation of state, Eq. (2). Values calculated from a Bender equation of state which was fitted to the same data set as Eq. (2) are plotted for comparison.

again agree with the data by Abdulagatov et al. [166] well within the demanded uncertainty. Larger deviations in the extended critical region had to be expected for simple technical equations of state. As an example of the performance of the new equation of state, Fig. 13 shows deviations between experimental results for the isobaric heat capacity of liquid normal octane and values calculated from Eq. (2). Since no widely accepted reference equation of state is available for normal octane, a Bender equation of state [142] was fitted to the same data set as Eq. (2) for comparison.

Table XIII.   Summary of the Data Sets Selected for Normal Octane and Average Absolute Deviations Between Values Calculated from the New Equation of State and the Selected Data

Authors	No. of data	Temperature and pressure range		Average absolute deviations (AAD), %					
		T (K)	p (MPa)	Gas	Liq.	Crit. reg.	Supercritical fluid LD[a]	MD[a]	HD[a]
$p\rho T$ data[b]									
Felsing and Watson [182]	87	373–548	0.5–30.4	–	0.289	–	–	–	–
Benson and Winnick [183]	56	258	0.1–96.4	–	0.090	–	–	–	–
Banipal et al. [184]	66	318–373	0.1–10.0	–	0.077	–	–	–	–
Dix et al. [185]	22	299–323	0.1–90.1	–	0.092	–	–	–	–
Tanaka et al. [186]	13	298–348	0.1–80.3	–	0.126	–	–	–	–
Goodwin et al. [187]	14	298–303	0.7–32.6	–	0.072	–	–	–	–
Isochoric heat capacities									
Abdulagatov [166]	399[c]	443–693	0.3–26.2	1.476	0.700	2.807	0.495	0.630	1.045
Isobaric/saturated liquid heat capacities									
Banipal et al. [184]	60	318–373	0.1–10.0	–	0.216	–	–	–	–
Osborne and Ginnings [169]	6	283–308	Sat. liq.	–	0.158	–	–	–	–
Second virial coefficients									
McGlashan and Potter [152]	10	373–414	–	1.148	–	–	–	–	–

Authors	No of data	Temp. range T (K)	Average absolute deviations (AAD), %		
			$T/T_c < 0.6$	$0.6 \leqslant T/T_c \leqslant 0.98$	$T/T_c > 0.98$
Vapor pressures[d]					
Felsing and Watson [182]	4	423–548	–	0.236	–
Willingham et al. [138]	29	326–400	0.442	0.123	–
Cook [175]	3	273–308	0.117	–	–
McMicking and Kay [12]	18	399–563	–	0.094	0.065
Carruth and Kobayashi [83]	8	217–278	0.046	–	–
Gregorowicz et al. [188]	15	359–393	–	0.056	–
Weiguo et al. [159]	2	298–303	0.166	–	–
Saturated liquid densities					
McMicking and Kay [12]	16	403–553	–	0.263	–
Chappelow et al. [189]	30	246–390	0.061	0.033	–
Lopez Alanon et al. [190]	1	298	0.044	–	–
Weiguo et al. [159]	1	298	0.033	–	–
Kumar et al. [191]	2	303	0.044	–	–

[a] LD: $\rho/\rho_c \leqslant 0.6$; MD: $0.6 < \rho/\rho_c < 1.5$; HD: $\rho/\rho_c \geqslant 1.5$.
[b] In the extended critical region, pressure deviations are given instead of density deviations.
[c] Data used only for comparison.
[d] At temperatures $T/T_c < 0.6$, average absolute deviations in hPa are given.
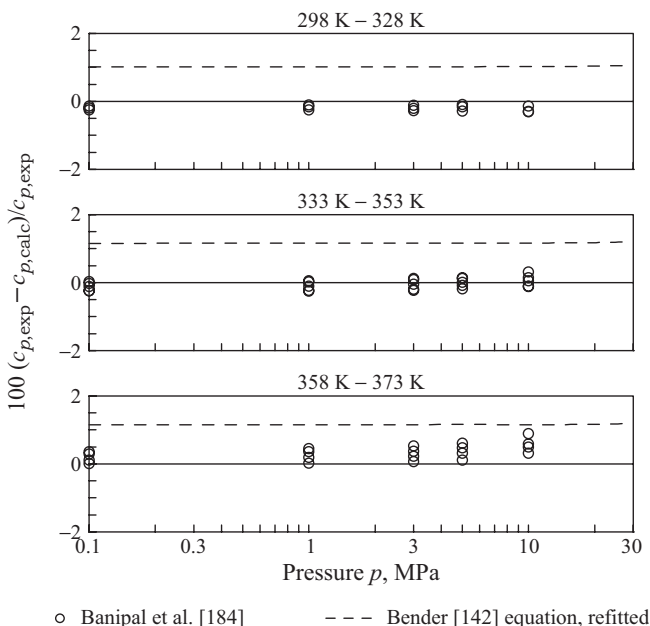
Fig. 13. Percentage deviations between selected experimental results for the isobaric heat capacity of normal octane and values calculated from the new equation of state, Eq. (2). Values calculated from a Bender equation of state which was fitted to the same data set as Eq. (2) are plotted for comparison.

3.10. Results for Argon

The data set which is available for argon was recently described in detail by Tegeler et al. [13]. The selected data set covers fluid states from the triple-point temperature at $T_t \approx 83.8$ K ($T_t/T_c \approx 0.556$) to a temperature of $T_{max} \approx 520$ K ($T_{max}/T_c \approx 3.45$) at pressures up to $p_{max} = 100$ MPa. Data which describe thermal and caloric properties on the vapor-liquid phase boundary are available from the triple-point temperature to the critical temperature including the highly accurate data published by Gilgen et al. [192]. With regard to thermal properties, the quality of the available data set has significantly been improved by the results of Gilgen et al. [193] and Klimeck et al. [194]. The publications of Estrada-Alexanders and Trusler [195, 196] greatly improved the information available for caloric properties at gaseous states. Table XIV summarizes the selected data sets for argon and gives percentage average absolute deviations between the selected experimental data and values calculated from Eq. (2).

Table XIV. Summary of the Data Sets Selected for Argon and Average Absolute Deviations Between Values Calculated from the New Equation of State and the Selected Data

Authors	No. of data	Temperature and pressure range		Average absolute deviations (AAD), %					
		T (K)	p (MPa)	Gas	Liq.	Crit. reg.	LD[a]	MD[a]	HD[a]
***p ρ T* data**[b]									
Michels et al. [197]	153	273–423	26.1–98.6	–	–	–	0.104	0.208	0.113
Barreiros et al. [198][c]	46	129–147	15.8–99.5	–	0.039	–	–	–	–
Biswas et al. [199]	1	298	100.0	–	–	–	–	–	0.297
Hoinkis [200]	6	298	21.9–58.2	–	–	–	–	0.087	–
Gilgen et al. [193]	638	90–340	0.2–12.1	0.036	0.062	0.071	0.028	0.101	0.062
Estrada-Alexanders and Trusler [196]	565[d]	110–450	0.0–27.2	0.032	–	–	0.025	–	–
Klimeck et al. [194]	237	235–520	2.0–30.1	–	–	–	0.034	0.081	–
Isochoric heat capacities									
Gladun [201]	82	88–151	1.4–11.5	–	1.602	0.730	–	–	–
Anisimov et al. [202]	57	152–263	5.2–26.6	–	–	2.118	–	2.565	–
Anisimov et al. [203]	306	134–267	2.6–41.6	6.147	1.852	8.648	0.898	1.583	0.965
Estrada-Alexanders and Trusler [196]	565[d]	110–450	0.0–27.2	1.214	–	–	0.369	–	–
Speeds of sound									
Radoviskii [204]	25	84–147	Sat. vap.	1.193	–	–	–	–	–
Aziz et al. [205]	14	84–146	Sat. liq.	–	1.049	–	–	–	–
Bowman et al. [206]	46	86–147	0.4–6.6	–	0.680	–	–	–	–
Pitaevskaya et al. [207]	25	323–423	50–100	–	–	–	–	0.894	0.500
Thoen et al. [208]	6	100–145	Sat. liq.	–	1.196	–	–	–	–
Thoen et al. [209]	18	110–148	Sat. vap.	1.746	–	–	–	–	–
Streett and Costantino [210]	137	90–160	0.3–99.3	–	0.779	–	–	–	0.578
Kachanov et al. [211]	2	373–423	100.0	–	–	–	–	0.188	0.504
Kortbeek et al. [212]	6	173–298	100.0	–	–	–	–	–	0.913
Boyes [76]	151	252–350	0.1–10.2	–	–	–	0.069	–	–
Ewing and Goodwin [213]	50	255–300	0.1–7.0	–	–	–	0.069	–	–
Estrada-Alexanders and Trusler [195]	225	110–450	0.0–19.3	0.365	–	–	0.143	–	–
Second virial coefficients									
Tegeler et al. [13]	15	120–340	–	0.623	–	–	–	–	–

Authors	No of data	Temp. range T (K)	Average absolute deviations (AAD), %		
			$T/T_c < 0.6$	$0.6 \leqslant T/T_c \leqslant 0.98$	$T/T_c > 0.98$
Vapor pressures[e]					
Gilgen et al. [192]	47	84–151	1.379	0.075	0.054
Saturated liquid densities					
Gilgen et al. [192]	27	84–151	0.089	0.048	0.398
Saturated vapor densities					
Gilgen et al. [192]	23	84–151	0.250	0.155	1.653
Tegeler et al. [13]	28	84–110	0.225	0.074	–

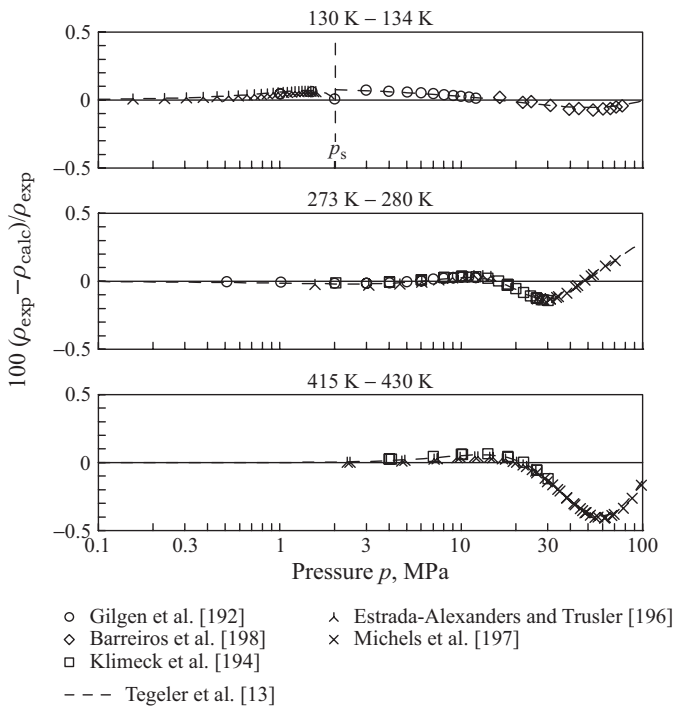[a] LD: $\rho/\rho_c \leqslant 0.6$; MD: $0.6 < \rho/\rho_c < 1.5$; HD: $\rho/\rho_c \geqslant 1.5$.

[b] In the extended critical region, pressure deviations are given instead of density deviations.

[c] The data of Barreiros et al. [198] were adjusted according to Tegeler et al. [13].

[d] Data calculated from speed of sound measurements.

[e] At temperatures $T/T_c < 0.6$, average absolute deviations in hPa are given.

Fig. 14. Percentage deviations between selected experimental results for the density of argon and values calculated from the new equation of state, Eq. (2). Values calculated from the reference equation of state by Tegeler et al. [13] are plotted for comparison.

In general, the new equation of state describes the selected data set within the uncertainties claimed in Table IV. Figure 14 shows deviations between accurate experimental results for the density of argon and values calculated from the new equation of state. Values calculated from the recent reference equation by Tegeler et al. [13] are included for comparison. At high temperatures and pressures, the observed absolute deviations exceed 0.2%, but they remain within the limit of $|\Delta\rho|/\rho \leqslant 0.5\%$ which is claimed for pressures above 30 MPa. For speeds of sound at low temperature liquid states, the limit of $|\Delta w|/w = 2\%$ is exceeded at $p \approx 60$ MPa, with maximum deviations of $\Delta w/w \approx -3\%$ at $p = 100$ MPa. However, at higher temperatures, speed of sound data are represented well within the claimed uncertainty; see Fig. 15.
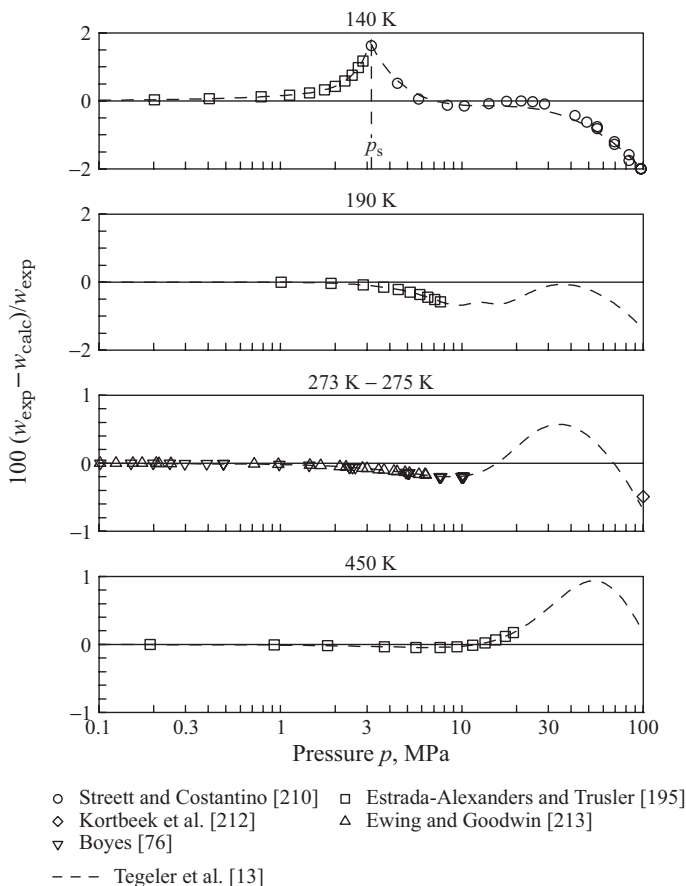
Fig. 15. Percentage deviations between selected experimental results for the speed of sound in argon and values calculated from the new equation of state, Eq. (2). Values calculated from the reference equation of state by Tegeler et al. [13] are plotted for comparison.

3.11. Results for Oxygen

At pressures up to $p_{max} \approx 92\,\text{MPa}$, the data set available for oxygen covers a temperature range from close to the triple-point temperature at $T_t \approx 54.4\,\text{K}$ ($T_t/T_c \approx 0.352$) to $T_{max} \approx 303\,\text{K}$ ($T_{max}/T_c \approx 1.96$). The available experimental data are at least 20 years old and are clearly less accurate than recent reference data, which are available, e.g., for fluids like nitrogen or argon. However, for the development of an equation of state for technical applications, the data situation is very satisfactory both with regard

Table XV. Summary of the Data Sets Selected for Oxygen and Average Absolute Deviations Between Values Calculated from the New Equation of State and the Selected Data

Authors	No. of data	Temperature and pressure range		Average absolute deviations (AAD), %					
		T (K)	p (MPa)	Gas	Liq.	Crit. reg.	LD[a]	MD[a]	HD[a]
$p\rho T$ data[b]									
Weber [215]	1452	56–300	0.2–36.2	0.114	0.033	0.066	0.037	0.063	0.052
Weber [216]	346	58–300	3.6–81.8	–	0.097	–	–	0.073	0.161
Pentermann and Wagner [217]	320	68–301	0.0–7.1	0.101	0.082	0.068	0.069	0.415	–
Isochoric heat capacities									
Goodwin and Weber [218]	150	56–284	2.1–35.5	–	0.586	5.701	1.542	0.589	0.133
Speeds of sound									
van Itterbeek and Zink [219]	93	232–303	0.1–7.0	–	–	–	0.263	–	–
van Itterbeek and van Dael [220]	16	90	0.4–7.2	–	1.077	–	–	–	–
van Itterbeek and van Dael [221]	101	68–90	0.2–92.2	–	1.376	–	–	–	–
Straty and Younglove [222]	117	70–300	2.8–34.7	–	0.749	0.589	0.174	0.494	0.723

Authors	No of data	Temp. range T (K)	Average absolute deviations (AAD), %		
			$T/T_c < 0.6$	$0.6 \leqslant T/T_c \leqslant 0.98$	$T/T_c > 0.98$
Vapor pressures[c]					
Anscin [223]	59	55–90	0.200	–	–
Wagner et al. [224]	166	93–155	–	0.095	0.104
Saturated liquid densities					
Lisman and Keesom [225][d]	9	67–117	0.033	0.010	–
Weber [215]	23	120–153	–	0.019	0.297
Saturated vapor densities					
Pool et al. [226][d]	8	85–90	0.328	–	–
Anscin [223][d]	8	68–91	0.309	–	–
Pentermann and Wagner [217]	20	99–154	–	0.077	0.754

[a] LD: $\rho/\rho_c \leqslant 0.6$; MD: $0.6 < \rho/\rho_c < 1.5$; HD: $\rho/\rho_c \geqslant 1.5$.
[b] In the extended critical region, pressure deviations are given instead of density deviations.
[c] At temperatures $T/T_c < 0.6$, average absolute deviations in hPa are given.
[d] Data calculated from experimental results for different properties; see Wagner and de Reuck [214].

to thermal and caloric properties in the homogeneous region and on the vapor-liquid phase boundary. The IUPAC book by Wagner and de Reuck [214] contains a comprehensive review of the available data sets. Table XV summarizes the data sets selected in this project and gives percentage average absolute deviations between the selected experimental data and values calculated from the new equation of state, Eq. (2).

In general, the new equation of state describes the selected data set well within the claimed uncertainties. Figure 16 shows deviations between experimental results for the isochoric heat capacity of oxygen and values
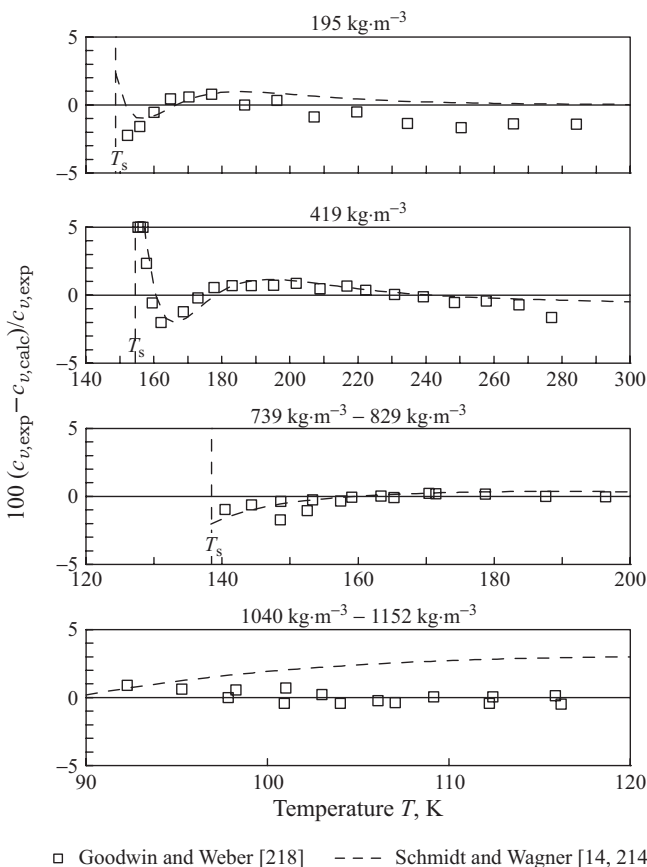
Fig. 16. Percentage deviations between selected experimental results for the isochoric heat capacity of oxygen and values calculated from the new equation of state, Eq. (2). Values calculated from the reference equation of state by Schmidt and Wagner [14, 214] are plotted for comparison.

calculated from Eq. (2). Deviations which exceed the limit of $\pm 2\%$ are observed only in the extended critical region, where simple technical equations of state cannot be expected to yield an accurate representation of isochoric heat capacities. For gaseous states, where the available experimental data show a considerable scatter, results calculated from the reference equation by Schmidt and Wagner [14, 214] and from Eq. (2) agree with each other much better than with the experimental data. Again, larger deviations occur for speeds of sound at low temperature liquid states,

where the limit of $|\Delta w|/w = 2\%$ is exceeded at $p \approx 60$ MPa. However, compared to existing technical equations of state, maximum deviations of $\Delta w/w \approx -3\%$ at $p \approx 90$ MPa are still very good. Fitted to the same data set, a Bender equation [142] results in deviations which are about twice as large.

Table XVI. Summary of the Data Sets Selected for Nitrogen and Average Absolute Deviations Between Values Calculated from the New Equation of State and the Selected Data

| Authors | No. of data | Temperature and pressure range | | Average absolute deviations (AAD), % | | | | | |
		T (K)	p (MPa)	Gas	Liq.	Crit. reg.	LD[a]	MD[a]	HD[a]
$p\rho T$ **data**[b]									
Michels et al. [235]	109	273–423	19.5–100	–	–	–	–	0.266	0.071
Saurel [236]	68	573–1074	1.0–91.2	–	–	–	0.153	0.784	–
Straty and Diller [237]	287	80–300	0.8–34.8	–	0.067	0.080	–	0.094	0.068
Duschek et al. [238]	127	273–323	0.5–8.0	–	–	–	0.025	–	–
Jaeschke and Humpreys [70]	94	279–308	3.7–6.7	–	–	–	0.038	–	–
Jaeschke and Hinze [36][c]	129	273–353	0.2–30.2	–	–	–	0.029	0.133	–
Jaeschke and Hinze [36][d]	499	269–353	0.2–28.7	–	–	–	0.041	0.130	–
Pieperbeck et al. [37]	124	273–323	0.1–12.1	–	–	–	0.041	–	–
Fenghour et al. [239]	50	290–680	3.5–37.0	–	–	–	0.106	–	–
Nowak et al. [227]	920	66–340	0.1–12.0	0.021	0.045	0.050	0.038	0.112	0.042
Klimeck et al. [228]	264	240–520	1.1–30.1	–	–	–	0.056	0.160	–
Isochoric heat capacities									
Weber [240]	61	91–242	1.7–33.2	–	0.847	2.459	–	0.596	0.490
Magee [232]	173	66–307	3.1–33.7	–	1.672	2.278	0.806	0.732	0.626
Speeds of sound									
Dobbs and Finegold [241]	29	77–90	0.3–13.6	–	0.377	–	–	–	–
van Itterbeek and van Dael [242]	44	77–90	0.4–19.7	–	0.548	–	–	–	–
van Itterbeek and van Dael [221]	91	64–91	0.1–97.0	–	1.827	–	–	–	–
Vassermann and Selevanyuk [243]	78	500–1001	0.1–100	–	–	–	0.370	0.638	–
Younglove and McCarty [244]	237	80–350	0.0–1.5	0.329	–	–	0.054	–	–
Kortbeek et al. [245]	16	123–298	85.0–100	–	2.915	–	–	–	1.242
Boyes [76]	112	250–325	0.1–6.6	–	–	–	0.053	–	–
Ewing and Trusler [230]	100	80–373	0.0–0.6	0.026	–	–	0.004	–	–
Costa Gomes and Trusler [231]	72	250–350	0.0–30.1	–	–	–	0.062	0.478	–
Isobaric/saturated liquid heat capacities									
Mage et al. [246]	20	172–274	1.0–13.8	–	–	–	0.354	0.177	–
Magee [232]	102	65–121	Sat. liq.	–	0.536	–	–	–	–
Enthalpy differences									
Grini and Owren [233]	19	160–270	0.3–15.0	–	–	–	0.233	0.378	–
Second virial coefficients									
Nowak et al. [227]	29	98–340	–	1.070	–	–	–	–	–
Duschek et al. [238]	6	273–323	–	2.656	–	–	–	–	–
Ewing and Trusler [230]	14	75–700	–	2.051	–	–	–	–	–

Table XVI.   *(Continued)*

Authors	No of data	Temp. range T (K)	Average absolute deviations (AAD), %		
			$T/T_c < 0.6$	$0.6 \leqslant T/T_c \leqslant 0.98$	$T/T_c > 0.98$
Vapor pressures[e]					
Nowak et al. [229]	58	63–126	0.470	0.098	0.039
Saturated liquid densities					
Nowak et al. [229]	52	64–126	0.065	0.046	0.180
Saturated vapor densities					
Nowak et al. [229]	51	63–126	0.277	0.050	1.288

[a] LD: $\rho/\rho_c \leqslant 0.6$; MD: $0.6 < \rho/\rho_c < 1.5$; HD: $\rho/\rho_c \geqslant 1.5$.

[b] In the extended critical region, pressure deviations are given instead of density deviations.

[c] Burnett measurements.

[d] Refractive index measurements.

[e] At temperatures $T/T_c < 0.6$, average absolute deviations in hPa are given.

3.12. Results for Nitrogen

In terms of reduced properties, the data set which is available for nitrogen covers by far the broadest range of temperatures. At pressures up to $p_{max} = 100$ MPa, data were used for temperatures from the triple-point temperature at $T_t \approx 63.2$ K $(T_t/T_c \approx 0.500)$ to $T_{max} \approx 1074$ K $(T_{max}/T_c \approx 8.51)$. Most of the available data sets describe supercritical states, but for gaseous, critical, and liquid states highly accurate data are available as well. The state-of-the-art data sets that are most important for the development of an accurate equation of state include the density data measured by Nowak et al. [227] and Klimeck et al. [228], the vapor pressures and saturation densities by Nowak et al. [229], the speeds of sound by Boyes [76], Ewing and Trusler [230], and Costa Gomes and Trusler [231], the isochoric heat capacities by Magee [232], and the enthalpy differences measured by Grini and Owren [233]. Caloric properties on the vapor-liquid phase boundary are also well known. A recent review of the available data set was published by Span et al. [234]. Table XVI summarizes the selected data sets and gives percentage average absolute deviations between the selected experimental data and values calculated from the new equation of state, Eq. (2).

In general, the new equation of state represents the data which are available for nitrogen within the demanded uncertainties. Figure 17 illustrates this fact using caloric properties at saturation as an example. The saturated liquid heat capacities (c_σ) by Magee [232] were included in the data set used to establish Eq. (2), but neither the plotted speeds of sound at saturated liquid states (w') nor the enthalpies of evaporation (Δh_v) were
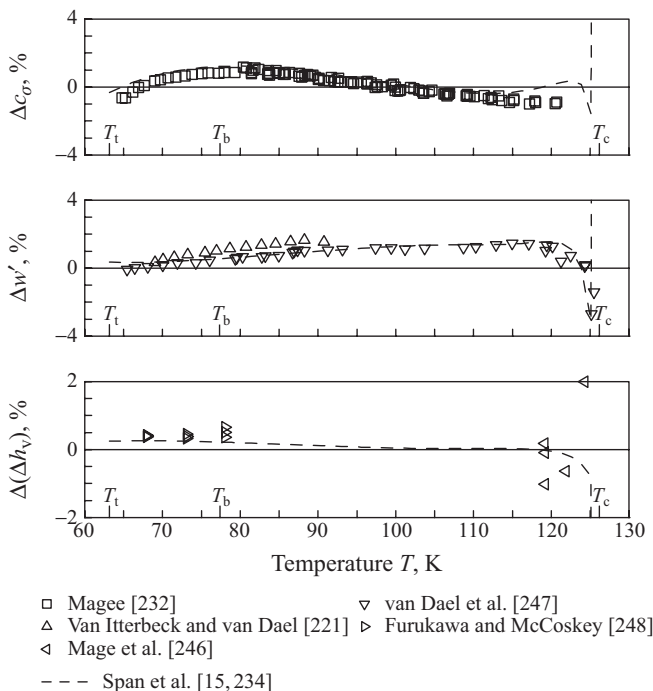
Fig. 17. Percentage deviations $\Delta y, \% = 100(y_{exp} - y_{calc})/y_{exp}$ with $y = c_\sigma$, w', Δh_v between selected experimental results for nitrogen and values calculated from the new equation of state, Eq. (2). Values calculated from the reference equation of state by Span et al. [15, 234] are plotted for comparison.

considered when fitting the new equation. Since accurate data are available for several properties of nitrogen, it was possible to use these data to test the consistency of the description of different properties.

Larger deviations occur again for speeds of sound at low temperature liquid states, where the limit of $|\Delta w|/w = 2\%$ is exceeded at $p \approx 30$ MPa with maximum deviations of $\Delta w/w \approx -4\%$ at $p = 100$ MPa. At temperatures of $T \gtrsim 500$ K ($T/T_c \gtrsim 4$) the deviations observed for $p\rho T$ data exceed $|\Delta\rho|/\rho = 0.5\%$ at $p \approx 50$ MPa with maximum deviations up to $|\Delta\rho|/\rho \approx 1\%$ at $p = 100$ MPa. This fact is illustrated in Fig. 18. No data have been used at such high reduced temperatures for any of the other substances and, based only on the data set for nitrogen, the representation of data in this region could not be improved in the simultaneous optimization process without affecting the overall performance of the resulting functional form;
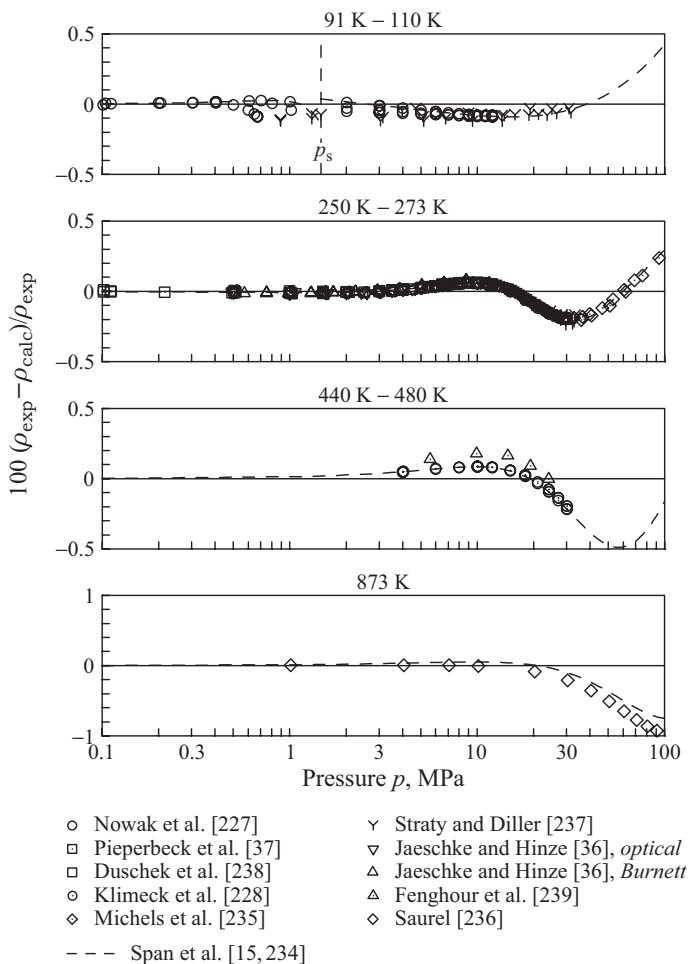
Fig. 18. Percentage deviations between selected experimental results for the density of nitrogen and values calculated from the new equation of state, Eq. (2). Values calculated from the reference equation of state by Span et al. [15, 234] are plotted for comparison.

see Ref. 2. Finally, nitrogen was excluded from the group of substances used in the simultaneous optimization and was used as an ambitious test for the transferability of the simultaneously optimized functional form. However, problems at extreme states should not obscure the fact that the new equation of state yields excellent results in the technically most important regions as shown in Figs. 17 and 18 and in Table XVI.

3.13. Results for Ethylene

For ethylene, reliable data are available from the triple-point temperature at $T_t \approx 104.0$ K ($T_t/T_c \approx 0.368$) to $T_{max} \approx 473$ K ($T_{max}/T_c \approx 1.68$) and the data set used was again restricted to $p_{max} = 100$ MPa. Highly accurate data are available for thermal properties in the homogeneous regions as well as at vapor-liquid equilibrium states. The experimental results for caloric properties show larger uncertainties and inconsistencies, but on the

Table XVII. Summary of the Data Sets Selected for Ethylene and Average Absolute Deviations Between Values Calculated from the New Equation of State and the Selected Data

Authors	No. of data	Temperature and pressure range T (K)	p (MPa)	Gas	Liq.	Crit. reg.	Supercritical fluid LD[a]	MD[a]	HD[a]
pρT data[b]									
Michels and Geldermans [253]	28	274–424	50.2–98.6	–	0.044	–	–	–	0.138
Turlington and McKetta [254]	10	243–303	0.1–0.2	0.075	–	–	0.013	–	–
Thomas and Zander [255]	42	273–323	0.3–3.0	0.048	–	–	0.033	–	–
Golovskii et al. [256]	87	200–307	1.4–59.5	–	0.077	–	–	–	0.093
Golovskii et al. [257]	107	199–324	5.7–99.9	–	0.048	–	–	–	0.040
Golovskii et al. [258]	114	106–232	1.2–59.8	–	0.074	–	–	–	–
Douslin and Harison [259]	634	238–448	1.3–39.6	0.060	0.129	0.052	0.055	0.142	0.094
Trappeniers et al. [260]	650	273–423	1.7–99.2	0.037	0.048	0.068	0.038	0.103	0.057
Hastings et al. [261]	138	279–303	4.7–8.4	–	–	0.046	–	–	–
Straty [262]	243	105–320	0.6–37.1	–	0.051	–	–	–	0.035
Thomas and Zander [263]	199	244–362	0.3–25.4	0.044	0.079	0.071	0.052	0.119	0.079
Levelt Sengers and Hastings [264]	60	223–273	0.2–3.5	0.017	–	–	–	–	–
Calado et al. [265]	412	140–240	0.0–99.2	–	0.068	–	–	–	–
Waxman [266]	111	273–448	0.2–3.6	0.013	–	–	0.037	–	–
Mollerup [267]	106	310	0.0–71.8	–	–	0.019	0.018	0.010	0.105
Achtermann et al. [268]	540	283–373	0.3–30.0	–	–	0.077	0.041	0.111	0.086
Achtermann et al. [269]	158	283–373	0.8–5.1	–	–	–	0.028	–	–
Nowak et al. [250]	800	104–340	0.0–12.1	0.069	0.040	0.043	0.034	0.105	0.035
Claus et al. [252]	87	235–370	2.0–30.1	–	0.074	–	0.034	0.080	0.037
Isochoric heat capacities									
Weber [270]	45	144–336	2.4–27.5	–	0.377	1.385	–	1.647	0.896
Speeds of sound									
Soldatenko and Dregulyas [271]	181	193–473	0.1–9.9	0.343	–	0.657	0.270	0.398	0.713
Gammon [272]	186	104–298	0.0–7.9	0.263	0.557	2.430	0.138	0.883	–
Mehl and Moldover [273]	24	273–373	0.1–1.0	0.010	–	–	0.010	–	–
Degrulyas and Stavtsev [274]	83	193–473	0.2–5.1	0.115	–	–	0.098	–	–
Dregulyas and Stavtsev [275]	106	193–282	0.2–59.1	0.244	0.382	1.587	–	–	–
Isobaric heat capacities									
Watanabe [276]	27	245–363	0.5–3.0	1.004	–	–	0.975	–	–
Second virial coefficients									
Bird et al. [277]	6	298–423	–	0.751	–	–	–	–	–
Trappeniers et al. [260]	13	273–423	–	0.685	–	–	–	–	–
Nowak et al. [250]	19	205–340	–	0.317	–	–	–	–	–

Table XVII. *(Continued)*

Authors	No of data	Temp. range T (K)	Average absolute deviations (AAD), %		
			$T/T_c < 0.6$	$0.6 \leqslant T/T_c \leqslant 0.98$	$T/T_c > 0.98$
Vapor pressures[c]					
Nowak et al. [251]	62	104–282	0.129	0.043	0.048
Saturated liquid densities					
Nowak et al. [251]	65	104–282	0.016	0.048	0.509
Saturated vapor densities					
Nowak et al. [251]	54	104–282	0.213	0.155	0.994

[a] LD: $\rho/\rho_c \leqslant 0.6$; MD: $0.6 < \rho/\rho_c < 1.5$; HD: $\rho/\rho_c \geqslant 1.5$.
[b] In the extended critical region, pressure deviations are given instead of density deviations.
[c] At temperatures $T/T_c < 0.6$, average absolute deviations in hPa are given.

level of accuracy required here the data situation is satisfactory. An extensive review of the data set which is available for ethylene was published by Jacobsen et al. [249]. A more recent review can be found in the article by Smukala et al. [16]. Important recent data sets are especially those of Nowak et al. [250, 251] and Claus et al. [252]. Table XVII summarizes the selected data sets and gives percentage average absolute deviations between the selected experimental data and values calculated from the new equation of state, Eq. (2).

The new equation of state for ethylene represents the available data within the demanded uncertainties without exception. Figure 19 illustrates this fact showing density deviations for selected $p\rho T$ data over a broad range of temperatures and pressures. For ethylene, accurate data for properties in the region of ambient temperatures and typical pipeline pressures are frequently needed in technical applications. Data calculated from simple equations of state, such as cubic equations of state or the BWR equation and its simple modifications, are very uncertain in this range, since pipelining conditions correspond to states in the extended critical region of ethylene ($T_c = 282.35$ K, $p_c = 5.042$ MPa). On the 306 to 310 K isotherm larger deviations become visible for the new equation as well, but the corresponding deviations in pressure stay within $\Delta p/p \approx \pm 0.1\%$ and are thus on an order which is typical for older reference equations of state and not for technical equations of state. However, for calculations with high demands on accuracy, the use of the recent reference equation by Smukala et al. [16] has to be recommended.

3.14. Results for Isobutane

For isobutane, experimental data are available from the triple-point temperature at $T_t \approx 113.6$ K ($T_t/T_c \approx 0.278$) to $T_{max} \approx 573$ K ($T_{max}/T_c \approx 1.41$)

Fig. 19. Percentage deviations between selected experimental results for the density of ethylene and values calculated from the new equation of state, Eq. (2). Values calculated from the reference equation of state by Smukala et al. [16] are plotted for comparison.

and up to pressures of $p_{max} \approx 35$ MPa. The accuracy of most of the data sets for thermal properties is poor, and reliable data for caloric properties are available only up to pressures of 1 MPa. With regard to caloric properties for liquid states, only rather old data for the heat capacity along the saturated liquid line have been published. Reliable information on

the density of the saturated vapor is available only in the critical region. A comprehensive review of the data which are available for isobutane was published by Goodwin and Haynes [278] in 1982. Important data sets published after the work of Goodwin and Haynes include the highly accurate speed of sound data by Ewing and Goodwin [280]. These data

Table XVIII. Summary of the Data Sets Selected for Isobutane and Average Absolute Deviations Between Values Calculated from the New Equation of State and the Selected Data

Authors	No. of data	Temperature and pressure range T (K)	p (MPa)	Average absolute deviations (AAD), %					
				Gas	Liq.	Crit. reg.	Supercritical fluid LD[a]	MD[a]	HD[a]
$p\rho T$ data[b]									
Das and Kuloor [281]	169	380–1501	0.1–10.1	0.175	0.203	–	0.087	–	–
Waxman [282]	85	378–448	0.3–20.8	0.095	–	0.124	0.040	0.183	0.070
Haynes [283]	156	120–300	1.7–34.7	–	0.071	–	–	–	–
Nieuwoudt et al. [279]	268	296–631	1.1–107	–	0.249	0.148	0.222	0.418	0.191
Speeds of sound									
Ewing and Goodwin [280]	79	251–320	0.0–0.1	0.010	–	–	–	–	–
Isobaric/saturated liquid heat capacities									
Parks et al. [284]	19	115–258	Sat. liq.	–	2.442	–	–	–	–
Aston et al. [285]	23	117–257	Sat. liq.	–	2.440	–	–	–	–
Ernst and Büsser [110]	21	293–353	0.1–0.8	0.142	–	–	–	–	–
Second virial coefficients									
Ewing and Goodwin [280]	8	251–320	–	0.741	–	–	–	–	–

Authors	No of data	Temp. range T (K)	Average absolute deviations (AAD), %		
			$T/T_c < 0.6$	$0.6 \leqslant T/T_c \leqslant 0.98$	$T/T_c > 0.98$
Vapor pressures[c]					
Aston et al. [285]	9	188–262	0.081	0.049	–
Connolly [286]	5	344–407	–	0.018	0.013
Steele et al. [287]	10	278–344	–	0.120	–
Martinez-Ortiz and Manley [288]	10	278–344	–	0.060	–
Weber [289]	3	344–394	–	0.039	–
Saturated liquid densities					
Carney [141]	19	245–323	–	0.034	–
Das and Kuloor [281]	13	261–390	–	0.067	–
McClune [90]	12	118–173	0.104	–	–
Haynes and Hiza [91]	12	115–300	0.066	0.114	–
Orrit and Laupretre [92]	36	129–249	0.043	0.045	–
Kaminishi et al. [290]	6	273–323	–	0.048	–
Saturated vapor densities					
Levelt Sengers et al. [291]	8	404–408	–	–	0.788

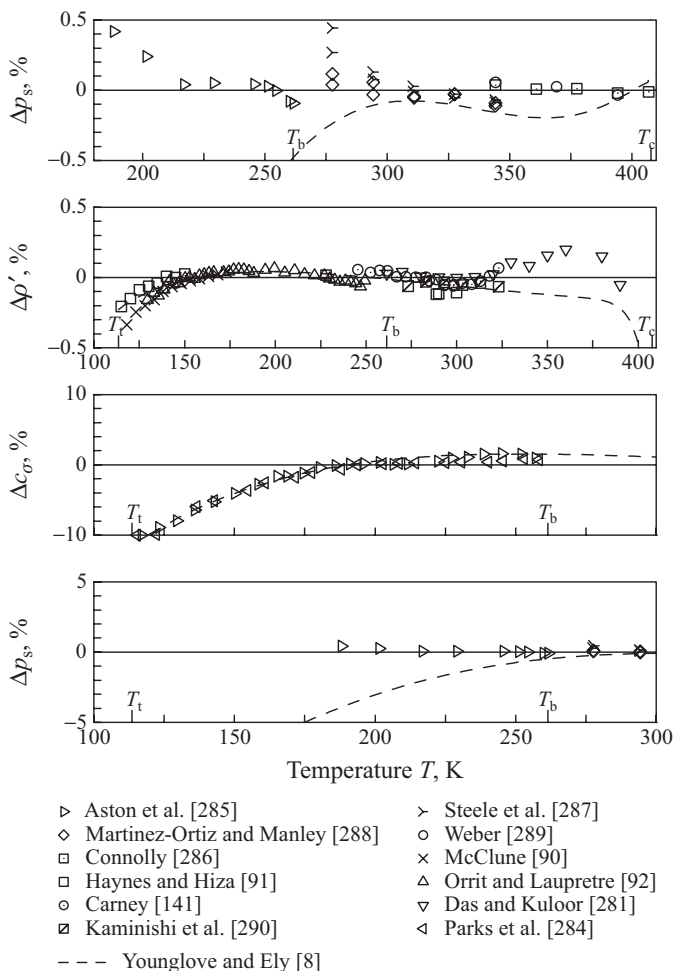[a] LD: $\rho/\rho_c \leqslant 0.6$; MD: $0.6 < \rho/\rho_c < 1.5$; HD: $\rho/\rho_c \geqslant 1.5$.
[b] In the extended critical region, pressure deviations are given instead of density deviations.
[c] At temperatures $T/T_c < 0.6$, average absolute deviations in hPa are given.

cover only gaseous states at pressures up to $p \approx 0.11$ MPa, but the derived virial coefficients yield important information on gaseous states at low and ambient temperatures. To extend the range of states covered by data, calculated $p\rho T$ data by Nieuwoudt et al. [279] and Das and Kuloor [281] were considered, which reach up to $T_{max} = 1501$ K ($T_{max}/T_c \approx 3.68$) and


> ▷ Aston et al. [285] ≻ Steele et al. [287]
> ◇ Martinez-Ortiz and Manley [288] ○ Weber [289]
> □ Connolly [286] × McClune [90]
> □ Haynes and Hiza [91] △ Orrit and Laupretre [92]
> ○ Carney [141] ▽ Das and Kuloor [281]
> ☒ Kaminishi et al. [290] ◁ Parks et al. [284]
>
> – – – Younglove and Ely [8]

Fig. 20. Percentage deviations $\Delta y,\% = 100(y_{exp} - y_{calc})/y_{exp}$ with $y = p_s$, ρ', c_σ between selected experimental results for properties on the phase boundary of isobutane and values calculated from the new equation of state, Eq. (2). Values calculated from the reference equation by Younglove and Ely [8] are plotted for comparison.

$p_{max} \approx 106$ MPa. Table XVIII summarizes the selected data sets and gives percentage average absolute deviations between the selected experimental data and values calculated from the new equation of state, Eq. (2).

In Ref. 2 a slightly increased weighted variance has been reported for the new equation of state for isobutane. This larger variance is caused by two major inconsistencies in the data set. Figure 20 illustrates the representation of thermal and caloric properties on the phase boundary of isobutane. Vapor pressures and saturated liquid densities are satisfactorily represented, but at low temperatures deviations up to $\Delta c_\sigma / c_\sigma \approx -10\%$ are observed for the heat capacity of the saturated liquid. Figure 21 highlights this effect in an absolute plot over the reduced temperature. The experimental data which are available for the saturated liquid heat capacity of isobutane give an almost straight line down to the triple-point temperature. For fluids for which more reliable experimental data are available such as normal butane, a flattening of the curve is observed at low reduced temperatures. However, at reduced temperatures below $T/T_c \approx 0.4$ ($T \lesssim 165$ K), Eq. (2) overemphasizes this tendency and results in a minimum in the saturated liquid heat capacity. Preliminary equations which more closely followed the experimental data for the saturated liquid heat capacity could not represent vapor pressures around the normal boiling temperature, just like the MBWR-type equation by Younglove and Ely [8]; see the first deviation diagram in Fig. 20. Most likely, the true shape lies somewhere in between, but without reliable experimental data both for the vapor pressure
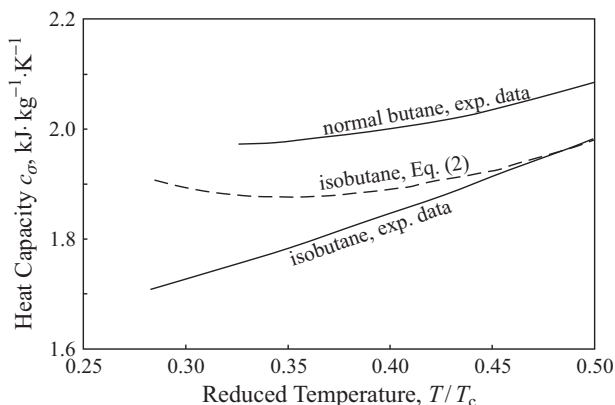
Fig. 21. Plots of the saturated liquid heat capacity versus the reduced temperature which result from experimental data for isobutane and normal butane and from Eq. (2) for isobutane.
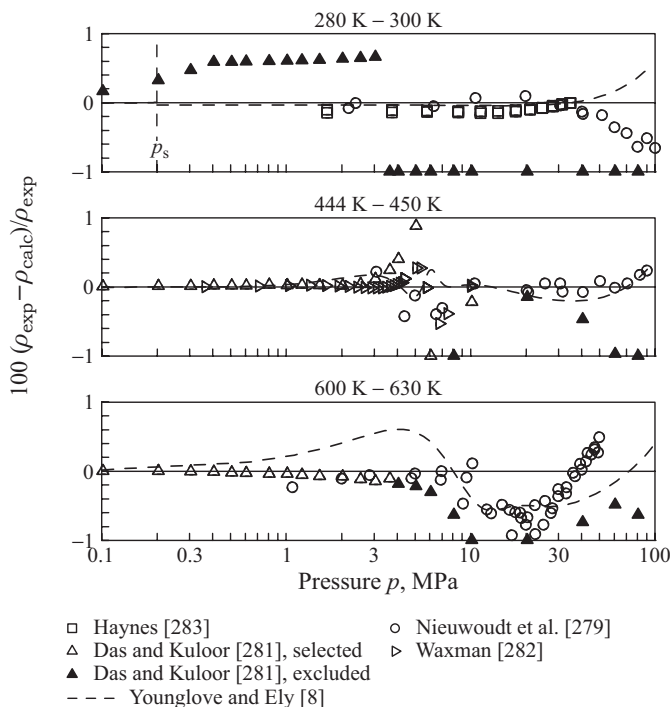
Fig. 22. Percentage deviations between selected experimental results for the density of isobutane and values calculated from the new equation of state, Eq. (2). Values calculated from the reference equation by Younglove and Ely [8] are plotted for comparison.

and for the saturated liquid heat capacity at low temperatures, no satisfactory solution could be found.

For high pressure liquid states and in particular for supercritical states, inconsistencies are observed between the data calculated by Nieuwoudt et al. [279] and other selected $p\rho T$ data sets. These inconsistencies could be reduced by excluding a part of the data calculated by Das and Kuloor [281], but the scatter of the selected data still exceeds the demands formulated on the accuracy of $p\rho T$ data; see Fig. 22 and Table IV. Without affecting the representation of more reliable data, the representation of the calculated $p\rho T$ data by Nieuwoudt et al. could not be improved. A comparison of the plots of the equation of Younglove and Ely [8] and of the new equation of state proves that a consistent description of calculated high temperature data and accurate experimental data at lower temperatures is obviously impossible. Even though reduced weights were applied, these inconsistencies led to a further increase of the weighted variance. To

Table XIX. Summary of the Data Sets Selected for Cyclohexane and Average Absolute Deviations Between Values Calculated from the New Equation of State and the Selected Data

Authors	No. of data	Temperature and pressure range T (K)	p (MPa)	Gas	Liq.	Crit. reg.	LD[a]	MD[a]	HD[a]
$p\rho T$ data[b]									
Rastorguev et al. [292]	136	298–473	0.1–85.4	–	0.058	–	–	–	–
Bich et al. [293]	38	372–621	0.1–0.2	0.029	–	–	0.032	–	–
Sun et al. [294]	52	288–323	0.1–30.0	–	0.014	–	–	–	–
Isochoric heat capacities									
Moelwyn-Hughes and Thorpe [295]	19	280–333	0.4–62.9	–	0.856	–	–	–	–
Asenbaum and Wilhelm [296]	7	283–343	0.2–1.6	–	0.357	–	–	–	–
Speeds of sound									
Wilhelm et al. [297]	3	293–313	Sat. liq.	–	0.127	–	–	–	–
Prakash and Srivastav [298]	1	308	Sat. liq.	–	0.683	–	–	–	–
Takagi [299]	39	283–333	0.1–107	–	0.212	–	–	–	–
Kiyohara al. [300]	1	298	0.1	–	0.181	–	–	–	–
Nath and Narain [301]	2	293–303	Sat. liq.	–	0.104	–	–	–	–
Nath and Dixit [302]	2	298–308	Sat. liq.	–	0.072	–	–	–	–
Sun et al. [294]	88	288–323	0.1–85.0	–	0.403	–	–	–	–
Isobaric heat capacities									
Parks et al. [303]	5	283–291	Sat. liq.	–	0.945	–	–	–	–
Moelwyn-Hughes and Thorpe [295]	4	298–328	Sat. liq.	–	0.088	–	–	–	–
Rührwein and Huffman [304]	7	282–301	Sat. liq.	–	0.554	–	–	–	–
Wilhelm et al. [297]	3	293–313	Sat. liq.	–	0.446	–	–	–	–
Safir et al. [305]	120	295–541	0.5–50.0	–	1.004	–	–	–	–
Rastorguev et al. [306]	64	548–669	12.0–50.0	–	1.938	–	–	4.320	2.838
Murdaev [307]	44	323–533	5.0–50.0	–	0.535	–	–	–	–
Sun et al. [294]	88	288–323	0.1–85.0	–	0.397	–	–	–	–
Vesely et al. [308]	3	298–318	Sat. liq.	–	0.163	–	–	–	–
Second virial coefficients									
Bich et al. [293]	11	373–623	–	0.711	–	–	–	–	–

Authors	No of data	Temp. range T (K)	$T/T_c < 0.6$	$0.6 \leqslant T/T_c \leqslant 0.98$	$T/T_c > 0.98$
Vapor pressures[c]					
Tatevskiy [309]	8	353–423	–	0.023	–
Ridgway and Butler [310]	1	353	–	0.033	–
Ewing [311]	5	288–328	0.101	–	–
French [312]	1	318	0.225	–	–
Weclawski and Bylicki [313]	15	298–349	0.056	0.030	–

Table XIX. *(Continued)*

Authors	No of data	Temp. range T (K)	Average absolute deviations (AAD), %		
			$T/T_c < 0.6$	$0.6 \leqslant T/T_c \leqslant 0.98$	$T/T_c > 0.98$
Saturated liquid densities					
Young and Fortey [314]	29	303–552	0.096	0.171	0.217
Reamer and Sage [315]	6	311–478	0.253	0.298	–
Tatevskiy [309]	17	283–353	0.021	0.089	–
Ridgway and Butler [310]	1	298	0.012	–	–
Wilhelm et al. [297]	3	293–313	0.019	–	–
Fortier et al. [316]	1	298	0.001	–	–
Kurumov et al. [317]	9	280–349	0.017	0.086	–
Goates et al. [318]	15	283–313	0.028	–	–
Karvo [319]	4	303–333	0.017	0.043	–
Asenbaum and Wilhelm [296]	7	283–343	0.016	0.059	–
Nath and Narain [301]	1	303	0.010	–	–
French [312]	5	288–318	0.014	–	–
Sun et al. [320]	12	281–336	0.020	0.022	–
Shibata and Sandler [321]	2	366–411	–	0.341	–
Arce et al. [322]	1	298	0.007	–	–
Richon et al. [323]	1	293	0.006	–	–

[a] LD: $\rho/\rho_c \leqslant 0.6$; MD: $0.6 < \rho/\rho_c < 1.5$; HD: $\rho/\rho_c \geqslant 1.5$.
[b] In the extended critical region, pressure deviations are given instead of density deviations.
[c] At temperatures $T/T_c < 0.6$, average absolute deviations in hPa are given.

verify the results found for supercritical isobutene, additional experimental data are required.
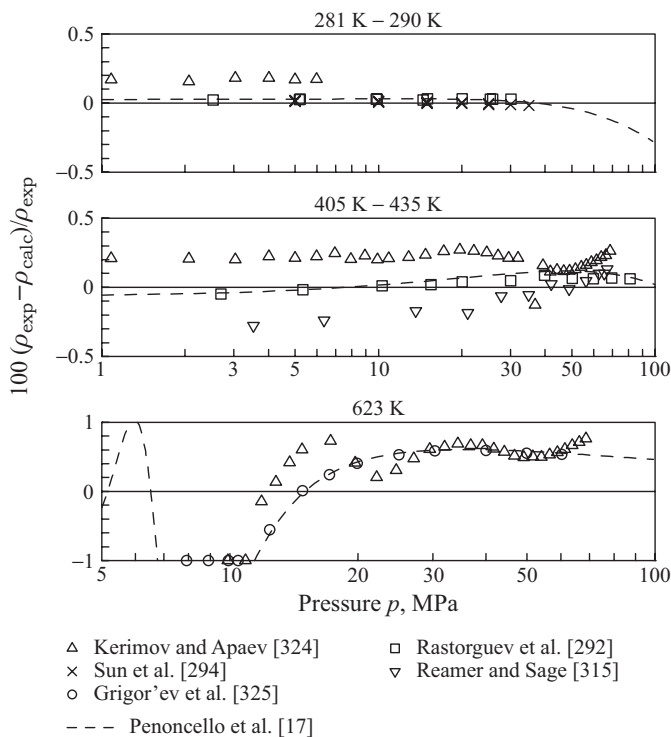
3.15. Results for Cyclohexane

For cyclohexane, a large data set of questionable quality is available. For temperatures from the triple-point at $T_t \approx 279.5$ K ($T_t/T_c \approx 0.505$) to 473 K ($T/T_c \approx 0.85$), reliable data are available both for thermal and caloric properties at liquid states. At temperatures above $T \approx 350$ K, the data sets which are available for the vapor pressure and the saturated liquid density show inconsistencies which clearly exceed the demanded value of $|\Delta y|/y = 0.2\%$. A recent review of the data which are available for the thermodynamic properties of cyclohexane was published by Penoncello et al. [17]. Table XIX summarizes the data sets selected for this project and gives percentage average absolute deviations between the selected experimental data and values calculated from the new equation of state, Eq. (2).

At ambient temperatures, Eq. (2) consistently describes the thermal and caloric properties of cyclohexane. The observed deviations remain far
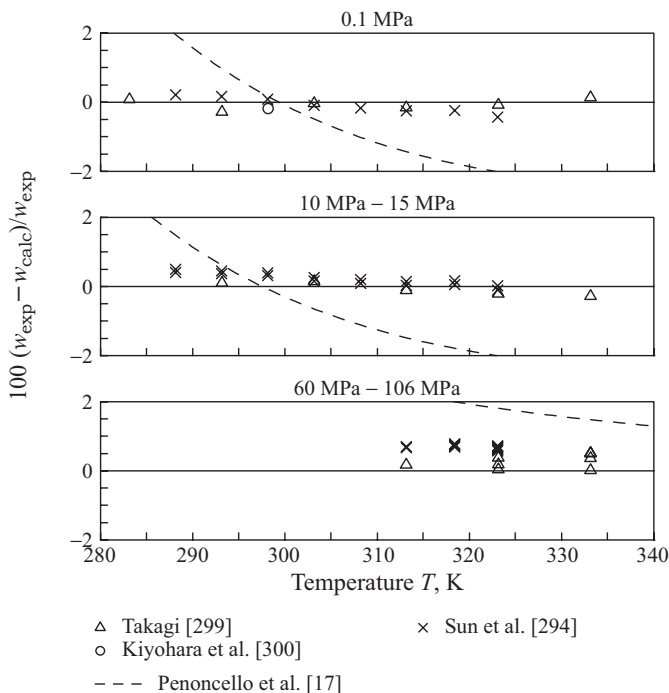
Fig. 23. Percentage deviations between selected experimental results for the speed of sound in liquid cyclohexane and values calculated from the new equation of state, Eq. (2). Values calculated from the reference equation by Penoncello et al. [17] are plotted for comparison.

within the limits formulated in Table IV. With regard to the representation of caloric properties at liquid states, the new equation is even superior to the equation by Penoncello et al. [17] which is internationally used as a reference for the properties of cyclohexane; see Fig. 23 for an example. However, at temperatures above $T \approx 350$ K, the inconsistencies in the available data set increase. At temperatures above $T \approx 473$ K, Penoncello et al. relied mostly on $p\rho T$ data [324, 325], which could not be satisfactorily represented using the simultaneously optimized functional form of Eq. (2); see Fig. 24. Any attempt to better fit these data distorted the representation of the data for caloric properties and of more reliable data at lower temperatures, and thus the data were excluded from the final data set summarized in Table XIX. The same is true for the majority of the vapor pressure data available at temperatures above $T \approx 450$ K. However, Fig. 25 shows that Eq. (2) is superior to the reference equation by Penoncello et al. [17] with regard to the representation of isobaric heat capacities at supercritical

Fig. 24. Percentage deviations between experimental results for the density of cyclohexane and values calculated from the new equation of state, Eq. (2). Values calculated from the reference equation by Penoncello et al. [17] are plotted for comparison.

states. At these states, results calculated for the isobaric heat capacity are strongly related to results for the derivatives $(\partial p/\partial \rho)_T$ and $(\partial p/\partial T)_\rho$. Obviously, neither the reference equation with its substance-specifically optimized functional form nor Eq. (2) with its simultaneously optimized functional form can yield a consistent description of the high temperature data available for cyclohexane.

Based on the available data set, it cannot be clarified whether the problems observed for cyclohexane depend on inconsistencies or whether the simultaneously optimized functional form for nonpolar fluids is unsuitable for the description of cyclic alkanes at high temperatures. Based on experiences made in a different context [4], it seems likely that the observed problems are at least partly caused by systematic errors of experimental results for the saturated liquid density at high temperatures. To
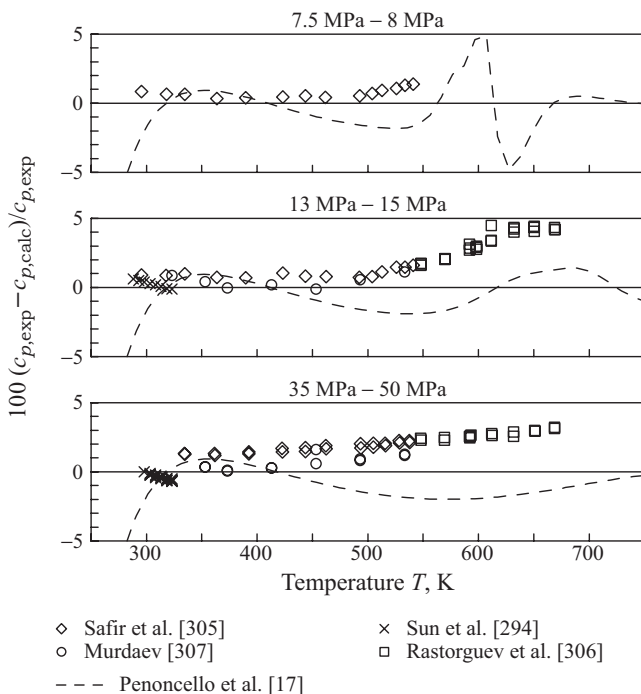
Fig. 25. Percentage deviations between selected experimental results for the isobaric heat capacity of cyclohexane and values calculated from the new equation of state, Eq. (2). Values calculated from the reference equation by Penoncello et al. [17] are plotted for comparison.

clarify the situation, accurate data for the $p\rho T$ relation and for the saturated liquid density at high temperatures would be most helpful.

3.16. Results for Sulfur Hexafluoride

The data set which was used for sulfur hexafluoride (SF_6) covers the range from the triple-point temperature at $T_t \approx 223.6$ K ($T_t/T_c \approx 0.701$) to $T_{max} \approx 521$ K ($T_{max}/T_c \approx 1.73$) at pressures up to $p_{max} \approx 59$ MPa. Data are available for thermal and caloric properties in homogeneous states and for the thermal phase equilibrium properties. Reviews of the available data set were published by Cole and de Reuck [18] and de Reuck et al. [326]. Recently, the data situation was improved drastically by the experimental results of Funke et al. [327, 328]. Sulfur hexafluoride is regarded as one of the most important reference fluids for the investigation of critical phenomena, and thus the available data set is characterized by an enormous

amount of data in the critical region. Since properties in the critical region were considered as less important for the development of technical equations of state, data sets which are restricted to the critical region were considered neither in the simultaneous optimization procedure nor in the substance-specific nonlinear fit. Table XX summarizes the data sets selected for this project and gives percentage average absolute deviations between

Table XX. Summary of the Data Sets Selected for Sulfur Hexafluoride and Average Absolute Deviations Between Values Calculated from the New Equation of State and the Selected Data

| Authors | No. of data | Temperature and pressure range | | Average absolute deviations (AAD), % | | | | | |
		T (K)	p (MPa)	Gas	Liq.	Crit. reg.	LD[a]	MD[a]	HD[a]
$p\rho T$ data[b]									
Mears et al. [329]	15	251–521	0.6–7.9	–	0.070	0.091	0.229	0.092	–
Ulybin and Zherdev [330]	73	233–473	0.7–55.0	–	0.120	–	–	0.134	0.158
Watanabe et al. [331]	75	273–363	2.0–19.6	–	0.066	0.110	0.186	0.072	0.120
Likhatskii et al. [332]	12	373	0.2–15.0	–	–	–	0.035	0.214	0.003
Biswas et al. [333]	272	308–333	0.1–10.5	0.140	0.156	0.042	0.090	0.156	0.266
Mollerup [334]	126	260–340	0.0–2.5	0.048	–	–	0.054	–	–
Freyhof [335]	11	333	0.2–0.9	–	–	–	0.015	–	–
Blanke et al. [336]	69	293–340	1.6–6.0	0.282	–	0.068	0.163	0.205	0.043
Hoinkis [200]	17	298	0.2–2.0	0.047	–	–	–	–	–
Kamimura et al. [337]	16	320–360	3.8–6.0	–	–	0.117	–	0.630	–
Gilgen et al. [338]	170	321–333	0.2–8.0	–	–	0.062	0.108	0.143	0.089
Blanke et al. [339]	223	225–453	2.5–30.2	–	0.059	–	–	–	0.067
Funke et al. [327]	311	225–340	0.1–12.1	0.091	0.065	0.063	0.084	0.103	0.113
Speeds of sound									
Vacek and Zollweg [340]	137	231–334	2.1–59.4	–	1.223	–	–	–	1.594
Isobaric heat capacities									
Sirota et al. [341]	251	298–425	2.4–20.0	–	0.659	0.712	0.799	1.055	0.605
Bier et al. [342]	24	298–398	0.1–1.5	0.388	–	–	0.461	–	–

| Authors | No of data | Temp. range T (K) | Average absolute deviations (AAD), % | | |
			$T/T_c < 0.6$	$0.6 \leqslant T/T_c \leqslant 0.98$	$T/T_c > 0.98$
Vapor pressures					
Funke et al. [328]	33	224–319	–	0.150	0.011
Saturated liquid densities					
Funke et al. [328]	31	224–319	–	0.110	0.691
Saturated vapor densities					
Funke et al. [328]	32	224–319	–	0.165	0.903

[a] LD: $\rho/\rho_c \leqslant 0.6$; MD: $0.6 < \rho/\rho_c < 1.5$; HD: $\rho/\rho_c \geqslant 1.5$.
[b] In the extended critical region, pressure deviations are given instead of density deviations.
[c] Due to the large reduced triple-point temperature, no vapor-liquid equilibria are possible at $T/T_c < 0.6$.

the selected experimental data and values calculated from the new equation of state, Eq. (2).

The new equation of state generally satisfies the demands summarized in Table IV, even though a slightly enlarged weighted variance was reported for sulfur hexafluoride in Ref. 2. The larger weighted variance results from three different effects. The selected set of $p\rho T$ data shows considerable inconsistencies, especially at temperatures close to the critical temperature. For high density gaseous states, the inconsistencies between different data sets and the differences between measured and calculated data remain within $|\Delta p|/p = 0.2\%$, see Fig. 26, but the corresponding density deviations exceed $\pm 0.2\%$ in several cases. At densities above the critical density, even larger inconsistencies are observed. The isobaric heat capacity data by Sirota et al. [341] are generally represented within $|\Delta c_p|/c_p = 2\%$ but with a clearly systematic trend which results in an increased weighted variance. Finally, enlarged deviations are observed when comparing results of Eq. (2) with the speed of sound data by Vacek and Zollweg [340]; see Fig. 27. The slightly increased deviations for high pressure liquid states agree with experiences for different fluids, but the large deviations which are observed when approaching the extended critical region seem to result from experimental problems. In this region, speeds of sound calculated from Eq. (2) agree well with values calculated from the equation by de Reuck et al. [326] which is the most recent reference equation published for sulfur hexafluoride.

4. SUMMARY AND PROSPECTS

Based on the simultaneously optimized functional form for non- and weakly polar fluids presented in Ref. 2, state-of-the-art technical equations of state have been developed for 15 fluids. A total of 36036 selected data points from more than 300 references were used to fit and evaluate these equations. The results of comparisons with the selected data are summarized in Tables VI–XX. The number of data points which were not selected for different reasons and which are thus not documented here was even larger. It has been shown that the simultaneously optimized functional form presented in Ref. 2 is suitable for a sufficiently accurate description of a broad variety of non- and weakly polar fluids. On average, the new equations are far superior to older technical equations of state. In many cases, their performance comes close to the performance of typical reference equations, and for some fluids they are superior to the available reference equations. However, up to this point obsolete technical equations of state have been replaced by more accurate and more reliable ones—multiparameter equations of state were previously available for all of the fluids
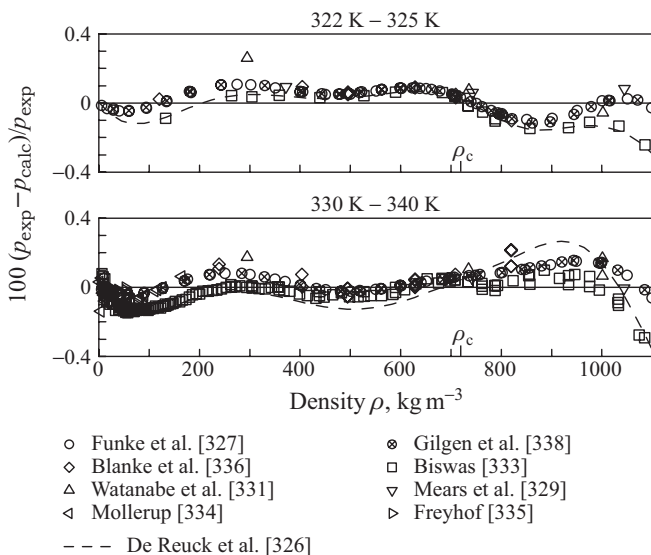
Fig. 26. Percentage pressure deviations between selected $p\rho T$ data for sulfur hexafluoride and values calculated from the new equation of state, Eq. (2). Values calculated from the reference equation by de Reuck et al. [326] are plotted for comparison.
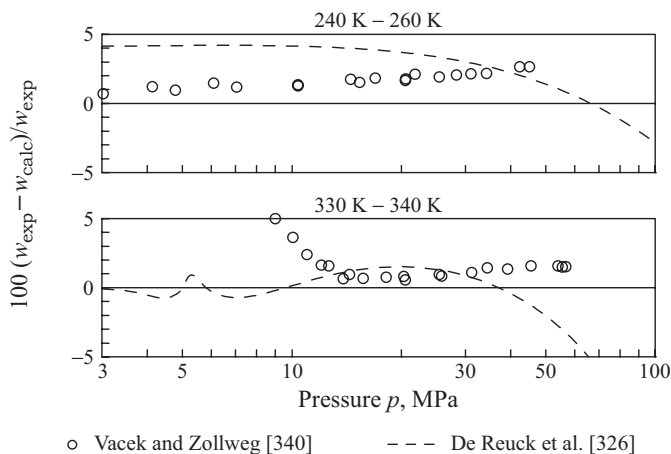
Fig. 27. Percentage deviations between experimental results for the speed of sound in sulfur hexafluoride and values calculated from the new equation of state, Eq. (2). Values calculated from the reference equation by de Reuck et al. [326] are plotted for comparison.

discussed here. The upcoming challenge is to describe fluids with this new class of accurate and numerically stable equations of state which have not yet been described with multiparameter equations. Equations of state for other fluids belonging to the group of non- and weakly polar fluids are being developed and will be published in further articles of this series.

Limitations of the functional forms proposed here need to be investigated in more detail. For example, it is yet not known, whether restrictions apply for the description of cyclic hydrocarbons or for the description of fluids with strongly elongated molecules at far supercritical temperatures; see Sections 3.7 and 3.15. Requirements on the data sets which are needed to establish further equations have been discussed in Ref. 2. Software for fitting equations of state based on the new functional form can be made available to other scientists who desire to use their own data sets as input.

ACKNOWLEDGMENTS

REFERENCES

1. R. Span, H.-J. Collmann, and W. Wagner, *Int. J. Thermophys.* **19**:491 (1998).
2. R. Span and W. Wagner, *Int. J. Thermophys.* **24**:1 (2003).
3. R. Span and W. Wagner, *Int. J. Thermophys.* **24**:111 (2003).
4. R. Span, *Multiparameter Equations of State—An Accurate Source of Thermodynamic Property Data* (Springer, Berlin, 2000).
5. U. Setzmann and W. Wagner, *J. Phys. Chem. Ref. Data* **20**:1061 (1991).
6. M. Jaeschke and P. Schley, *Int. J. Thermophys.* **16**:1381 (1995).
7. D. R. Douslin and R. H. Harrison, *J. Chem. Thermodyn.* **5**:491 (1973).
8. B. A. Younglove and J. F. Ely, *J. Phys. Chem. Ref. Data* **16**:577 (1987).
9. E. Fransson, A. Barreau, and J. Vidal, *J. Chem. Eng. Data* **37**:521 (1992).
10. J. B. Opfell, B. H. Sage, and K. S. Pitzer, *Ind. Eng. Chem.* **11**:2069 (1956).
11. M. Gomez-Nieto and G. Thodos, *Ind. Eng. Chem. Fundam.* **16**:254 (1977).
12. J. H. McMicking and W. B. Kay, *Proc. Am. Pet. Inst., Sect. 3,* **45**:75 (1965).
13. C. Tegeler, R. Span, and W. Wagner, *J. Phys. Chem. Ref. Data* **28**:779 (1999).
14. R. Schmidt and W. Wagner, *Fluid Phase Equil.* **19**:175 (1985).
15. R. Span, E. W. Lemmon, R. T Jacobsen, and W. Wagner, *Int. J. Thermophys.* **19**:1121 (1998).
16. J. Smukala, R. Span, and W. Wagner, *J. Phys. Chem. Ref. Data* **29**:1053 (2000).
17. S. G. Penoncello, R. T Jacobsen, and A. R. H. Goodwin, *Int. J. Thermophys.* **16**:519 (1995).
18. W. A. Cole and K. M. de Reuck, *Int. J. Thermophys.* **11**:189 (1990).

19. N. Kurzeja, Th. Tielkes, and W. Wagner, *The Nearly Classical Behavior of a Pure Fluid on the Critical Isochore Very Near the Critical Point under the Influence of Gravity*, in W. M. Haynes, ed., *Proc. 13th Symp. Thermophys. Prop., Preprint Volume,* Boulder, Colorado (1997).
20. H. Preston-Thomas, *Metrologia* **12**:7 (1990).
21. R. L. Rusby, *J. Chem. Thermodyn.* **23**:1153 (1990).
22. T. B. Coplen, *J. Phys. Chem. Ref. Data* **26**:1239 (1997).
23. E. R. Cohen and B. N. Taylor, *J. Phys. Chem. Ref. Data* **17**:1795 (1988).
24. P. J. Mohr and B. N. Taylor, *J. Phys. Chem. Ref. Data* **28**:1713 (1999).
25. W. Wagner and K. M. de Reuck, *International Thermodynamic Tables of the Fluid State–13–Methane* (Blackwell, Oxford, 1996).
26. H. W. Schamp Jr., E. A. Mason, A. C. B. Richardson, and A. Altman, *Phys. Fluids* **1**:329 (1958).
27. D. R. Douslin, R. H. Harrison, R. T. Moore, and J. P. McCullough, *J. Chem. Eng. Data* **9**:358 (1964).
28. G. A. Pope, *Calculation of Argon, Methane and Ethane Virial Coefficients at Low Reduced Temperatures Based on Data Obtained by Isochorically Coupled Burnett Experiments* (Ph.D. thesis, Rice University, 1972).
29. D. R. Roe, *Thermodynamic Properties of Gases and Gas Mixtures at Low Temperatures and High Pressures* (Ph.D. thesis, University of London, 1972).
30. R. D. Goodwin, *The Thermophysical Properties of Methane from 90 to 500 K at Pressures up to 700 bar*, Nat. Bur. Stand. (US), Tech. Note 653 (1974).
31. N. J. Trappeniers, T. Wassenaar, and J. C. Abels, *Physica A* **98**:289 (1979); Erratum: *Physica A* **100**:660 (1980).
32. J. Mollerup, *J. Chem. Thermodyn.* **17**:489 (1985).
33. H. J. Achtermann, T. K. Bose, H. Rögner, and J. M. St.-Arnaud, *Int. J. Thermophys.* **7**:709 (1986).
34. R. Kleinrahm, W. Duschek, and W. Wagner, *J. Chem. Thermodyn.* **18**:1103 (1986).
35. R. Kleinrahm, W. Duschek, W. Wagner, and M. Jaeschke, *J. Chem. Thermodyn.* **20**:621 (1988).
36. M. Jaeschke and M. Hinze, *Ermittlung des Realgasverhaltens von Methan und Stickstoff und deren Gemische im Temperaturbereich von 270 K bis 353 K und Drücken bis 30 MPa.* Fortschr.-Ber. VDI, Reihe **6**, 262 (1991).
37. N. Pieperbeck, R. Kleinrahm, W. Wagner, and M. Jaeschke, *J. Chem. Thermodyn.* **23**:175 (1991).
38. H. J. Achtermann, J. Hong, W. Wagner, and A. Pruß, *J. Chem. Eng. Data* **37**:414 (1992).
39. G. Händel, R. Kleinrahm, and W. Wagner, *J. Chem. Thermodyn.* **24**:685 (1992).
40. B. A. Younglove, *J. Res. Nat. Bur. Stand.* **78**:401 (1974).
41. H. M. Roder, *J. Res. Nat. Bur. Stand. A* **80**:739 (1976).
42. W. van Dael, A. van Itterbeek, J. Thoen, and A. Cops, *Physica* **31**:1643 (1965).
43. A. van Itterbeek, J. Thoen, A. Cops, and W. van Dael, *Physica* **35**:162 (1967).
44. G. C. Straty, *Cryogenics* **14**:367 (1974).
45. G. C. Straty, *Cryogenics* **15**:729 (1975).
46. B. E. Gammon and D. R. Douslin, *J. Chem. Phys.* **64**:203 (1976).
47. V. G. Baidakov, A. M. Kaverin, and V. P. Skripov, *J. Chem. Thermodyn.* **14**:1003 (1982).
48. A. Sivaraman and B. E. Gammon, *Speed of Sound Measurements in Natural Gas Fluids*, GRI Report 86/0043 (1986).
49. A. R. H. Goodwin, *Thermophysical Properties from the Speed of Sound* (Ph.D. thesis, University of London, 1988).

50. W. Lemming, *Experimentelle Bestimmung akustischer und thermischer Virialkoeffizienten von Arbeitsstoffen der Energietechnik*. Fortschr.-Ber. VDI, Reihe **19**, 32 (1989).
51. J. P. M. Trusler and M. P. Zarari, *J. Chem. Thermodyn.* **24**:973 (1992).
52. D. Fawcett, *Measurement and Prediction of Speed of Sound, with Application to Gas Flow Metering in Australian Natural Gases* (Ph.D. thesis, Murdoch University, 1995).
53. J. P. M. Trusler and M. F. Costa Gomes, *Final Report to GERG WG 1.3* (Imperial College, London, 1996).
54. R. A. Dawe and P. N. Snowdown, *J. Chem. Eng. Data* **19**:220.
55. P. G. Grini, *Flow Calorimetry and Enthalpy Increment Measurements for Natural Gases* (Ph.D. thesis, University of Trondheim, 1994).
56. G. Owren, P. G. Grini, H. S. Maehlum, and O. Jorstad, *Final Report to GERG WG 1.3* (University of Trondheim, 1996).
57. C. Day, M. Stephan, and L. R. Oellrich, *J. Chem. Thermodyn.* **29**:949 (1997).
58. R. Kleinrahm and W. Wagner, *J. Chem. Thermodyn.* **18**:739 (1986).
59. D. G. Friend, H. Ingham, and J. F. Ely, *J. Phys. Chem. Ref. Data* **20**:275 (1991).
60. P. Sliwinski, *Z. Phys. Chem. N. F.* **63**:263 (1969).
61. D. R. Douslin and R. H. Harrison, *J. Chem. Thermodyn.* **5**:491 (1973).
62. M. Funke, R. Kleinrahm, and W. Wagner, submitted to *J. Chem. Thermodyn.*
63. M. Funke, R. Kleinrahm, and W. Wagner, submitted to *J. Chem. Thermodyn.*
64. A. Michels and W. Nederbragt, *Physica* **6**:656 (1939).
65. A. Michels, W. van Straaten, and J. Dawson, *Physica* **20**:17 (1954).
66. G. C. Straty and R. Tsumura, *J. Res. Nat. Bur. Stand. A* **80**:35 (1976).
67. J. G. Young, M. S. Thesis, Texas A&M University (1978).
68. H. Mansoorian, K. R. Hall, J. C. Holste, and P. T. Eubank, *J. Chem. Thermodyn.* **13**:1001 (1981).
69. W.-W. R. Lau, *A Continuosly Weighed Pycnometer Providing Densities for Carbon Dioxide + Ethane Mixtures Between 240 and 350 K at Pressures up to 35 MPa* (Ph.D. thesis, Texas A&M University, 1986).
70. M. Jaeschke and A. E. Humphreys, *The GERG Databank of High Accuracy Compressibility Measurements*, GERG Tech. Monograph 4, VDI, Düsseldorf (1990).
71. X.-Y. Guo, R. Kleinrahm, and W. Wagner, *Final report to Ruhrgas AG, Part I* (Ruhr-Universität Bochum, 1992).
72. L. A. Weber, *Int. J. Thermophys.* **13**:1011 (1992).
73. H. Hou, J. C. Holste, and K. R. Hall, *J. Chem. Eng. Data* **41**:344 (1996).
74. A. F. Estrada-Alexanders and J. P. M. Trusler, *J. Chem. Thermodyn.* **29**:991 (1997).
75. R. Tsumura and G. C. Straty, *Cryogenics* **17**:195 (1977).
76. S. J. Boyes, *The Speed of Sound in Gases with Application to Equations of State and Sonic Nozzles* (Ph.D. thesis, University of London, 1992).
77. K. Bier, J. Kunze, and G. Maurer, *J. Chem. Thermodyn.* **8**:857 (1976).
78. R. Bender, *Untersuchungen zur zwischenmolekularen Wechselwirkung in binären Gemischen niedriger Dichte* (Ph.D. thesis, Universität Karlsruhe, 1982).
79. G. Ernst and U. E. Hochberg, *J. Chem. Thermodyn.* **21**:407 (1989).
80. A. W. Tickner and F. P. Lossing, *J. Phys. Coll. Chem.* **55**:733 (1951).
81. V. M. Miniovich and G. A. Sorina, *Russ. J. Phys. Chem.* **45**:306 (1971).
82. J. Regnier, *J. Chim. Phys. Phys.-Chim. Biol.* **69**:942 (1972).
83. G. F. Carruth and R. Kobayashi, *J. Chem. Eng. Data* **18**:115 (1973).
84. A. Fredenslund and J. Mollerup, *J. Chem. Soc. Far. Trans.* I:1653 (1974).
85. A. K. Pal, G. A. Pope, Y. Arai, N. F. Carnahan, and R. Kobayashi, *J. Chem. Eng. Data* **21**:394 (1976).
86. D. A. Barclay, J. L. Fiebbe, and D. B. Manley, *J. Chem. Eng. Data* **27**:135 (1982).

87. J. Klosek and C. McKinley, *Densities of Liquefied Natural Gas and of Low Molecular Weight Hydrocarbons*. Proc. 1st. Int. Conf. LNG, Chicago (1968).
88. J. R. Tomlinson, *Liquid Densities of Ethane, Propane, and Ethane-Propane Mixtures*. Tech. Pub. TP-1, Nat. Gas Proc. Assoc., Tulsa (1971).
89. L. C. Kahre, *J. Chem. Eng. Data* **18**:267 (1973).
90. C. R. McClune, *Cryogenics* **16**:289 (1976).
91. W. M. Haynes and M. J. Hiza, *J. Chem. Thermodyn.* **9**:179 (1977).
92. J. E. Orrit and J. M. Laupretre, *Adv. Cryo. Eng.* **23**:573 (1978).
93. C. C. Luo and R. C. Miller, *Cryogenics* **21**:85 (1981).
94. M. W. Pestak, R. E. Goldstein, M. H. W. Chan, J. R. de Bruyn, D. A. Balzarini, and N. W. Ashcroft, *Phys. Rev.* **B36**:599 (1987).
95. H. Miyamoto and K. Watanabe, *Int. J. Thermophys.* **21**:1045 (2000).
96. J. P. M. Trusler and M. P. Zarari, *J. Chem. Thermodyn.* **28**:329 (1996).
97. P. Dittmar, F. Schulz, and G. Strese, *Chemie Ing. Technik* **34**:437 (1962).
98. S. E. Babb and S. L. Robertson, *J. Chem. Phys.* **53**:1097 (1970).
99. J. F. Ely and R. Kobayashi, *J. Chem. Eng. Data* **23**:221 (1978).
100. W. Warowny, P. Wielopolski, and J. Stecki, *Physica A* **91**:73 (1978).
101. R. H. P. Thomas and R. H. Harrison, *J. Chem. Eng. Data* **27**:1 (1982).
102. W. M. Haynes, *J. Chem. Thermodyn.* **15**:419 (1983).
103. H. Kratzke and S. Müller, *J. Chem. Thermodyn.* **16**:1157 (1984).
104. K. E. Starling, *Propane*. In: M. Jaeschke and A. E. Humphreys, *The GERG Databank of High Accuracy Compressibility Measurements*. GERG Tech. Monograph 4, VDI, Düsseldorf (1990).
105. G. C. Straty and A. M. F. Palavra, *J. Res. Nat. Bur. Stand.* **89**:375 (1984).
106. A. Lacam, *J. Recherches CNRS* **34**:25 (1956).
107. B. A. Younglove, *J. Res. Nat. Bur. Stand.* **86**:165 (1981).
108. R. Niepmann, *J. Chem. Thermodyn.* **16**:851 (1984).
109. V. F. Yesavage, D. L. Katz, and J. E. Powers, *J. Chem. Eng. Data* **14**:197 (1969).
110. G. Ernst and J. Büsser, *J. Chem. Thermodyn.* **2**:787 (1970).
111. J. D. Kemp and C. J. Egan, *J. Am. Chem. Soc.* **60**:1521 (1938).
112. H. Kratzke, *J. Chem. Thermodyn.* **12**:305 (1980).
113. N. L. Helgeson and B. H. Sage, *J. Chem. Eng. Data* **12**:47 (1967).
114. I. M. Abdulagatov, L. N. Levina, Z. R. Zakaryaev, and O. N. Mamchenkova, *J. Chem. Thermodyn.* **27**:1385 (1995).
115. I. M. Abdulagatov, L. N. Levina, Z. R. Zakaryaev, and O. N. Mamchenkova, *Fluid Phase Equil.* **127**:205 (1997).
116. R. D. Goodwin and W. M. Haynes, *Thermophysical Properties of Normal Butane from 135 to 700 K at Pressures to 70 MPa*. Nat. Bur. Stand. Monograph 169, Boulder, Colorado (1982).
117. D. Gupta and P. T. Eubank, *J. Chem. Eng. Data* **42**:961 (1997).
118. M. B. Ewing, A. R. H. Goodwin, M. L. McGlashan, and J. P. M. Trusler, *J. Chem. Thermodyn.* **20**:243 (1988).
119. J. W. Magee and T. O. D. Lüddecke, *Int. J. Thermophys.* **19**:129 (1998).
120. J. A. Beattie, G. L. Simard, and G.-J. Su, *J. Am. Chem. Soc.* **61**:24 (1939).
121. R. H. Olds, H. H. Reamer, B. H. Sage, and W. N. Lacey, *Ind. Eng. Chem.* **36**:282 (1944).
122. W. M. Haynes, *J. Chem. Thermodyn.* **15**:801 (1983).
123. J. G. Aston and G. H. Messerly, *J. Am. Chem. Soc.* **62**:1917 (1940).
124. B. P. Dailey and W. A. Felsing, *J. Am. Chem. Soc.* **65**:44 (1943).
125. W. Brostow, D. M. McEachern, and S. Perez-Guttierez, *J. Chem. Phys.* **71**:2716 (1979).
126. W. B. Kay, *Ind. Eng. Chem.* **32**:358 (1940).

127. H. Holldorf and H. Knapp, *Fluid Phase Equil.* **40**:113 (1988).

128. W. D. Machin and P. D. Golding, *J. Chem. Soc. Faraday Trans.* **I**:2229 (1989).

129. T. Sako, S. Horiguchi, H. Ichimaru, and S. Nakagawa, *J. Chem. Eng. Data* **42**:169 (1997).

130. H. Kratzke, S. Müller, M. Bohn, and R. Kohlen, *J. Chem. Thermodyn.* **17**:283 (1985).

131. M. B. Ewing, A. R. H. Goodwin, and J. P. M. Trusler, *J. Chem. Thermodyn.* **21**:867 (1989).

132. I. Cibulka and L. Hnedkovsky, *J. Chem. Eng. Data* **41**:657 (1996).

133. E. W. Lemmon and A. R. H. Goodwin, *J. Phys. Chem. Ref. Data* **29**:1 (2000).

134. B. H. Sage and W. N. Lacey, *Ind. Eng. Chem.* **34**:730 (1942).

135. J. A. Beattie, D. R. Douslin, and S. W. Levin, *J. Chem. Phys.* **19**:948 (1951).

136. J. A. Huff and T. M. Reed, *J. Chem. Eng. Data* **8**:306 (1963).

137. B. J. Mair, *J. Res. Nat. Bur. Stand.* **16**:457 (1932).

138. C. B. Willingham, W. J. Taylor, J. M. Pignocco, and F. D. Rossini, *J. Res. Nat. Bur. Stand.* **35**:219 (1945).

139. K. Li and L. N. Canjar, *Chem. Eng. Prog. Symp. Ser.* **49 (7)**:147 (1953).

140. A. G. Osborn and D. R. Douslin, *J. Chem. Eng. Data* **19**:114 (1974).

141. B. R. Carney, *Petroleum Refiner* **21 (9)**:84 (1942).

142. E. Bender, *Equations of State Exactly Representing the Phase Behavior of Pure Substance* In: C. F. Bonila, ed., *Proc. 5th Symp. Thermophys. Prop.*, ASME, New York (1970), p. 227.

143. P. Sauermann, K. Holzapfel, J. Oprzynski, F. Kohler, W. Poot, and T. W. de Loos, *Fluid Phase Equil.* **112**:249 (1995).

144. I. M. Abdulagatov, A. R. Bazaev, R. K. Gasanov, and A. E. Ramazanova, *J. Chem. Thermodyn.* **28**:1037 (1996).

145. E. A. Kelso and W. A. Felsing, *J. Am. Chem. Soc.* **62**:3132 (1940).

146. D. E. Stewart, B. H. Sage, and W. N. Lacey, *Ind. Eng. Chem.* **46**:2529 (1954).

147. E. Kuss and M. Taslimi, *Chem. Ing. Tech.* **42**:1073 (1970).

148. J. H. Dymond and K. J. Young, *J. Chem. Thermodyn.* **11**:887 (1979).

149. E. Kiran and Y. L. Sen, *Int. J. Thermophys.* **13**:411 (1992).

150. S. S. Susnar, C. J. Budziak, H. A. Hamza, and A. W. Neumann, *Int. J. Thermophys.* **13**:443 (1992).

151. G. Waddington and D. R. Douslin, *J. Am. Chem. Soc.* **69**:2275 (1947).

152. M. L. McGlashan and D. J. B. Potter, *Proc. Royal Soc.* **A267**:478 (1962).

153. A. F. Hajjar, W. B. Kay, and G. F. Leverett, *J. Chem. Eng. Data* **14**:377 (1969).

154. V. Rodriguez, J. Pardo, M. C. Lopez, F. M. Royo, and J. S. Urieta, *J. Chem. Eng. Data* **38**:350 (1993).

155. A. H. N. Mousa, *J. Chem. Thermodyn.* **9**:1063 (1977).

156. S. A. Wieczorek and J. Stecki, *J. Chem. Thermodyn.* **10**:177 (1978).

157. H. Wolff, J. Szydlowski, and L. Dill-Staffenberger, *J. Chem. Thermodyn.* **12**:641 (1980).

158. H. Wolff and A. Shadiaky, *Fluid Phase Equil.* **7**:309 (1981).

159. S. Weiguo, A. X. Qin, P. J. McElroy, and A. G. Williamson, *J. Chem. Thermodyn.* **22**:905 (1990).

160. M. R. W. Maciel and A. Z. Francesconi, *Fluid Phase Equil.* **50**:201 (1989).

161. D. Fenclova and V. Dohnal, *J. Chem. Thermodyn.* **25**:689 (1993).

162. F. Vesely, L. Svab, R. Provaznik, and V. Svoboda, *J. Chem. Thermodyn.* **20**:981 (1988).

163. M. J. P. Muringer, N. J. Trappeniers, and S. N. Biswas, *Phys. Chem. Liq.* **14**:273 (1985).

164. T. F. Sun, S. A. R. C. Bominaar, C. A. ten Seldam, and S. N. Biswas, *Ber. Bunsenges. Phys. Chem.* **95**:696 (1991).

165. W. B. Nichols, H. H. Reamer, and B. H. Sage, *Ind. Eng. Chem.* **47**:2219 (1955).

166. I. M. Abdulagatov, *Experimental results for the isochoric heat capacity of n-heptane and n-octane*, Private communication, National Institute of Standards and Technology, Boulder, Colorado (1998).
167. L. B. Smith, J. A. Beattie, and W. C. Kay, *J. Am. Chem. Soc.* **59**:1587 (1937).
168. S. Toscani, P. Figuiere, and H. Szwarc, *J. Chem. Thermodyn.* **21**:1263 (1989).
169. N. S. Osborne and D. C. Ginnings, *J. Res. Nat. Bur. Stand.* **39**:453 (1947).
170. M. Zábranský and V. Růžicka Jr., *J. Phys. Chem. Ref. Data* **23**:55 (1994).
171. R. C. Castro-Gomez, K. R. Hall, J. C. Holste, B. E. Gammon, and K. N. Marsh, *J. Chem. Thermodyn.* **22**:269 (1990).
172. J. O. Hirschfelder, F. T. McClure, and I. F. Weeks, *J. Chem. Phys.* **10**:201 (1942).
173. J. A. Beattie and W. C. Kay, *J. Am. Chem. Soc.* **59**:1586 (1937).
174. A. F. Forziatti, W. R. Norris, and F. D. Rossini, *J. Res. Nat. Bur. Stand.* **43**:555 (1949).
175. M. W. Cook, *Rev. Sci. Instrum.* **29**:399 (1958).
176. J. H. McMicking, *Vapor Pressures and Saturated Liquid and Vapor Densities of Isomeric Heptanes and Octanes* (Ph.D. thesis, Ohio State University, 1961).
177. L. A. Weber, *J. Chem. Eng. Data* **45**:173 (2000).
178. R. Bravo, M. Pintos, and A. Amigo, *J. Chem. Thermodyn.* **23**:905 (1991).
179. I. G. de la Fuente, J. A. Gonzalez, J. C. Cobos, and C. Casanova, *J. Chem. Eng. Data* **37**:535 (1992).
180. B. Pittau, B. Maronglu, and S. Porcedda, *J. Chem. Eng. Data* **37**:124 (1992).
181. L. Romani, J. Peleteiro, T. P. Iglesias, E. Carballo, R. Escudero, and J. L. Legido, *J. Chem. Eng. Data* **39**:19 (1994).
182. W. A. Felsing and G. M. Watson, *J. Am. Chem. Soc.* **64**:1822 (1942).
183. M. S. Benson and J. Winnick, *J. Chem. Eng. Data* **16**:154 (1971).
184. T. S. Banipal, S. K. Garg, and J. C. Ahluwalia, *J. Chem. Thermodyn.* **23**:923 (1991).
185. M. Dix, J. M. N. A. Fareleira, Y. Takaishi, and W. A. Wakeham, *Int. J. Thermophys.* **12**:357 (1991).
186. Y. Tanaka, H. Hosokawa, H. Kubota, and T. Makita, *Int. J. Thermophys.* **12**:245 (1991).
187. A. R. H. Goodwin, C. H. Bradsell, and L. S. Toczylkin, *J. Chem. Thermodyn.* **28**:637 (1996).
188. J. Gregorowicz, K. Kiciak, and S. Malanowski, *Fluid Phase Equil.* **38**:97 (1987).
189. C. C. Chappelow, P. S. Snyder, and J. Winnick, *J. Chem. Eng. Data* **16**:440 (1971).
190. M. R. Lopez Alanon, M. Caceres, R. G. Rubio, and J. Nunez, *J. Chem. Soc. Faraday Trans. 1* **85**:3425 (1989).
191. K. S. Kumar, P. R. Naidu, W. E. Acre Jr., *J. Chem. Eng. Data* **39**:2 (1994).
192. R. Gilgen, R. Kleinrahm, and W. Wagner, *J. Chem. Thermodyn.* **26**:399 (1994).
193. R. Gilgen, R. Kleinrahm, and W. Wagner, *J. Chem. Thermodyn.* **26**:383 (1994).
194. J. Klimeck, R. Kleinrahm, and W. Wagner, *J. Chem. Thermodyn.* **30**:1571 (1998).
195. A. F. Estrada-Alexanders and J. P. M. Trusler, *J. Chem. Thermodyn.* **27**:1075 (1995).
196. A. F. Estrada-Alexanders and J. P. M. Trusler, *Int. J. Thermophys.* **17**:1325 (1996).
197. A. Michels, H. Wijker, and H. K. Wijker, *Physica* **15**:627 (1949).
198. S. F. Barreiros, J. C. G. Calado, P. Clancy, M. Nunes da Ponte, and W. B. Strett, *J. Phys. Chem.* **86**:1722 (1982).
199. S. N. Biswas, N. J. Trappeniers, P. J. Kortbeek, and C. A. ten Seldam, *Rev. Sci. Inst.* **59**:470 (1988).
200. J. Hoinkis, *Untersuchungen zum thermischen Verhalten von binären Gasmischungen mit Kohlendioxid* (Ph.D. thesis, Universität Karlsruhe, 1989).
201. C. Gladun, *Cryogenics* **11**:205 (1971).
202. M. A. Anisimov, B. A. Koval'chuk, V. A. Rabinovich, and V. A. Smirnov, *Teplofiz. Svoistva Vesh. Mat.* **8**:237 (1975).

203. M. A. Anisimov, B. A. Koval'chuk, V. A. Rabinovich, and V. A. Smirnov, *Teplofiz. Svoistva Vesh. Mat.* **12**:86 (1978).
204. I. S. Radovskii, *Z. Prikl. Mech. Tech. Fiz.* **3**:159 (1963).
205. R. A. Aziz, D. H. Bowman, and C. C. Lim, *Can. J. Chem.* **45**:2079 (1967).
206. D. H. Bowman, C. C. Lim, and R. A. Aziz, *Can. J. Chem.* **46**:1175 (1968).
207. L. L. Pitaevskaya, A. V. Bilevich, and N. B. Isakova, *Rus. J. Phys. Chem.* **43**:1197 (1969).
208. J. Thoen, E. Vangeel, and W. van Dael, *Physica* **45**:339 (1969).
209. J. Thoen, E. Vangeel, and W. van Dael, *Physica* **52**:205 (1971).
210. W. B. Streett and M. S. Costantino, *Physica* **75**:283 (1974).
211. Yu. L. Kachanov, B. E. Kanishchev, and L. L. Pitaevskaya, *J. Eng. Phys.* **44**:1 (1983).
212. P. J. Kortbeek, M. J. P. Muringer, N. J. Trappeniers, and S. N. Biswas, *Rev. Sci. Inst.* **56**:1269 (1985).
213. M. B. Ewing, and A. R. H. Goodwin, *J. Chem. Thermodyn.* **24**:531 (1992).
214. W. Wagner and K. M. de Reuck, *International Thermodynamic Tables of the Fluid State–9–Oxygen* (Blackwell, Oxford, 1987).
215. L. A. Weber, *J. Res. Nat. Bur. Stand. A* **74**:93 (1970).
216. L. A. Weber, *Thermodynamic and Related Properties of Oxygen from the Triple Point to 300–K at Pressures to 1000–bar*, NASA Ref. Publ. 1011, NBSIR 77-865 (1977).
217. W. Pentermann and W. Wagner, *J. Chem. Thermodyn.* **10**:1161 (1978).
218. R. D. Goodwin and L. A. Weber, *J. Res. Nat. Bur. Stand. A* **73**:15 (1969).
219. A. van Itterbeek and J. Zink, *Appl. Sci. Res. A* **7**:375 (1958).
220. A. van Itterbeek and W. van Dael, *Bull. Int. Inst. Refrig. Annexe* 295 (1958).
221. A. van Itterbeek and W. van Dael, *Physica* **28**:861 (1962).
222. G. C. Straty and B. A. Younglove, *J. Chem. Thermodyn.* **5**:305 (1973).
223. J. Anscin, *Can. J. Phys.* **52**:2305 (1974).
224. W. Wagner, J. Ewers, and W. Pentermann, *J. Chem. Thermodyn.* **8**:1049 (1976).
225. J. H. C. Lisman and W. H. Keesom, *Physica* **2**:901 (1935).
226. R. A. H. Pool, G. Saville, T. M. Herrington, B. D. C. Shields, and L. A. K. Staveley, *Trans. Farraday Soc.* **58**:1692 (1962).
227. P. Nowak, R. Kleinrahm, and W. Wagner, *J. Chem. Thermodyn.* **29**:1137 (1997).
228. J. Klimeck, R. Kleinrahm, and W. Wagner, *J. Chem. Thermodyn.* **30**:1571 (1998).
229. P. Nowak, R. Kleinrahm, and W. Wagner, *J. Chem. Thermodyn.* **29**:1157 (1997).
230. M. B. Ewing and J. P. M. Trusler, *Physica A* **184**:415 (1992).
231. M. F. Costa Gomes and J. P. M. Trusler, *J. Chem. Thermodyn.* **30**:527 (1998).
232. J. W. Magee, *J. Res. NIST* **96**:725 (1991).
233. P. G. Grini and G. A. Owren, *J. Chem. Thermodyn.* **29**:37 (1997).
234. R. Span, E. W. Lemmon, R. T Jacobsen, W. Wagner, and A. Yokozeki, *J. Phys. Chem. Ref. Data* **29**:1361 (2000).
235. A. Michels, H. Wouters, and J. DeBoer, *Physica* **3**:585 (1936).
236. J. Saurel, *J. Rech. CNRS* **42**:22 (1958).
237. G. C. Straty and D. E. Diller, *J. Chem. Thermodyn.* **12**:927 (1980).
238. W. Duschek, R. Kleinrahm, W. Wagner, and M. Jaeschke, *J. Chem. Thermodyn.* **20**:1069 (1988).
239. A. Fenghour, W. A. Wakeham, D. Ferguson, A. C. Scott, and J. T. R. Watson, *J. Chem. Thermodyn.* **25**:831 (1993).
240. L. A. Weber, *J. Chem. Thermodyn.* **13**:389 (1981).
241. E. R. Dobbs and L. Finegold, *J. Acoust. Soc. Am.* **32**:1215 (1960).
242. A. van Itterbeek and W. van Dael, *Cryogenics* **1**:226 (1961).
243. A. A. Vassermann and V. I. Selevanyuk, *Akust. Zh.* **13**:131 (1967).

244. B. A. Younglove and R. C. McCarty, *J. Chem. Thermodyn.* **12**:1121 (1980).
245. P. J. Kortbeek, N. J. Trappeniers, and S. N. Biswas, *Int. J. Thermophys.* **9**:103 (1988).
246. D. T. Mage, M. L. Jones Jr., D. L. Katz, and J. R. Roebuck, *Chem. Eng. Prog.* **59**:61 (1963).
247. W. van Dael, A. van Itterbeek, A. Cops, and J. Thoen, *Physica* **32**:611 (1966).
248. G. T. Furukawa and R. E. McCoskey, *The Condensation Line of Air and Heats of Vaporization of Oxygen and Nitrogen*, National Advisory Committee for Aeronautics, Tech. Note No. 2969 (1953).
249. R. T Jacobsen, M. Jahangiri, R. B. Stewart, R. D. McCarty, J. M. H. Levelt Sengers, H. J. White Jr., J. V. Sengers, and G. A. Olchowy, *International Thermodynamic Tables of the Fluid State, Vol. 10: Ethylene* (Blackwell Scientific Pubs., Oxford, 1988).
250. P. Nowak, R. Kleinrahm, and W. Wagner, *J. Chem. Thermodyn.* **28**:1423 (1996).
251. P. Nowak, R. Kleinrahm, and W. Wagner, *J. Chem. Thermodyn.* **28**:1441 (1996).
252. P. Claus, R. Kleinrahm, and W. Wagner, *$\rho\rho T$ Data for Ethylene*, Private communication, Ruhr-Universität Bochum (1998).
253. A. Michels and M. Geldermans, *Physica* **9**:967 (1942).
254. L. Turlington and J. J. McKetta, *Petroleum Refiner* **40**:245 (1961).
255. W. Thomas and M. Zander, *Z. angew. Phys.* **20**:417 (1966).
256. E. A. Golovskii, V. A. Elema, V. A. Zagoruchenko, and V. A. Tsymarnii, *Izv. Vys. Uchebuykh Zavedenii, Neft Gaz* **12**:85 (1969).
257. E. A. Golovskii, V. A. Zagoruchenko, and V. A. Tsymarnii, *Izv. Vys. Uchebuykh Zavedenii, Neft Gaz.* **16**:73 (1973).
258. E. A. Golovskii, E. P. Mitsevich, and V. A. Tsymarnii, *Izv. Vys. Uchebuykh Zavedenii, Neft Gaz.* **19**:95 (1976).
259. D. R. Douslin and R. H. Harrison, *J. Chem. Thermodyn.* **8**:301 (1976).
260. N. J. Trappeniers, T. Wassenaar, and G. J. Wolkers, *Physica A* **82**:305 (1976).
261. J. R. Hastings, J. M. H. Levelt Sengers, and F. W. Balfour, *J. Chem. Thermodyn.* **12**:1009 (1980).
262. G. C. Straty, *J. Chem. Thermodyn.* **12**:709 (1980).
263. W. Thomas and M. Zander, *Int. J. Thermophys.* **1**:383 (1980).
264. J. M. H. Levelt Sengers and J. R. Hastings, *Int. J. Thermophys.* **2**:269 (1981).
265. J. C. G. Calado, P. Clancy, A. Heintz, and W. B. Streett, *J. Chem. Eng. Data* **27**:376 (1982).
266. M. Waxman, *Ethylene PVT Data*. Private communication to M. Jahangiri (1983). Values published in Ref. 249.
267. J. Mollerup, *J. Chem. Thermodyn.* **17**:489 (1985).
268. H. J. Achtermann, H. D. Baehr, and T. K. Bose, *J. Chem. Thermodyn.* **21**:1023 (1989).
269. H. J. Achtermann, T. K. Bose, and G. Magnus, *Int. J. Thermophys.* **11**:133 (1990).
270. L. A. Weber, *J. Chem. Eng. Data* **27**:203 (1982).
271. Y. A. Soldatenko and E. K. Dregulyas, *Teplofiz. Svoistva Vesh.* **3**:344 (1968).
272. B. E. Gammon, *Values of the Velocity of Sound in Ethylene and Related Variables*. In: *Industrial needs for critically evaluated state data of ethylene and related substances*, Minutes Ninth Mtg. Joint Industry-Government Project Thermophys. Props. Ethylene, Boulder, Colorado (1978).
273. J. B. Mehl and M. R. Moldover, *J. Chem. Phys.* **74**:4062 (1981).
274. E. K. Dregulyas and A. F. Stavtsev, *High Temp.* **20**:210 (1982).
275. E. K. Dregulyas and A. F. Stavtsev, *High Temp.* **22**:849 (1985).
276. K. Watanabe, *Experimental Isobaric Heat Capacity Values for Ethylene*, Private communication to R. B. Stewart (1980). Values published in M. Jahangiri, R. T Jacobsen, R. B. Stewart, and R. D. McCarty, *J. Phys. Chem. Ref. Data* **15**:593 (1986).

277. R. B. Bird, E. L. Spotz, and J. O. Hirschfelder, *J. Chem. Phys.* **18**:1395 (1950).
278. R. D. Goodwin and W. M. Haynes, *Thermophysical Properties of Isobutane from 114 to 700 K at Pressures to 70 MPa.* Nat. Bur. Stand. Tech. Note 1051, Boulder, Colorado (1982).
279. J. C. Nieuwoudt, B. L. Neindre, R. Tufeu, and J. V. Sengers, *J. Chem. Eng. Data* **32**:1 (1987).
280. M. B. Ewing and A. R. H. Goodwin, *J. Chem. Thermodyn.* **23**:1107 (1991).
281. T. R. Das and N. R. Kuloor, *Indian J. Tech.* **5**:40 (1967).
282. M. Waxman, *PVT data for isobutane*, Private communication to R. D. Goodwin and W. M. Haynes; Values published in Ref. 278.
283. W. M. Haynes, *J. Chem. Eng. Data* **28**:367 (1983).
284. G. S. Parks, C. H. Shomate, W. D. Kennedy, and B. L. Crawford, *J. Chem. Phys.* **5**:359 (1937).
285. J. G. Aston, R. M. Kennedy, and S. C. Schumann, *J. Am. Chem. Soc.* **62**:2059 (1940).
286. J. F. Connolly, *J. Phys. Chem.* **66**:1082 (1962).
287. K. Steele, B. E. Poling, and D. B. Manley, *J. Chem. Eng. Data* **21**:399 (1976).
288. J. A. Martinez-Ortiz and D. B. Manley, *J. Chem. Eng. Data* **23**:165 (1978).
289. L. A. Weber, *J. Chem. Eng. Data* **34**:171 (1989).
290. G.-I. Kaminishi, C. Yokoyama, and S. Takahashi, *Sekiyu Gakkaishi* **31**:433 (1988).
291. J. M. H. Levelt Sengers, B. Kamgar-Parsi, and J. V. Sengers, *J. Chem. Eng. Data* **28**:354 (1983).
292. Y. L. Rastorguev, B. A. Grigor'ev, and R. M. Murdaev, *Izv. Vyssh. Uchebn. Zaved. Neft Gaz.* **18**:66 (1975).
293. E. Bich, G. Opel, R. Pietsch, R. Schmal, and E. Vogel, *Z. Phys. Chem.* **265**:101 (1984).
294. T. F. Sun, P. J. Kortbeek, N. J. Trappeniers, and S. N. Biswas, *Phys. Chem. Liq.* **16**:163 (1987).
295. E. A. Moelwyn-Hughes and P. L. Thorpe, *Proc. Royal Soc. A* **278**:574 (1963).
296. A. Asenbaum and E. Wilhelm, *Adv. Mol. Relax. Int. Proc.* **22**:187 (1982).
297. E. W. Wilhelm, R. Schano, G. Becker, G. H. Findenegg, and F. Kohler, *Trans. Far. Soc.* **65**:1443 (1968).
298. S. Prakash and S. B. Srivastav, *J. Chem. Thermodyn.* **7**:997 (1975).
299. T. Takagi, *Kyoto Techn. Univ. Sci. Technol.* **25**:51 (1976).
300. O. Kiyohara, C. J. Halpin, and G. C. Benson, *J. Chem. Thermodyn.* **10**:721 (1978).
301. J. Nath and B. Narain, *J. Chem. Eng. Data* **27**:308 (1982).
302. J. Nath and A. P. Dixit, *J. Chem. Eng. Data* **29**:313 (1984).
303. G. S. Parks, H. M. Huffman, and S. B. Thomas, *J. Am. Chem. Soc.* **52**:1032 (1930).
304. R. A. Rührwein and H. M. Huffman, *J. Am. Chem. Soc.* **6**:1620 (1943).
305. L. I. Safir, A. A. Gerasimov, and B. A. Grigor'ev, *Izv. Vyssh. Uchebn. Zaved. Gaz.* **11**:No. 11, 61 (1975).
306. Y. L. Rastorguev, B. A. Grigor'ev, and L. I. Safir, *Izv. Sev. Kavk. Nauchn. Tsentra Vyssh. Shk.* **4**:107 (1976).
307. R. M. Murdaev, *Elekt. Auto. Ob'ektov. Neft. Prom-sti, Grozngi* 217 (1980).
308. F. Vesley, M. Zabransky, V. Svoboda, and J. Pick, *Collect. Czech. Chem. Comm.* **44**:3529 (1979).
309. V. M. Tatevskiy, *Physico-chemical Properties of Individual Hydrocarbons.* Gostoptech Press (1960). See also: N. B. Vargatik, *Handbook of Physical Properties of Liquids and Gases, 2nd edn.* (Hemisphere Publishing, Washington, 1975).
310. K. Ridgway and A. Butler, *J. Chem. Eng. Data* **12**:509 (1967).
311. M. B. Ewing, *Excess Free Energies, Excess Enthalpies and Isothermal Compressibilities of Mixtures of Approximately Spherical Molecules* (Ph.D. thesis, University of New England, 1974).

312. H. T. French, *J. Sol. Chem.* **12**:869 (1983).

313. J. Weclawski and A. Bylicki, *Fluid Phase Equil.* **12**:143 (1983).

314. S. Young and E. C. Fortey, *J. Chem. Soc. Trans.* **75**:873 (1899).

315. H. H. Reamer and B. H. Sage, *J. Chem. Eng. Data* **2**:9 (1957).

316. J. Fortier, G. C. Benson, and P. Picker, *J. Chem. Thermodyn.* **8**:289 (1976).

317. D. S. Kurumov, R. M. Murdaev, and B. A. Grigor'ev, *Izv. Vyssh. Uchebn. Zaved. Neft Gaz.* **20**:75 (1977).

318. J. R. Goates, J. B. Ott, and R. B. Grigg, *J. Chem. Thermodyn.* **11**:497 (1979).

319. M. Karvo, *Finn. Chem. Lett.* 196 (1980).

320. T. F. Sun, P. J. Kortbeek, N. J. Trappeniers, and S. N. Biswas, *J. Chem. Thermodyn.* **20**:1089 (1988).

321. S. K. Shibata and S. I. Sandler, *J. Chem. Eng. Data* **34**:419 (1989).

322. A. Arce, A. Dominguez, and J. Tojo, *J. Chem. Eng. Data* **35**:30 (1990).

323. D. Richon, S. Laugier, and H. Renon, *J. Chem. Eng. Data* **36**:104 (1991).

324. A. M. Kerimov and T. A. Apaev, *Fluid Mech.–Sov. Res.* **3**:100 (1974).

325. B. A. Grigor'ev, R. M. Murdaev, and Y. L. Rastorguev, *Izv. Vyssh. Uchebn. Zaved. Neft Gaz.* **18**:61 (1975).

326. K. M. de Reuck, R. J. B. Craven, and W. A. Cole, *Report on the Development of an Equation of State for Sulphur Hexafluoride*, Report PC/D44, Imperial College Thermodyn. Tables Project Centre, London (1991).

327. M. Funke, R. Kleinrahm, and W. Wagner, *J. Chem. Thermodyn.* **34**:717 (2002).

328. M. Funke, R. Kleinrahm, and W. Wagner, *J. Chem. Thermodyn.* **34**:735 (2002).

329. W. H. Mears, E. Rosenthal, and J. V. Sinka, *J. Phys. Chem.* **73**:2254 (1969).

330. S. A. Ulybin and E. P. Zherdev, *Dokl. Akad. Nauk.* **191**:572 (1970).

331. K. Watanabe, H. Watanabe, and K. Oguchi, *Proc. 7th Symp. Thermophys. Prop.* (Am. Soc. Mech. Eng., New York, 1977).

332. M. A. Likhatskii, V. V. Altunin, and N. Y. Filatov, *Therm. Eng.* **29**:576 (1982).

333. S. N. Biswas, N. J. Trappeniers, and J. H. B. Hoogland, *Physica A* **126**:384 (1984).

334. J. Mollerup, *J. Chem. Eng. Data* **30**:21 (1985).

335. R. Freyhof, *Untersuchungen zur Temperaturabhängigkeit des thermischen Verhaltens binärer Gasmischungen in einem großen Dichtebereich* (Ph.D. thesis, TH Karlsruhe, 1986).

336. W. Blanke, H. Häusler, and R. Weiss, *Int. J. Thermophys.* **9**:791 (1988).

337. T. Kamimura, A. Iso, Y. Higashi, M. Uematsu, and K. Watanabe, *Rev. Sci. Instrum.* **60**:3055 (1989).

338. R. Gilgen, R. Kleinrahm, and W. Wagner, *J. Chem. Thermodyn.* **24**:953 (1992).

339. W. Blanke, G. Klingenberg, and R. Weiß, *PTB-Mitteilungen* **103**:27 (1993).

340. V. Vacek and J. A. Zollweg, *Fluid Phase Equil.* **88**:219 (1993).

341. A. M. Sirota, Y. A. Khromykh, and I. I. Goldstein, *Therm. Eng.* **26**:733 (1979).

342. K. Bier, G. Maurer, and H. Sand, *Ber. Bunsenges. Phys. Chem.* **84**:430 (1980).